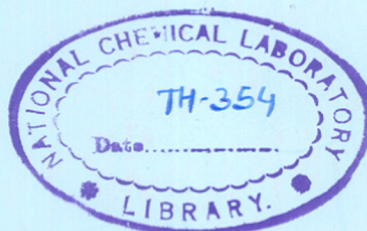


STRUCTURAL, ELECTRICAL AND
PHOTOCONDUCTING PROPERTIES
OF CADMIUM SULPHIDE THICK FILMS

A THESIS
SUBMITTED TO THE
UNIVERSITY OF POONA
FOR THE DEGREE OF
DOCTOR OF PHILOSOPHY
IN CHEMISTRY

COMPUTERISED

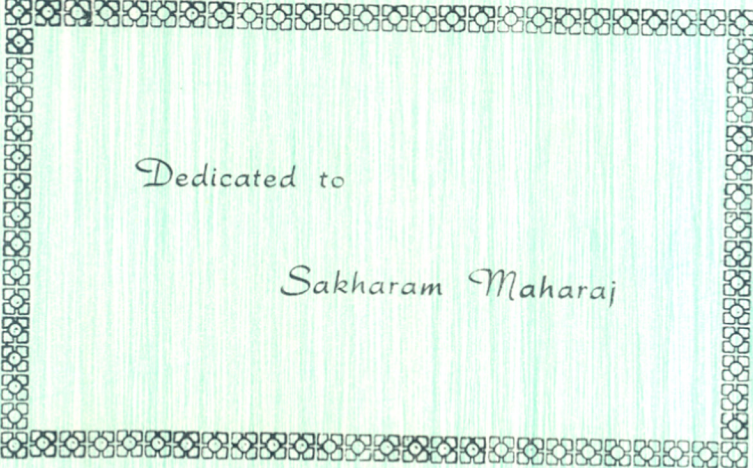


BY
D. P. AMALNERKAR
M. Sc.

621.382:541.6 (043)
AMA

NATIONAL CHEMICAL LABORATORY
POONA-411008 (INDIA)

MAY 1982



Dedicated to

Sakharam Maharaj

Certified that the work incorporated in the thesis "Structural, electrical and photoconducting properties of cadmium sulphide thick films" submitted by Shri D.P. Amalnerkar was carried out by the candidate under my supervision. Such material as has been obtained from other sources has been duly acknowledged in the thesis.



Dr. A.P.B. Sinha
(Supervisor)

C O N T E N T S

	<u>Page</u>
GENERAL INTRODUCTION	
(I) Theoretical background of photo-conductivity phenomenon	1
(II) Scope and objectives of the present work	14
(III) Outline of the thesis	18
CHAPTER – 1 HISTORICAL SURVEY	
1.0. General features of CdS	21
1.1. Studies on single crystal of CdS	23
1.2. Studies on powder layers of CdS	30
1.3. Studies on sintered films or layers Of CdS	34
1.4. Studies on thin films of photo-Conducting CdS:	
1.4.1. Studies on vacuum-evaporated films of CdS	43
1.4.2. Studies on sputtered films of CdS	50
1.4.3. Studies on chemically deposited CdS films	51
1.5. Studies on thick films of CdS	57
1.6. Summary and conclusions	59
1.7. Chemisorption of oxygen on CdS	61
REFERENCES	72
CHAPTER – 2 EXPERIMENTAL	
2.1. Preparation	84
2.2. Preparation of the test samples	90
2.3. Surface morphology	93
2.4. Structure	93

	<u>Page</u>
2.5. Electrical contacts	94
2.6. Measurements on electrical and photoconducting properties	95
2.7. Chemisorption of oxygen	98
 CHAPTER – 3 RESULTS AND DISCUSSION	
3.1. Effect of preparation conditions on photosensitivity :	
3.1.1. Effect of firing temperature	102
3.1.2. Effect of copper concentration	105
3.2. Structure	
3.2.1. Analysis of X-ray	107
3.2.2. Predominance of cubic phase in undoped films	115
3.2.3. Cubic to hexagonal phase transformation	116
3.3. Surface morphology	131
3.4. Electrical contacts and current-voltage characteristics	134
3.5. Dark conductivity as a function of temperature	138
3.6. Photosensitivity	145
3.6.1 Photosensitivity and oxygen chemisorption	146
3.6.2. Kinetics of oxygen chemisorption	157
3.6.3. X-ray photoelectron spectroscopic studies of oxygen chemisorption	160
3.7. Dependence of photocurrent on the intensity of illumination	168
3.8. Spectral Response	176
REFERENCES	187
CHAPTER – 4 SUMMARY	191
ACKNOWLEDGEMENT	

GENERAL INTRODUCTION

1

The phenomenon of photoconductivity, i.e., the enhancement of the electrical conductivity of a material by the absorption of suitable photons, although discovered more than hundred years ago by W. Smith, still continues to attract a great deal of attention as is evident from the growing number of papers devoted to all the facets of this subject. Solid state research in the past three decades has greatly improved our understanding of this phenomenon which has culminated in the development of highly sensitive materials for use in electronic devices. There are several excellent contributions to this subject in the form of books¹⁻⁴, proceedings of conferences^{5,6} and review articles⁷⁻¹⁰.

(I) THEORETICAL BACKGROUND OF
PHOTOCONDUCTIVITY PHENOMENON^{1,2,3,7,8}

[A] General Mechanism

Generally speaking, every insulator and semiconductor should exhibit photoconductivity when illuminated by a suitable radiation.

The expression for electrical conductivity (σ) of a material (semiconductor/insulator), in which one type of charge carriers is considered to dominate (for the sake of simplicity) is given below:

$$\sigma = ne\mu \quad \dots (1)$$

where n , e and μ are the density, charge and mobility of the free carriers respectively.

A change in conductivity ($\Delta\sigma$) with illumination may arise from either (i) a change in the density of free carriers (Δn), or (ii) a change in their mobility ($\Delta\mu$).

$$\text{Thus, } \Delta\sigma = e\mu \Delta n + e n \Delta\mu \quad \dots (2)$$

(for small values of Δn and $\Delta\mu$).

The term 'n' is directly related to the intensity of excitation 'f' through the free carrier lifetime ' τ ', perhaps the key parameter in photoconductivity, by the expression

$$n = f\tau \quad \dots (3)$$

This expression implies that a change in free carrier density (Δn) can be caused either (i) by a change in the rate of photoexcitation (Δf) or (ii) by a change in free carrier lifetime ($\Delta\tau$), i.e.

$$\Delta n = \tau \Delta f + f \Delta\tau \quad \dots (4)$$

By substituting the value of Δn from expression (4) in expression (2), we get

$$\Delta\sigma = e\mu\tau\Delta f + e\mu f\Delta\tau + ne\Delta\mu \quad \dots (5)$$

Each of the terms involved in expression (5) represent atleast one and in some cases more than one mechanism responsible for photoconductivity.

[B] Dependence of the photoconductivity on the lifetime and the mobility of free carriers

Let us consider an n-type of semiconducting material for the sake of simplicity. Fig. (I) shows a unit cross-sectional area of the insulator exposed to a uniform volume excitation which generates free electrons at the total rate of 'f' per second. The total number of photogenerated (free) electrons, in the steady state, will be given by;

$$n = f\tau \quad \dots(3)$$

[Here ' τ ' counts only the time spent by an electron in the conduction band. If the electron is trapped and thermally re-emitted to the conduction band, the time spent in traps is not included in ' τ '].

From the simple definition of current, expression for the photocurrent can be written as,

$$I_p = \frac{ne}{T_r} \quad \dots(6)$$

where I_p = magnitude of the photocurrent,
 n = total number of the photogenerated electrons,
 e = the electronic charge,
 T_r = transit time of free electrons in moving from cathode to anode under the influence of the applied electrical field.

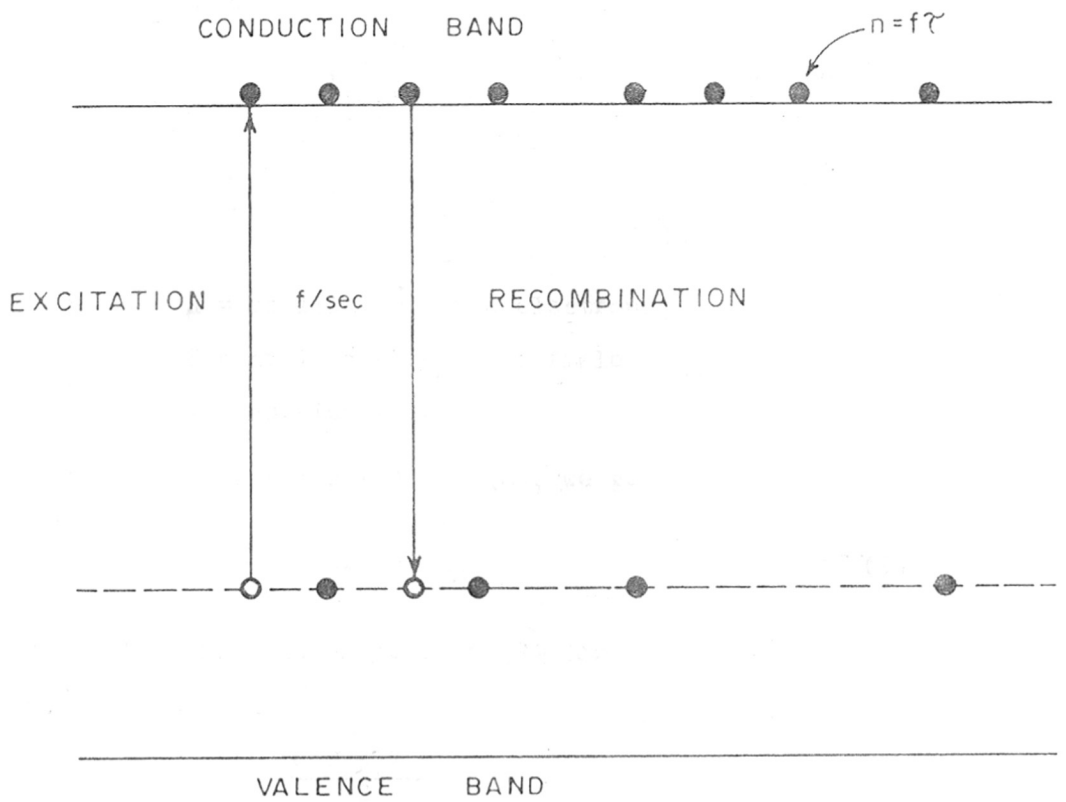


FIG. (1) PHOTOEXCITATION AND RECOMBINATION

Transit time (T_r) can be written in terms of the drift velocity (V_d) of free electrons and inter-electrode spacing (L), as

$$T_r = \frac{L}{V_d} \quad \dots (7)$$

$$\begin{aligned} \text{and } V_d &= \mu E \quad \dots (8) \\ &= \mu \frac{V}{L} \end{aligned}$$

where μ = mobility of free electrons,
 E = applied electrical field = $\frac{V}{L}$,
 V = applied voltage.

Combining expressions (7) and (8), we get

$$T_r = \frac{L}{V_d} = \frac{L}{\mu E} = \frac{L^2}{V\mu} \quad \dots (9)$$

By substituting the expression (9) for T_r in expression (6), we get

$$I_p = \frac{e f \tau V \mu}{L^2}$$

or, on rearranging

$$I_p = \frac{e f V}{L^2} (\mu \tau) \quad \dots (10)$$

Expression (10) indicates that under constant conditions of f , v and L , photoconductivity is directly proportional to the product of mobility and lifetime of free carriers ($\mu \tau$) which, therefore, is used as the "figure of merit"

for photosensitivity. The mobility varies only slightly between different II-VI materials, whereas the lifetime may vary by many orders of magnitude. Majority carrier lifetime (τ) is, therefore, the key parameter in photoconductivity. It is associated predominantly with the specific compensated acceptor type of imperfections added and/or formed in the photoconducting material. These imperfections, for example in n-type of photoconductor, possess a large capture cross-section for photoexcited holes and small capture cross-section for photoexcited electrons thereby increasing lifetime of the photoexcited electrons. According to expression (10), this situation results in high photosensitivity. An energy level representation of the sensitization process is given in Fig. (II).

(C) Performance Criteria

In order to compare and evaluate different photoconductors, it is necessary to have a detailed information of the following properties:

- (a) Photosensitivity,
- (b) Speed of response,
- (c) Region of spectral sensitivity, i.e. spectral response.

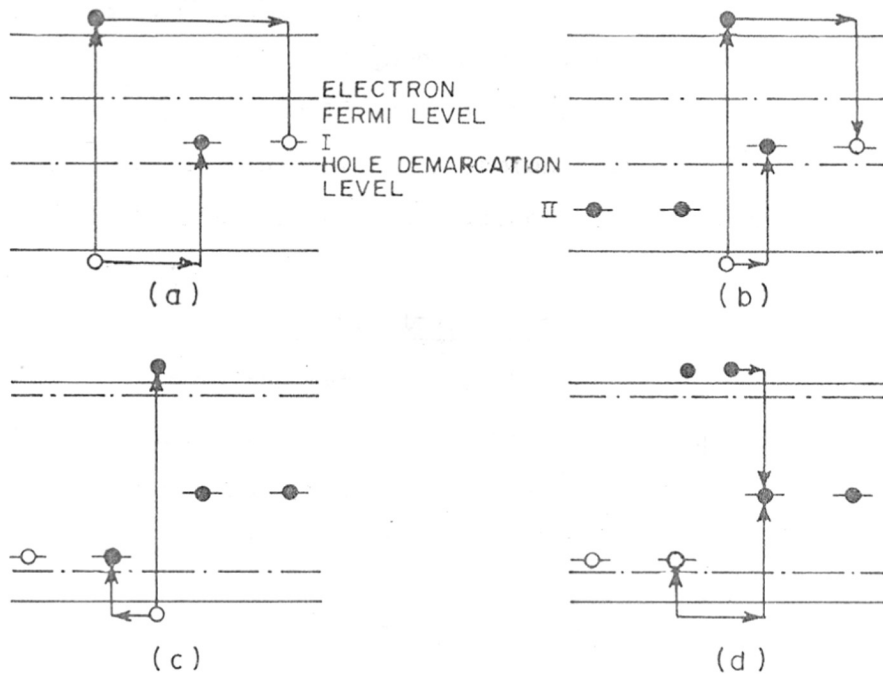


FIG. (II) IMPERFECTION SENSITIZATION OF PHOTOCONDUCTIVITY :

- a) MATERIAL WITH ONLY FAST RECOMBINATION CENTERS RESULTS IN LOW FREE CARRIER LIFETIMES.
- b) SENSITIZING CENTERS INCORPORATED, BUT ACTING ONLY AS HOLE TRAPS.
- c) SENSITIZING CENTERS ACTING AS RECOMBINATION CENTERS AND OCCUPIED LARGELY BY HOLES.
- d) OPTICAL QUENCHING OF PHOTOCONDUCTIVITY BY OPTICAL FREEING OF HOLE FROM SENSITIZING CENTER.

a: Photosensitivity

The value assigned to the photosensitivity of a photoconductor should express how efficient the photoconductor is, in converting photon flux into the electrical current. It can be defined in various ways as given below:

(i) Photoconductivity gain (G)

It is the ratio of the number of charge carriers passing between the electrodes per unit time to the number of photons absorbed in an electron-hole creation process per unit time which can be given by the expression,

$$G = \frac{T}{T_r} \quad \dots (11)$$

(ii) Specific sensitivity/photo-response (S)

It is given by the expression

$$S = \frac{I_p/V \cdot L^2}{p} \quad \dots (12)$$

where I_p = photocurrent,

L = interelectrode spacing,

V = applied voltage,

p = absorbed radiation power.

(iii) Often photosensitivity is defined as the ratio of photoconductivity to dark conductivity, i.e.

$$\begin{aligned} \text{Photosensitivity} &= \frac{\text{Photocurrent}}{\text{Dark current}} \quad \dots (13) \\ &= \frac{\text{Dark resistance}}{\text{Photoresistance}} \end{aligned}$$

b : Speed of Response

A finite time is required for a photoconductor to adjust to an abrupt change in the intensity of photo-excitation. It is called response time. The shortest possible adjustment time can be the majority carrier lifetime. Frequently, the required adjustment time (rise or decay) is longer than the lifetime by many orders of magnitude. These long adjustment times are caused by the presence of trapping centers. When a photoconductor is being used as a light detector, its performance is judged by the dual criteria of photosensitivity and speed of response.

c : Spectral Response

Spectral response is the variation in the photo-conductivity with the wavelength of excitation. It gets modified according to absorption characteristics because that component with higher α (absorption constant) gets absorbed near the surface, whereas that with lower α goes deep into the bulk. Since the surface lifetime is considerably shorter than the volume lifetime, the photosensitivity of a material for surface-absorbed light is usually less than that for volume-absorbed light. A maximum response is usually found at the wavelength for which the absorption constant is approximately equal to the reciprocal of the crystal thickness. Light with wavelengths longer than that

corresponding to the photoconductivity maximum is only partially absorbed and hence the photosensitivity is also less. The presence of imperfection centers extends the spectral response to longer wavelengths because of the direct excitation of carriers from the imperfection levels into the conduction band.

The photosensitivity, the speed of response and the spectral response depend upon (i) the material used, (ii) the method of preparation, (iii) the impurities introduced, (iv) the nature of the electrical contacts made to the photoconductor and (v) the ambient atmosphere and temperature.

(D) Basic electronic processes
in a photoconductor

Fig. (III) shows the basic electronic processes in a photoconductor shown specifically for an n-type photoconductor like CdS. The processes are:

(1) Excitation of the host crystal by absorption of light with energy equal to or greater than the band gap.

(2) Excitation of a bound electron at an imperfection level.

(3) Capture of a photoexcited hole by an imperfection center.

(4) Capture of a photoexcited electron.

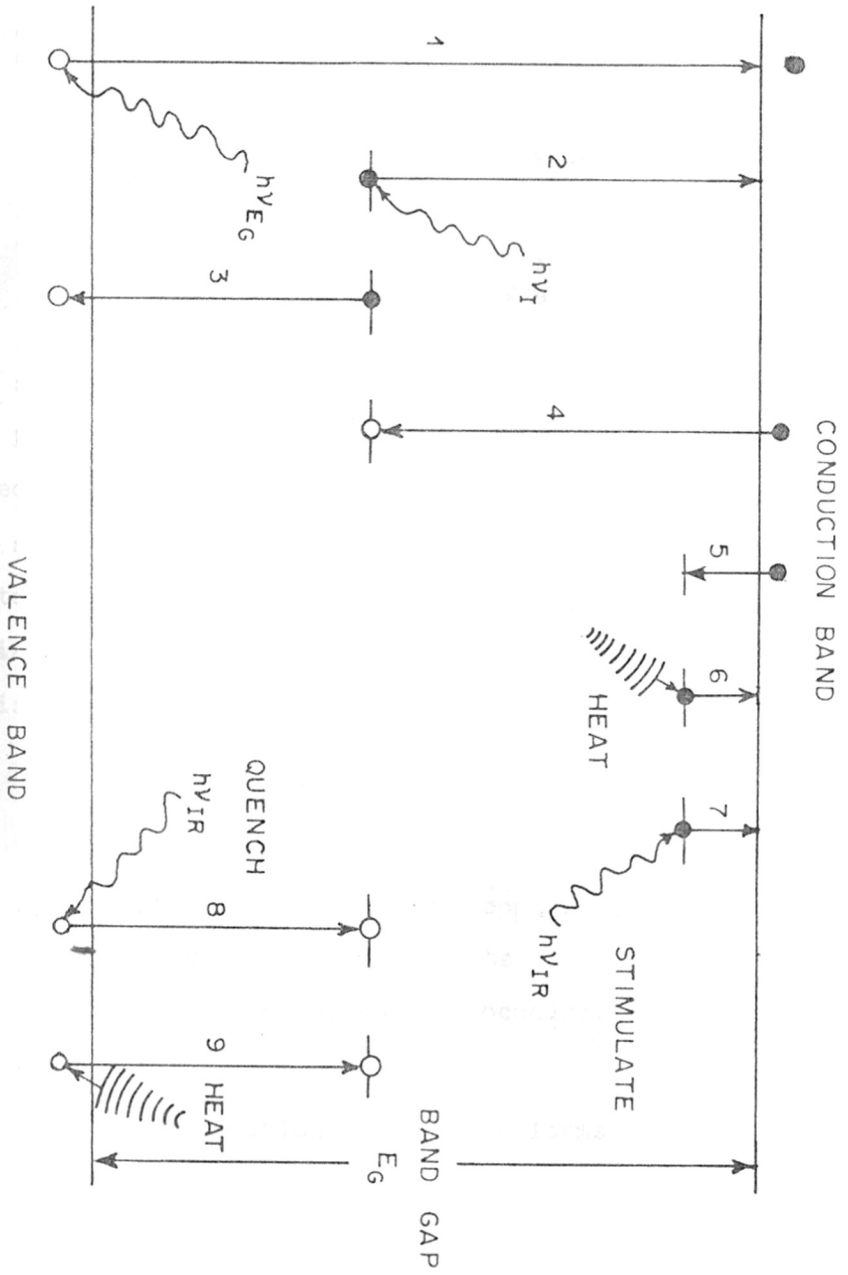


FIG. (III) TYPICAL ELECTRONIC TRANSITIONS IN AN n-TYPE PHOTOCONDUCTOR

by a center which has previously captured a photoexcited hole, resulting in recombination of the carriers.

(5) Capture of a photoexcited electron by an electron trapping center.

(6) Thermal freeing of a trapped electron.

(7) Optical freeing of a trapped electron.

(8) Optical freeing of a captured hole.

(9) Thermal freeing of a captured hole.

Processes (1) and (2) determine the spectral response; (3) and (4) determine free-electron lifetime and through it the photosensitivity; (5) and (6) frequently determine the speed of response; (7) causes stimulation of conductivity; (8) and (9) correspond to optical and thermal quenching of photoconductivity. Transitions (3) and (4) may be either **radiative** (i.e., give rise to luminescence emission) or non-radiative (i.e., dissipate the heat energy).

(E) A Photoconductor in Operation

A typical n-type photoconductor in operation is depicted in Fig. (IV). Two ohmic contacts to the photoconductor are shown. These contacts are assumed to supply the free carriers required by the photoconductivity process. The processes are:

(1) Absorption of a photon forms a free electron-hole pair.

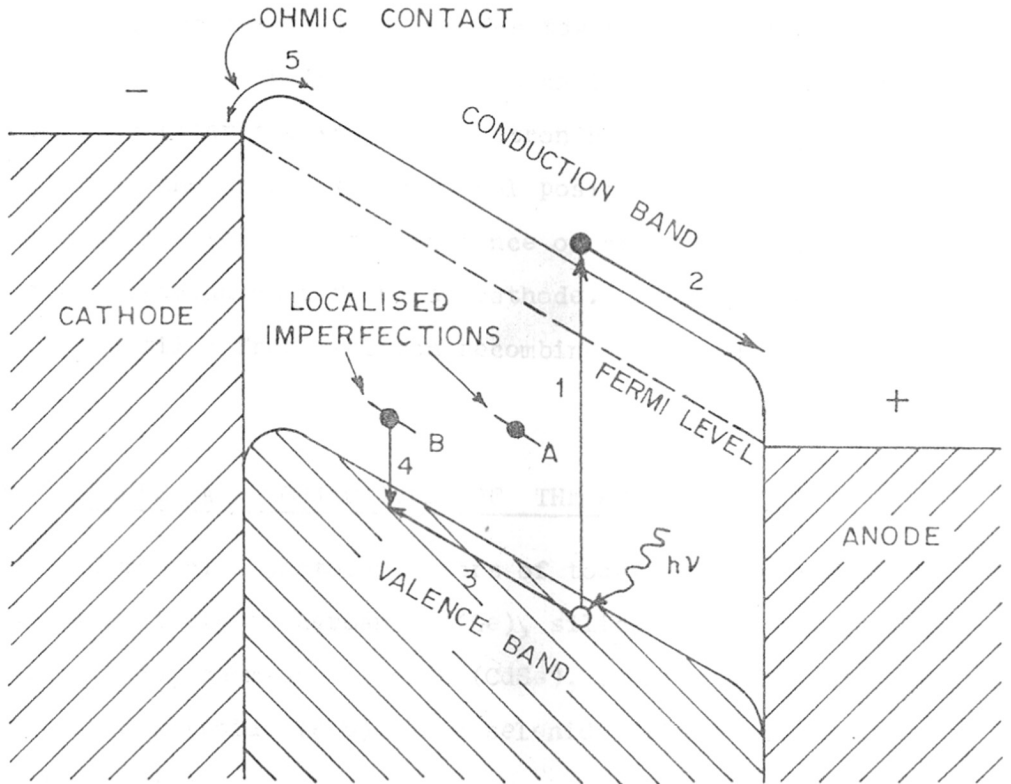


FIG. (IV) AN n-TYPE PHOTOCONDUCTOR IN OPERATION

(2) Under the applied electric field, the photoexcited electron moves towards the anode.

(3) Photoexcited hole moves towards the cathode.

(4) The hole is captured at an imperfection center.

(5) After the initial electron has left the photoconductor at the anode, the residual positive charge left in the material leads to the entrance of another electron into the photoconductor from the cathode. Photocurrent continues until a free electron recombines with the captured hole.

(II) SCOPE AND OBJECTIVES OF THE PRESENT WORK

Commercial photoconductors of today are based almost exclusively on germanium (Ge), silicon (Si), cadmium sulphide (CdS), cadmium selenide (CdSe), cadmium telluride (CdTe), lead sulphide (PbS), lead selenide (PbSe) and lead telluride (PbTe).

CdS possesses most of the desirable properties of an ideal photoconductor namely;

(i) It has sufficiently large band gap to provide the required high value of dark resistivity and in turn, high photosensitivity.

(ii) It possesses response in the desired spectral range i.e. visible.

(iii) A small density of trapping states in CdS permits the theoretical speed of response to be obtained at low intensities.

CdS, therefore, meets the needs of various opto-electronic devices and finds a variety of applications as listed in Table I.

TABLE - I

APPLICATIONS OF PHOTOCONDUCTING CdS CELLS

	<u>Analog devices</u>	<u>Digital devices</u>	<u>Large-area devices</u>
1.	Auto-bright-control circuits in TV sets	Automatic switching of out-door electric lamps	Electro-photography
2.	Auto-gain-control in transceivers	Optical encoders	Picture reproduction and display
3.	Exposure meters of cameras	Card readers	Image intensifiers
4.	Expression circuits of electronic organs	Contactless meter relays	
5.	Automatic light controls of digital watches	Electronic camera-shutters	
6.	Smoke detectors	Pulse meters	
7.	Densitometers		

In view of these wide-ranging applications, CdS photoconductors have received immense attention particularly in the last three decades. They have been studied in the form of single crystals¹¹ and in the form of thin films or layers prepared by various techniques like sintering^{12,13}, vacuum-deposition /evaporation¹⁴⁻¹⁶, sputtering^{17,18}, spraying¹⁹⁻²¹, chemical deposition²²⁻²⁴, etc. Efforts are still being made all over the world (i) to get a better characterised material with improved performance and (ii) to develop a simple and economical method for commercial fabrication.

Thick film technology, which is essentially a screen-printing and firing process, is comparatively less known in the field of photoconducting materials. It is of recent origin, relatively simple, less expensive and has become an extremely versatile and flexible method in the field of hybrid microelectronics^{25,26}. It is also quite amenable for large-area fabrication. In spite of all these advantages, this method is not seriously tried so far for the preparation of CdS photoconductors^{27,28}. An attempt has, therefore, been made (i) to prepare thick films of photoconducting CdS and (ii) to study the relevant characteristics.

The immensely complex issues of the surface states originating through physisorption and chemisorption of

various gases which play a key role in the photoconductivity phenomenon are important areas of investigation which have received renewed impetus through advances in surface-sensitive techniques like X-ray and Ultra-violet photoelectron spectroscopy (XPS and UPS), Auger electron spectroscopy (AES), etc. An XPS examination of oxygen-chemisorption on thick films of CdS forms a salient feature of our work.

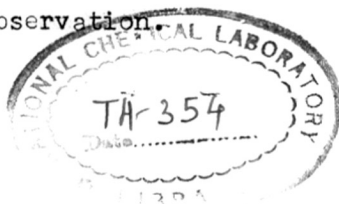
The highlights of the present investigation are as follows:

(i) CdS films with superior photosensitivity and acceptable shelf-life have been successfully fabricated using the thick film technique. Photosensitivity of the order of 10^9 associated with these films is the highest reported so far for CdS photoconductors.

(ii) A strong chemisorption of oxygen is found to be responsible for the high photosensitivity.

(iii) XPS examination of such films shows that chemisorbed oxygen is preferentially bonded to sulphur sites in SO_4^{--} and SO_2 type configurations on the surface.

(iv) X-ray diffraction (XRD) studies reveal the occurrence of cubic dominated mixed (cubic+hexagonal) phase in undoped film and only hexagonal phase in doped film. Predominance of cubic phase in photoconducting CdS is an interesting observation.



621.382:541.6(643)
AMA

(v) Undoped film shows an anomalous spectral response behaviour at 300°K .

(III) OUTLINE OF THE THESIS

An account of the preparation and characterisation of CdS thick films is given in the present thesis comprising of four chapters.

Chapter 1 is the historical survey in which physical, electrical, optical and photoconducting properties of single crystals, powder layers, sintered layers and thin films of CdS have been chronologically reviewed. Oxygen chemisorption on CdS, which is of basic importance in the photoconductive processes, is also covered separately in the same chapter.

Chapter 2 describes the detailed preparation procedure based on the standard screen-printing and firing processes. It also deals with some experimental techniques and methods of measurements chosen to characterise the photoconducting films.

The experimental results are presented and discussed in Chapter 3.

A concise summary of this work is given in Chapter 4. A complete bibliography is provided at the end of each chapter.

REFERENCES

1. R. H. Bube;
"Photoconductivity of Solids", John Wiley and Sons,
Inc. New York, (1960).
2. A. Rose;
"Concepts in photoconductivity and allied problems",
Interscience Publishers - Wiley, New York (1963).
3. B. Ray;
"II-VI Compounds", Pergamon Press, Oxford, (1969).
4. S. M. Ryvkin;
"Photoelectric effects in semiconductors",
Consultants Bureau, New York, (1964).
5. H. Levinstein (Ed.);
"Photoconductivity", Pergamon Press, Oxford, (1962).
6. E. M. Pell (Ed.);
"Proc. Third Int. Conf. on photoconductivity",
Pergamon Press, Oxford, (1971).
7. R. H. Bube;
In S. Larach (Ed.); "Photoelectronic materials and
devices", Van Nostrand Co. Inc; New York, (1965),
p. 100.
8. R. H. Bube;
In M. Aven and J. S. Prener (Eds.);
"Physics and chemistry of II-VI compounds",
North-Holland Publishing Co., (1967), p. 657.
9. R. H. Bube;
In H. Eyring, D. Henderson and W. Jost (Eds.);
"Physical Chemistry ; Vol. X, Solid State,
Academic Press, New York, (1970), p. 515.
10. R. H. Bube;
In J. Mort and D. M. Pai (Eds.),
"Photoconductivity and related phenomena",
Elsevier Scientific Publishing Company,
Amsterdam, (1976), p. 117.
11. R. H. Bube and S. M. Thomsen;
J. Chem. Phys., 23, p. 15 (1955).

12. S. M. Thomsen and R. H. Bube;
Rev. Sci. Instrum., 26, p. 664 (1955).
13. M. J. B. Thomas and E. J. Zdanuk;
J. Electrochem. Soc., 106, p. 964 (1959).
14. W. Veith,
Compt. Rend., 230, p. 947 (1950).
15. W. Veith,
Z. Angew Physik, 7, p. 1 (1955).
16. J. Dresner and F. V. Shallcross;
J. Appl. Phys., 34, p. 2390 (1963).
17. G. Helwig and M. König;
Z. Angew Physik, 7, p. 323 (1955).
18. D. B. Fraser and H. Melchior;
J. Appl. Phys., 43, p. 3120 (1972).
19. C. H. Wu and R. H. Bube;
J. Appl. Phys., 45, p. 648 (1974).
20. Y. Y. Ma and R. H. Bube;
J. Electrochem. Soc., 124, p. 1430 (1977).
21. B. K. Gupta, O. P. Agnihotri and A. Raza;
Thin Sol. Films, 48, p. 153 (1978).
22. S. D. Sathaye and A. P. B. Sinha;
Thin Sol. Films, 37, p. 15 (1976).
23. N. R. Pavaskar, C. A. Menezes and A. P. B. Sinha;
J. Electrochem. Soc., 124, p. 743 (1977).
24. N. Croitoru and S. Jakobson;
Thin Sol. Films, 56, L5 (1979).
25. C. A. Harper;
"Handbook of Thick Film Hybrid Microelectronics",
McGraw Hill Book Company, New York, (1974).
26. R. A. Rikoski;
"Hybrid Microelectronic Circuits - The Thick Film",
John Wiley and Sons, Inc., New York, (1973).
27. F. B. Micheletti and P. Mark;
J. Appl. Phys., 39, p. 5274 (1968).
28. Y. Moriwaki;
Japan Kokai 7551, 286 (Cl. H. 01 L) 8 May 1975;
C. A. 83:156842a.

CHAPTER — 1
HISTORICAL SURVEY

1.0. Before embarking on the actual literature survey, let us make a note of some general features of CdS¹:

- (A) CdS crystallises in two forms;
 - (i) Wurtzite or hexagonal structure (α)
 - (ii) Zinc blende or cubic structure (β).
- (B) It is generally 'n' type.

(C) The band gap of CdS has been estimated mainly from the optical absorption data. Though the values reported in the literature vary from 2.4 to 2.7 eV, 2.4 eV is the generally accepted value.

(D) The absorption edge is found at $\lambda \approx 5100\text{\AA}$ with a sharp cut-off. The spectral response of CdS has the peak sensitivity in the visible region.

(E) A typical room temperature value for electron mobility in CdS in dark is $200 \text{ cm}^2/\text{volt sec}$.

A great deal of work has been done on the electrical, optical and photoconducting properties of CdS in the form of single crystals, powder layers, sintered layers and thin films. Since a comprehensive review (of these studies) is not available in the literature, an attempt is made to review the photoconducting and related properties of CdS in each of the above mentioned forms.

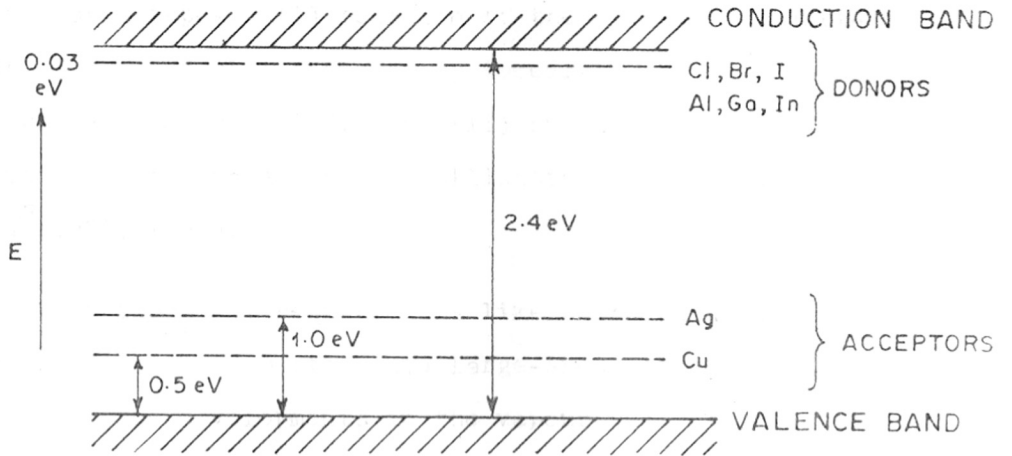


FIG. 1-1 CdS BAND DIAGRAM WITH IMPURITY LEVELS

1.1. STUDIES ON SINGLE CRYSTALS OF CdS

1.1.1. Methods for growing single crystals

Single crystals of CdS are mainly grown from the vapour-phase technique. This technique can be separated into two main types : (i) reaction of the elemental constituents of the material followed by immediate crystal growth e.g. Frerichs method²(1947) and (ii) sublimation of the compound with subsequent recrystallisation e.g. Reynolds method³(1952, 1958).

The important requirements like reproducibility and uniformity in the properties and large-area applications have led to the developments in the vapour-phase techniques. Notable contributions are due to Beun et al.¹⁴, (1962), Clark and Woods^{36,37} (1966, 1968), etc.

1.1.2. Photoconductivity and associated properties

Since the revival of Lorenz method (1891) of growing CdS single crystals by Frerichs (1947), the photoconducting properties of this material have been extensively investigated. The first thorough attempt goes to the credit of Bube and Thomsen⁴ (1955). They have studied photoconductivity and crystal imperfections in CdS crystals which were grown by the modified Frerichs technique and activated by copper and chlorine impurities. This study is in two parts^{4a,4b}. Part I deals with the effect of impurities and

their role in the enhancement of the photosensitivity. Part II deals with the determination of characteristic photoconductivity quantities from various photoconducting measurements such as (1) spectral response, (2) thermally stimulated current, (3) conductivity as a function of temperature, (4) photocurrent as a function of light intensity at various temperatures, (5) photocurrent decay time as a function of light intensity at various temperatures. Bube⁵ (1955) further presented infrared quenching and a unified description of photoconductivity phenomenon in CdS single crystals. He (1956) has also determined rise and decay times of photoconductivity in CdS single crystals under high intensity of excitation⁶.

Almost in the same period, Reynolds et al.⁷ (1955) have reported optical absorption, refraction, spectral response, response time, current-voltage characteristics, photovoltaic and rectification effects in CdS single crystals which were grown by the sublimation method.

Woods⁸ (1957) suggested an alternative way of activating CdS crystals grown by Frerichs' technique. It involves heat treatment in vacuum or in air. He (1958) has further investigated the effects of heat treatment in oxygen on the photoconductivity of a number of differently activated CdS crystals with particular reference to shallow electron

trapping effects⁹. Kitamura¹⁰ (1961) specified the ionization energies and the electron trap-depths in CdS single crystals which were heat-treated in vacuum or in oxygen. He noticed an increase in photosensitivity in the longer wavelength region.

Bube and Barton¹¹ (1959) have demonstrated that highly photosensitive crystals of CdS can be grown by introducing a trace of halogen impurity such as iodine during the preparation. Bube¹² (1959) reported the existence of relatively shallow acceptor levels with ionization energy in the range of 0.1 to 0.3 eV in certain CdS crystals annealed in sulphur atmosphere. According to him, the reversible variations of photosensitivity in these crystals can be caused by making the shallow levels effective or by removing their effectiveness. Bube¹³ (1960) has investigated saturation of photoconductivity due to photoexcited emptying of sensitizing centers in CdS crystals.

Beun et al.¹⁴ (1962) have analysed photoconductivity in CdS single crystals which were grown from the vapour phase by the method of chemical transport with iodine as a carrier. They have found that annealing of such crystals in various atmospheres (sulphur, cadmium and potassium vapour) causes large changes in the optical and electrical properties although iodine content could not be altered by any of these treatments. Bube¹⁵ (1961) reported monotonic

trap distributions for such crystals. Additionally, he and his co-workers¹⁶ (1962) have described the photoelectronic properties of CdS single crystals grown by chemical transport method and containing high proportions of incorporated impurities. According to their hypothesis, the electrical and luminescent properties are to be associated with the specific acceptor impurity, whereas the photosensitivity is to be associated with the other defects such as cation vacancies. Bube and Young¹⁷ (1964) have presented the detailed measurements on the photoconductivity gain as a function of photon energy over the entire range of intrinsic absorption, copper impurity absorption and crystal defect absorption in such crystals providing an additional evidence for this hypothesis. Bube and Hemila¹⁸ (1967) have discussed the problems related to the distinction between the intrinsic defects and copper impurity defects. Cardon and Bube¹⁹ (1964) have published the theory of superlinear photoconductivity in CdS and related materials. They have developed several theoretical considerations in order to make the treatment of this phenomenon more consistent with the experimental data on CdS single crystals grown by the chemical transport method.

Crandall²⁰ (1967) presented the results of low temperature photocurrent measurements on Cu-doped CdS crystals grown by the vapour-phase method. He observed a

decrease in the photocurrent by several orders of magnitude below 30°K and explained it on the basis of an exponential distribution of electron traps.

1.1.3. Optical properties

Dutton²¹ (1958) has studied the absorption and reflection spectra of CdS single crystals and reported the value of the fundamental absorption edge. Balkanski and Waldron²² (1958) have studied the absorption spectra and the photoconductivity produced by illumination at a distance from the electrodes to determine the mechanisms of photon-electron interactions and the energy transport in CdS single crystals.

1.1.4. Thermally stimulated conductivity and photochemical phenomena

Trofimenko et al.²³ (1960) have studied the photo-sensitivity of variously treated CdS single crystals and their corresponding thermally induced conductivity. The results on the pulse excitation studies of gain and trapping in photoconducting CdS crystals have been presented by Bube²⁴ (1963). He has indicated that how a simple model of photoconductivity transients based on the concept of a quasi-uniform trap distribution can be used to give a quantitative correlation between pulse or transient data at a fixed temperature and thermally stimulated conductivity.

Nicholas and Woods²⁵ (1964) have made an extensive examination of the conductivity glow curves obtained for a variety of CdS crystals. They have computed six discrete sets of traps at depths of 0.05, 0.14, 0.25, 0.41, 0.63 and 0.83 eV. They have also pointed out that the concentration of these traps strongly depends on the preparation conditions and physical history of the crystals. They (1964) have further reported the number of photochemical phenomena in CdS single crystals which lead to the disappearance of some peaks from glow curves and appearance of others²⁶. An excellent summary of the photochemical phenomena in CdS single crystals is offered by Tscholl²⁷ (1968). Im et al.²⁸ (1970) have provided and discussed the actual evidence for the photochemical changes in traps in CdS crystals.

1.1.5. Hall-effect, Thermoelectric effect, Field effect, etc.

The importance of techniques like Hall effect and photo-Hall effect in understanding the photoconductive processes has been illustrated by Bube and MacDonald²⁹ (1961) with the example of CdS crystals. They have pointed out that the suitable use of photo-Hall effect can lead (i) to the knowledge about type, density and mobility of charge carriers, as well as, about the charge on imperfection centers, and (ii) to an independent determination of the various capture cross-sections.

Thermoelectric and photothermoelectric effects, having applications similar to Hall effect and photo-Hall effect, have been systematically investigated in case of CdS crystals by Birkholz et al.³⁰ (1968), Weichmann et al.³¹ (1968) and Kwok and Bube³² (1973).

Tyagai et al.³³ (1967) have shown that how the field effect measurements can be used to obtain quantitative information on the principal photoconductivity parameters of CdS single crystals. Similar measurements were also presented by Sawamoto³⁴ (1965) and Weber³⁵ (1969).

1.1.6. Miscellaneous

A new method of growing single crystals of CdS in the controlled atmospheres of the constituent elements is described by Clark and Woods^{36,37} (1966, 1968). Patil³⁸ (1973) has carried out extensive measurements of photoconductivity response, infrared quenching, trapping parameters and photochemical effects in CdS crystals prepared by this method. Similarly, Carter and Woods³⁹ (1973) have examined spectral response and infrared quenching of the photocurrent of such crystals having different stoichiometry.

Recently, Manshadi and Woods⁴⁰ (1977) have described the results of their investigation dealing with the stability of photosensitivity of CdS crystals doped with chlorine and

counterdoped with cuprous and cupric ions. It has been found that photosensitivity of crystals doped with cuprous ions is much more stable under illumination than that of crystals doped with cupric ions.

Table 1.1 presents some important results on photoconducting properties of CdS single crystals grown by various methods.

1.2. STUDIES ON POWDER LAYERS OF CdS

1.2.1. Preparative techniques

Before techniques for the preparation of other types of layers or single crystals had been developed, powder was the normal form with which photoconductors were made. Eventhough highly photosensitive single crystals of CdS were known in the latter years, considerable interest still remained in preparing photosensitive powder layers of CdS because of the ease of large-area fabrication.

Kolomiets⁴¹ (1952) attributed an early failure in obtaining a photosensitive CdS powder to high resistance between the grains. In latter years, several standard techniques have been developed to prepare powder-binder type layers of CdS⁴²⁻⁴⁵. General method of the preparation can be divided into three steps:

TABLE - 1.1
 SOME IMPORTANT RESULTS ON THE PHOTOCONDUCTING PROPERTIES OF CdS SINGLE CRYSTALS
 GROWN BY VARIOUS METHODS

IMPORTANT METHODS / MODIFICATIONS	CRYSTAL STRUCTURE	ACTIVATION BY	PHOTOSENSITIVITY	SPECTRAL RESPONSE	RESPONSE TIME (RISE / DECAY)	LIGHT-INTENSITY DEPENDENCE OF RESISTANCE / CURRENT
(14) Bube and Thomsen (1955)	Hexagonal	—	$\frac{\rho_D}{\rho_L} = 10^4$	$\lambda_{max} = 515 \text{ nm}$	$\sim 10^{-3}$ millisecc depending upon light intensity and temperature	Linear variation at lower intensities and square-root variation at higher intensities
		Cl compensated Cu, Ga, In, Al etc	$\frac{\rho_D}{\rho_L} = 10^5 - 10^6$ (Max)	—	—	—
(17) Reynolds (1955)	Hexagonal	Oxygen incorporation during growth	$\frac{\sigma_D}{\sigma_D} \approx 10^4$	Beyond the fundamental cut-off	Few seconds to days depending upon the concentration	—
(14) Beun et al (1962)	Hexagonal	Iodine (as a transporting agent) Untreated	$\frac{\rho_D}{\rho_L} \approx 5$	$\lambda_{max} = 620 \text{ nm}$	0.5 sec	—
		After treatment 'S' 375°C (12 hr) 'S' 600°C (12 hr) 'S' 800°C (12 hr) 'K' 800°C (12 hr) 'CuS' 800°C (12 hr)	≈ 2.5 $\approx 10^3$ $\approx 10^3$ $\approx 10^3 - 10^4$ $\approx 10^3$	$= 620 \text{ nm}$ $= 620 \text{ nm}$ $= 690 \text{ nm}$ $= 510 \text{ nm}$ $= 620 \text{ nm}$	0.5 sec 1.0 sec 10.0 sec 2×10^{-2} sec 2×10^{-3} sec	—
(16) Bube et al (1962)	—	I compensated Cu	$S = 1 - 10$ $\text{cm}^2 / \text{ohm Watt}$	Broad response about $\lambda_{max} = 650 \text{ nm}$ (frontsurface) $\lambda_{max} = 750$ (backsurface)	—	Linearity (for crystals with low Cu content) Superlinearity (high Cu content)
(37) Clark and Woods (1968)	Hexagonal	—	Absolute values not given. Dark resistivity and hence photosensitivity depends upon growth conditions	—	—	—
(38) Patil (1972)	—	Cu ₂ S addition to the CdS charge	—	Sharp response with $\lambda_{max} \approx 480 \text{ nm}$ and Broad response with $\lambda_{max} \approx 650 \text{ nm}$	—	—
(39) Carter and Woods (1973)	—	—	High photosensitivity for Cd rich crystals	$\lambda_{max} = 480 \text{ nm}$ with threshold of photoconductivity at about $\lambda = 710 - 750 \text{ nm}$ in Cd rich crystals $\lambda = 600 \text{ nm}$ in S rich crystals	—	—

(i) Activation of pure CdS powder with suitable impurities (e.g. Cu and Cl) by the standard phosphor technique.

(ii) Application of the mixture containing the activated CdS powder and a plastic binder in some volatile solvent onto substrates by conventional techniques such as painting, spraying, silk-screening or simply spreading.

(iii) Drying to harden the layer.

1.2.2. Photoconducting and related properties

Highly photosensitive powder layers of CdS with most of the equivalent characteristics of single crystals have been reported by Thomsen and Bube⁴³ (1955). They have studied properties such as photosensitivity, speed of response, spectral response, dependence of the photocurrent on the applied voltage and light intensity of these layers. In the same period, Nicoll and Kazan⁴⁴ (1955) have presented the characteristics of large-area high current photoconductive cells made by embedding CdS powder in the plastic binder. They have also emphasised the usefulness of the powder layer techniques in designing photoconductive cells of CdS having any arbitrary area and desired photosensitivity at almost any specified illumination without using lenses or other light concentrating means. Rothschild⁴⁶ (1956) studied the variations in spectral response of CdS powder.

layers occurring as a result of partial substitution of Zn for Cd and of Se for S. Bube and Dreeben⁴⁷ (1959) have performed photoconductivity measurements on a series of CdS:Cu:Ga powder layers to study the variation in the hole ionization energy of imperfection centers as a function of impurity concentration.

A different mechanism of photoconductivity phenomenon in powder layers of CdS has been proposed by Bube⁴⁸ (1960). Using the large amount of data obtained from the measurements on a variety of CdS powder-binder layers, he showed that there are four different regions encountered as the applied voltage is varied. He has also proposed a model to explain several observations such as current-voltage curves, photocurrent lag after periods of no applied voltage or of opposite polarity applied voltage, the existence of a semi-permanent polarised set, a.c. properties of the powders and the hysteresis or storage effects.

1.2.3. Miscellaneous

Lind and Bube⁴⁹ (1962) have reported photoelectronic properties of cubic CdS in the form of powder-binder layer.

Smith and Behringer⁵⁰ (1965) have studied the powder-binder layers of CdS with the objectives of examining and interpreting the photoinduced discharge characteristics of such layers in xerographic mode.

Miyake⁵¹ (1971) investigated a.c. and d.c. photoconductivities of CdS powdered layers. Misra et al.⁵² (1971) have presented the preparation and performance characteristics of luminescent and photoconducting layers of CdS powder.

1.2.4. Pellets

Another form in which the powder can be used is the pellet. It is prepared by press-moulding the activated CdS powder with a small quantity of binder. Angelov and Milyashev⁵³ (1972) have reported photoconductivity and electrically stimulated currents in pressed specimens of CdS. However, very soon the powder-binder type of layers have been replaced by the more attractive sintered layers.

Table 1.2 presents some important results on the photoconducting properties of powder-binder layers of CdS.

1.3. STUDIES ON SINTERED FILMS OR LAYERS OF CdS

A slight variation in the final treatment of the powder-binder layer produces a sintered layer. Its properties approach closer to those of single crystals.

1.3.1. Preparative technique

A general method for the preparation of sintered CdS layers can be described as follows:

TABLE - 1.2
SOME IMPORTANT RESULTS ON THE PHOTOCONDUCTING PROPERTIES OF POWDER - BINDER LAYERS
OF CdS

IMPORTANT METHODS / MODIFICATIONS	CRYSTAL STRUCTURE	ACTIVATION BY	PHOTOSENSITIVITY	SPECTRAL RESPONSE	RESPONSE TIME (RISE / DECAY)	LIGHT-INTENSITY DEPENDENCE OF RESISTANCE / CURRENT
Thomsen (43) and Bube (1955)	—	Cl compensated Cu	$\frac{\rho_D}{\rho_L} \approx 10^6$	Broad response with $\lambda_{max} \approx 670 \text{ nm}$	$\sim 10^3$ millisecond (depends upon the light intensity)	Square-root variation
Nicoll (44) and Kazan (1955)	—	Cl compensated Cu	$\frac{\sigma_L}{\sigma_D} \geq 10^6$	Fairly sharp response with $\lambda_{max} \approx 650 \text{ nm}$	0.1 sec	Linear variation
Misra et al (52) (1971)	—	Cl compensated Cu	—	Sharp response with $\lambda_{max} = 700 \text{ nm}$	—	Sublinear variation
Lind and Bube (1962)	Cubic	—	—	$E_{max} = 2.1 \text{ eV}$ $\lambda_{max} = 590 \text{ nm}$	—	—

(i) Highly pure CdS is activated with some suitable impurities by the standard phosphor technique.

(ii) The mixture of this activated CdS powder along with a binder in some volatile solvent in the form of slurry, ink or paste is applied onto the substrates by any one of the conventional techniques such as spraying, painting, mechanically spreading, silk-screening, flow-on and doctor blade.

(iii) The resulting powder layer is sintered at a sufficiently high temperature in a suitable atmosphere to yield a polycrystalline photoconductor.

1.3.2. Photoconducting and related properties

There exists a voluminous literature on the photoconducting properties of CdS sintered layers. The extensive investigation of the sintered layers of photoconducting CdS dates back to the report of Thomsen and Bube⁴³ (1955). They have reported preparation and properties such as photosensitivity, speed of response, spectral response, dependence of the photocurrent on the applied voltage and on the light intensity. This report has proved to be of unique importance as it initiated many investigators to work in this field in subsequent years.

Thomas and Zdanuk⁵⁴ (1959) have set forth the preparation and performance characteristics of sintered photoconductors of CdS. Although the photoconducting properties are directly dependent on the composition, the layer preparative techniques and the geometry of the unit; they have shown that these parameters can be predicted and controlled to obtain reproducible layers of the desired electrical and photoconducting properties.

Billups et al.⁵⁵ (1959) have presented the dependence of electrical and optical properties of CdS sintered layers on the variations (i) in activators and (ii) in sintering parameters such as atmosphere, temperature, time of sintering and method of cooling. Kitamura et al.⁵⁶ (1960) have prepared highly sensitive and stable films of CdS by sintering on a fused quartz plate and simultaneously adding impurities (e.g. Cu) with CdCl₂ flux. They have also investigated the effect of impurities on the optical and electrical properties of these films. In a separate note, Kitamura⁵⁷ (1960) has dealt with some consequences of the heat-treatment subjected to these films. Kitamura and his coworkers⁵⁸ (1960) have further examined the spectral response, rise and decay and the temperature dependence of the photocurrent of such films.

The effect of doping with In, Ga and also with InCl₃, GaCl₃ on the photoconductivity of sintered CdS layers is

reported by Zollei⁵⁹ (1966). Baczynski and Czajkowski⁶⁰ (1962) have determined the spectral sensitivity and the photocurrent decay curves of sintered CdS layers as a function of sintering temperature and time. Denga et al⁶¹ (1966) have investigated the effect of sintering temperature and time on the photocurrent as well as on the dark current of the sintered CdS films containing different Cu concentrations. They have reported stable and high photosensitivity in the ultra-violet region (350-420 nm).

Goldbach⁶² (1968) fabricated large-area photoconductive films by spraying water suspension of CdS with CuCl_2 on a suitable substrate and sintering the dry films obtained under the action of HCl. He characterised such films by studying the dependence of photosensitivity on the tempering time and temperature, HCl concentration and degree of doping. He also presented the results on the dependence of resistance on the illumination intensity, growth and decay times, partial sensitivity and temperature coefficient of photoconductivity.

A new process for sintering photoconductive CdS layers without any pinholes and cracks has been developed by Yamashita et al.⁶³ (1969) with which they have succeeded in designing sandwich type of photocells with high photoconducting gain ($\sim 10^5$). Main features of these cells are (i) high sensitivity for a very small active area,

(ii) feasibility of high degree integration, (iii) possibility of mass production and (iv) applications in pattern recognition systems, exposure meters for cameras, etc.

The principal preparation parameters of the sintered-CdS based-photoconductor for use in exposure meters have been optimised by Glukhova et al.⁶⁴ (1972). They have investigated spectral sensitivity, lux-ohm characteristics, current-voltage characteristics, time lag, temperature effects, fatigue and the light stability of such layers.

Pavelets et al.⁶⁵ (1973) have employed spray technique to prepare photosensitive sintered layers of CdS having high electron mobility values. He and his coworkers⁶⁶ (1974) have further investigated electrical, photoconducting and luminescent properties of sintered CdS:Cu:Cl layers as a function of Cu concentration.

Islam et al.⁶⁷ (1977) have reported photoconducting properties of sintered layers prepared by painting a slurry of CdS:Cu:Cl on ceramic substrates. The photosensitivity is $\sim 10^2$ for Cl doped CdS and $\sim 10^5$ for Cu and Cl doped CdS layers.

1.3.3. Miscellaneous

Zollei⁶⁸ (1971) studied the silver sensitization of sintered photoresistors prepared from colloidal CdS solution.

Chokalingam et al.⁶⁹ (1970) have reported current-voltage characteristics and spectral response of photo-conducting CdS layers prepared by the sintering technique. They have also analysed the effect of post-preparation treatments of these layers with the solution and the vapour of CdI₂.

Jakimavicius et al.⁷⁰ (1971) have examined micro-structure of sintered CdS layers by determining the crystallite size, regions of coherent scattering and micro-deformations by the analysis of X-ray diffraction lines. They have observed a cubic to hexagonal phase transformation.

Jakimavicius and his coworkers⁷¹ (1974) have deduced the dependence of the photocurrent relaxation time on the impurity concentration and on the layer recrystallisation methods for sintered CdS layers. They (1976) have further investigated charge-carrier mobilities in sintered CdS layers as a function of CuCl₂ concentration and illumination⁷². Variation in mobility with change in CuCl₂ concentration has been related to complex defects introduced by CuCl₂. Recently, Jakimavicius et al.⁷³ (1978) have discussed the distribution of energy levels associated with local centers in CdS:Cu:Cl sintered layers. They have also given the dependence of the trap levels upon sample illumination and the changes in defect parameters during photochemical reaction processes.

1.3.4. Sintered pellets/tablets

Sintered photoconductors can also be obtained in the form of pellets or tablets which actually bridge the gap between microcrystalline powders and single crystals. Yoshimatsu et al.⁷⁴ (1955) described sintered pellets of CdS made by press-moulding the powder with suitable binder followed by sintering. In the subsequent years, several reports dealing with various photoconducting properties of sintered CdS pellets have appeared in the literature. Important contributions are due to Bissinger⁷⁵ (1962), Wendland⁷⁶ (1962), Varvas et al.^{77,78} (1965, 1968), Ott⁷⁹ (1968) and Bunget et al.⁸⁰ (1979).

For most of the commercial applications, the sintered photoconductors are preferable because of certain advantages like large-area fabrication, uniformity, high mechanical strength and ease of impurity incorporation. As a result, the preparation techniques for sintered layers/films or pellets of CdS have become a matter of numerous patents⁸¹⁻⁹² which were filed from time to time (1949-1975).

Table 1.3 presents some important results on the photoconducting properties of sintered layers/pellets of CdS.

TABLE - 1.3

SOME IMPORTANT RESULTS ON THE PHOTOCONDUCTING PROPERTIES OF SINTERED-LAYERS / PELLETS OF CdS

IMPORTANT METHODS / MODIFICATIONS	CRYSTAL STRUCTURE	ACTIVATION BY	PHOTOSENSITIVITY	SPECTRAL RESPONSE	RESPONSE TIME (RISE / DECAY)	LIGHT-INTENSITY DEPENDENCE OF RESISTANCE / CURRENT
Thomsen and Bube (1955) (43)	—	Cl compensated Cu	$\frac{\sigma_L}{\sigma_D} \approx 10^6$	—	Less than powder-binder layers (Values not given)	Sublinear variation for the layers with low Cu content. Superlinear variation for the layers with high Cu content.
Thomas and Zdanuk (1959) (54)	—	Cl compensated Cu	$\frac{\sigma_L}{\sigma_D} \approx 10^7$	$\lambda_{max} = 625 \text{ nm}$ $= 700 \text{ nm}$ and also inbetween 625 nm - 700 nm (depending upon the mode of excitation, Cu content and thickness of the layer.)	2.5 to 10 millisecc	Linear variation
Kitamura et.al (1960) (56)	—	Cl compensated Cu	$\frac{\sigma_L}{\sigma_D} \approx 10^3$	—	10 millisecc	—
Chokalingam et al (1970) (69)	—	Cl compensated Cu	$\frac{\rho_D}{\rho_L} \approx 10^3$	$\lambda_{max} = 520 \text{ nm}$ $\lambda_{max} = 640 \text{ nm}$	—	—
Wendland (1962) (76)	—	Cl compensated Cu	—	$\lambda_{max} = 620 \text{ nm}$	20 millisecc	Sublinear variation (n = 0.73)

1.4. STUDIES ON THIN FILMS OF PHOTOCONDUCTING CdS

Thin films of photoconducting CdS can be obtained mainly by the following techniques:

- (i) Evaporation in vacuum.
- (ii) Sputtering.
- (iii) Chemical deposition.

The preparative techniques, being well established, will not be discussed in detail.

1.4.1. STUDIES ON VACUUM-EVAPORATED FILMS OF CdS

1.4.1.1. Photoconductivity and related properties

Extensive literature has grown on the preparation and properties of vacuum-evaporated films of photoconducting CdS. Such films are being studied since 1940s and the work upto 1955 has been reviewed by Bube¹ (1960). It begins with the work of Schwartz⁹³ (1948) who suggested several variations in the evaporation procedure including cathode sputtering, low-voltage arc and molecular beam techniques. Afterwards, investigations of Veith^{94,95} (1950, 1955) dealt with techniques for (i) increasing photosensitivity by heating the films in Cd vapour, (ii) decreasing photosensitivity by heating in S vapour, and (iii) affecting sensitivity, spectral response and speed of response by evaporating Cu on the films. Almost in the same period, Aitchison⁹⁶ (1951)

established the vacuum-evaporation conditions to get the photosensitive films of CdS having equivalent properties of single crystals. His results were repeated by Nelson⁹⁷ (1955) who pointed out the influence of the chemical purity of the starting material. Experiments of Bramley⁹⁸ (1955) have indicated the strong dependence of photosensitivity on the details of evaporation technique.

Kuwabara⁹⁹ (1954) has done a systematic study of the properties such as conductivity, photosensitivity and their temperature dependence for the evaporated films of CdS. Wlerick¹⁰⁰ (1954) determined photoconductivity as a function of illumination and discussed the role of traps in the conduction mechanism in CdS thin films.

Variations in performance characteristics such as sensitivity, spectral response and time constants of the CdS photoconductive layers prepared by (a) vacuum-evaporation, (b) sputtering and (c) chemical deposition from various cadmium salts have been investigated and discussed by Lawrance¹⁰¹ (1959).

Shalimova et al.¹⁰² (1961) have deposited thin films of CdS under various ambients such as vacuum, argon, hydrogen sulphide etc. and at different substrate temperatures. They have shown that the magnitude and the spectral distribution of photosensitivity are independent of the film thickness.

They also reported that the spectral distribution is independent of the substrate temperature and the ambient atmosphere.

Kaganovich et al.¹⁰³ (1968) have determined the parameters (like capture cross-sections, energy levels and the concentration) of the two types of recombination centers in the evaporated films of photoconducting CdS.

Woods and his coworkers¹⁰⁴ (1973) have investigated variations in electrical properties with the variations in thickness of the evaporated CdS films.

Photoconducting properties of evaporated films of CdS doped with Cu and Cl have been investigated with respect to (i) the intensity of illumination and (ii) the frequency of applied voltage by Porada et al.¹⁰⁵ (1980). Porada and Schabowska¹⁰⁶ (1980) have performed measurements on the surface and bulk photoconductivities of these films using the gap type and sandwich type of cells. They have found that the spectral response behaviour and the frequency dependence of photoconductivity differ for the surface cells and bulk cells.

Porada and Schabowska¹⁰⁷ (1980) have compared photoconductivity growth and decay time of vacuum-evaporated and screen-printed CdS:Cu:Cl films. In conclusion, they have emphasised the importance of vacuum-evaporation methods in the technology of short-decay time devices.

1.4.1.2. Optical properties

Kuwabara⁹⁹ (1954) studied the optical properties such as absorption edge, spectral sensitivity and their temperature dependence for evaporated CdS films.

Optical properties of evaporated thin films of CdS have been described by Gottesman and Ferguson¹⁰⁸ (1954) and later by Hall and Ferguson¹⁰⁹ (1955). Gottesman and Ferguson¹⁰⁸ have calculated the refractive index and the extinction coefficient of these films from the measurements of the film thickness and the reflectivity as a function of wavelength. Hall and Ferguson¹⁰⁹ have determined the refractive index and the absorption coefficient of these films by using spectrophotometric reflectance and transmittance measurements.

Shalimova et al.¹¹⁰ (1961) have reported the optical absorption in CdS thin films. Bujatti and Marcelja¹¹¹ (1972) have studied optical absorption in thin films of CdS evaporated under controlled conditions. Khawaja and Tomlin¹¹² (1975) have applied their thickness variational technique to determine optical constants (refractive and absorption indices) of the evaporated films of CdS. Wohlge-muth et al.¹¹³ (1976) have compared optical properties such as reflection and transmission of the vacuum-evaporated films of polycrystalline and amorphous CdS. The studies of Khawaja and Tomlin¹¹² and also of

Wohlgemuth et al.¹¹³ along with the recent one made by Cook and Christy¹¹⁴ (1980) on the optical properties of CdS thin films showed how the properties of these films differed from those of the single crystals.

1.4.1.3. Electrical, optical, photoconducting properties and crystal structure

Gilles and Cakenberghe¹¹⁵ (1958) have pointed out the dependence of the photosensitivity on the crystal size and hence on the crystallization conditions in the evaporated layers of CdS. Wendland¹¹⁶ (1962) examined properties such as crystalline structure, electrical resistivity and optical transmission of the evaporated CdS films as a function of the substrate and source temperature. He noticed that slight changes in the evaporation conditions over certain ranges can markedly alter the optical and electrical properties of the films. The effects of several post-evaporation processing treatments on the crystallinity and electronic properties of evaporated CdS films have been investigated by Dresner and Shallcross¹¹⁷ (1963).

X-ray diffraction study of the evaporated CdS films is presented by Behringer and Corrsin¹¹⁸ (1963). Sakai and Okimura¹¹⁹ (1964) have studied photoconductivity in evaporated CdS films and reported good photosensitivity for the hexagonal CdS. Aramu et al.¹²⁰ (1965) have compared rise and decay curves of photoconductivity in cubic and hexagonal CdS thin films.

The effect of a preferred orientation of the crystallites on the electrical properties of evaporated CdS films is established by Dresner and Shallcross¹¹⁷ (1963) and by Sakai and Okimura¹¹⁹ (1964). Afterwards, Vergunas et al.¹²¹ (1966) have verified the effect of substrate temperature on the structural formation of evaporated CdS films. They have deduced a correlation between the value of the electrical conductivity and the degree of crystal orientation in the photosensitive films.

Tyagi and Kumar¹²² (1975) have described the structural and electro-optical properties of the evaporated CdS films which were treated with thiourea to compensate the sulphur deficiency.

1.4.1.4. Hall-effect, Field-effect, etc.

Waxman et al.¹²³ (1965) have carried out Hall-effect and field-effect measurements to determine the surface mobility of electrons in evaporated films of CdS. Field-effect measurements on the evaporated CdS films have been presented also by Leviadi et al.¹²⁴ (1968) and Giraev et al.¹²⁵ (1965).

Table 1.4 presents some important results on the photoconducting properties of vacuum-evaporated films of CdS.

TABLE -1-4
SOME IMPORTANT RESULTS ON THE PHOTOCONDUCTING PROPERTIES OF VACUUM-EVAPORATED
FILMS OF CdS

IMPORTANT METHODS / MODIFICATIONS	CRYSTAL STRUCTURE	ACTIVATION BY	PHOTOSENSITIVITY	SPECTRAL RESPONSE	RESPONSE TIME (RISE / DECAY)	LIGHT-INTENSITY DEPENDENCE OF RESISTANCE / CURRENT
Veith (194, 95) (1950 ; 1955)	—	Cu	$\frac{\rho_D}{\rho_L} \approx 10^4 - 10^6$	$\lambda_{max} = 600 \text{ nm}$	10^{-4} sec	—
Kwabara (1954)	—	—	—	$\lambda_{max} = 520 \text{ nm}$	Few seconds	i) Linear variation for lower intensities ii) Sublinear variation ($n = 0.8$) for higher intensities
Lawrance (1959)	—	—	—	$\lambda_{max} = 400 \text{ nm}$	200 μsec	—
(105-107) Porada et al (1980)	—	Cl compensated Cu	—	$\lambda_{max} = 460 \text{ nm}$	—	—
(122) Tyagi and Kumar (1975)	—	Cl compensated Cu	—	$\lambda_{max} = 517 \text{ nm} = 600 \text{ nm}$	0.6 \pm 0.005 millisecc	Linear variation
				$\lambda_{max} = 420 \text{ nm}$ (without thiourea) $\approx 480 \text{ nm}$ (with thiourea)	—	—
		Ga compensated Cu	—	$\lambda_{max} = 540 \text{ nm}$ (with and without thiourea)	—	—

1.4.2. STUDIES ON SPUTTERED (SPUTTER-DEPOSITED) FILMS OF CdS

In contrast to evaporation techniques, very few references exist in regard to the sputter-deposition of CdS. The first sputter-deposited films of CdS were obtained by Helwig and Konig¹²⁶ (1955) who used Cd targets and Ar-H₂S mixtures. They have observed photoconductivity in the plane of the films with dark to light resistance ratio equal to 10^4 - 10^5 .

Sputter-deposition from bulk CdS targets using ultrapure argon has been described by Lagnado and Lichtensteiger¹²⁷ (1970). But these films displayed very little photoconductivity.

Fraser and Melchior¹²⁸ (1972) have reported photoconductivity through the thickness of the sputter-deposited CdS films. They have studied structural, mechanical, optical and photoconducting properties of such films. High photosensitivity ($\sim 10^5$) and fast response without activation or any other post-deposition treatment are the important characteristics of their films. Leighton¹²⁹ (1973) made exhaustive studies on the electrical properties of photoconducting CdS films which were prepared by d.c. sputter-deposition method without the use of post-deposition heat treatments.

By making use of Auger electron spectroscopy, Takagi et al.¹³⁰ (1978) have investigated the influence of non-stoichiometric surface layer on the photocurrent, dark current and decay time of sputter-deposited CdS films.

Table 1.5 presents some important results on the photoconducting properties of sputter-deposited films of CdS.

1.4.3. STUDIES ON CHEMICALLY DEPOSITED CdS FILMS

Among the established methods of chemical deposition of thin films; the solution-spray, the dip and the rotating substrate technique are well-known for CdS.

1.4.3.1. Chemical spraying/spray-pyrolysis

Chamberlin and Skarman¹³¹ (1966) have developed a method of producing large-area thin films of CdS by the solution-spraying technique. It basically consists of spraying a solution which produces the desired material on a heated substrate. However, this technique ^{has} not been seriously attempted until 1974, when Wu and Bube¹³² have published the photoconducting and related properties of solution-sprayed films of CdS. They have used thermoelectric and photothermoelectric data to analyse the electrical transport properties and have suggested that photoconductivity of solution-sprayed films is caused primarily by an increase in electron mobility.

TABLE - 1.5
SOME IMPORTANT RESULTS ON THE PHOTOCONDUCTING PROPERTIES OF SPUTTER-DEPOSITED
FILMS OF CdS

IMPORTANT METHODS / MODIFICATIONS	CRYSTAL STRUCTURE	ACTIVATION BY	PHOTOSENSITIVITY	SPECTRAL RESPONSE	RESPONSE TIME (RISE / DECAY)	LIGHT-INTENSITY DEPENDENCE OF RESISTANCE / CURRENT
Fraser (128) and Melchior (1972)	Hexagonal	— Cl compensated Cu	$\frac{\rho_D}{\rho_L} \approx 10^5$ $\approx 10^3$	— —	50 μ sec 60 μ sec 50 μ sec 100 μ sec	—
Leighton (129) (1973)	Hexagonal	—	$\frac{\sigma_L}{\sigma_D} \approx 10^5$	—	In μ sec region	Linear variation for lower intensities and square-root variation for higher intensities
Lowrance (101) (1959)	—	Baking in H ₂ S and then in air	$\frac{\sigma_L}{\sigma_D} \approx 10^2$	$\lambda_{max} = 500$ nm	~ 250 μ sec	—

Investigation by Ma and Bube¹³³ (1977) showed that the optical and electrical properties of these films can be strongly influenced by the nature of the substrate and its temperature, cooling rate, spraying rate and post-deposition heat treatments. They have stressed the essentiality of having careful control on the preparation conditions in order to get reproducible and high quality films.

The use of solution-spray technique for commercial production of CdS photocells of high photoconductive gain ($\sim 10^6$) has been described by Gogna et al.¹³⁴ (1977). They have optimised deposition parameters (viz. substrate temperature, solution concentration and spray rate) to yield high photosensitivity. They have also reported results on current-voltage characteristics, spectral response, rise and decay times and the intensity dependence of resistance for such cells.

Gupta and coworkers¹³⁵ (1978) have presented an exhaustive data on the electrical and photoconducting properties such as current-voltage characteristics, temperature dependence of resistance and spectral response of chemically sprayed CdS films having different cadmium to sulphur ionic ratios. They have also reported high photosensitivity ($\sim 10^6$). The effect of cation to anion ratio on the crystallinity and optical properties of such films has been investigated by Gupta and Agnihotri¹³⁶ (1977). They (1978)

have also done structural analysis of solution-sprayed films of CdS when doped with Cu, In and Ga¹³⁷.

Berg et al.¹³⁸ (1978) have studied structure and surface morphology of spray-deposited CdS films. Alaei and Rouhani¹³⁹ (1979) have examined physical and chemical properties of CdS films - sprayed at a relatively low temperature - by using techniques like XRD, AES, SEM and optical absorption measurements.

Recently, Chow et al.¹⁴⁰ (1981) have carried out a fairly comprehensive study of the surface morphology and electronic behaviour of chemically sprayed CdS films.

Table 1.6A presents some important results on the photoconducting properties of chemically spray-deposited films of CdS.

1.4.3.2. Chemical bath deposition technique(s)

Chemical bath deposition technique involves a slow film formation from a solution containing cadmium in a complex form and an organic-sulphur containing reducing agent which react to give CdS in thin film form. Very thin films of CdS have been chemically deposited by Mokrushin and Tkachev¹⁴¹ (1961) from an aqueous solution containing a cadmium salt, thiourea and ammonia. With a slight modification in Mokrushin's method, Nagao and Watanabe¹⁴² (1968) have obtained thick CdS films which were cubic in

TABLE - 1.6 A
SOME IMPORTANT RESULTS ON THE PHOTOCONDUCTING PROPERTIES OF CHEMICALLY SPRAY -
DEPOSITED FILMS OF CdS

IMPORTANT METHODS / MODIFICATIONS	CRYSTAL STRUCTURE	ACTIVATION BY	PHOTOSENSITIVITY	SPECTRAL RESPONSE	RESPONSE TIME (RISE / DECAY)	LIGHT-INTENSITY DEPENDENCE OF RESISTANCE / CURRENT
Wu and Bube (1974)	Hexagonal	—	$\frac{\sigma_L}{\sigma_D} \approx 10^2$	—	—	—
Gogga et al (1977)	Hexagonal	—	$\frac{\rho_D}{\rho_L} \approx 10^6$	$\lambda_{max} = 520 \text{ nm}$	1-3 / 6-8 millisec	Linear variation ($n = 0.7$)
Gupta et al (1978)	Hexagonal	—	$\frac{\sigma_L}{\sigma_D} \approx 10^5 - 10^6$	$\lambda_{max} = 490 \text{ nm}$	—	—

nature. They have reported photosensitivity, photo-conductivity excitation spectra and the dependence of photocurrent on the intensity of illumination for these films.

A new chemical bath deposition technique for the preparation of CdS thin films is described by Pavaskar et al.¹⁴³ (1977). In this method, films were formed on rotating substrates from a bath containing cadmium salt in a complex form. They have studied current-voltage characteristics, decay of photocurrent, spectral response and optical absorption of these films. Studies on field-effect, photo-field effect and photo-Hall effect also constitute important part of their work.

1.4.3.3. Miscellaneous

Sathaye and Sinha¹⁴⁴ (1976) have reported a novel method of chemical deposition to obtain thin films of photoconducting CdS. It consists of the formation of CdS thin films at the interface of a solution (containing a cation) and a gas (containing an anion). They have determined structural, electrical, optical and photoconducting properties of these films. The cubic nature of the films is the special feature of their work.

Croitoru and Jakobson¹⁴⁵ (1979) have reported the chemical printing method to prepare CdS films having good photosensitivity.

Table 1.6B presents some important results on the photoconducting properties of thin films of CdS prepared by chemical bath deposition and other techniques.

1.5. STUDIES ON THICK FILMS OF CdS

Thick film technique is the latest innovation in the microelectronics circuitry. In the thick film technology, specially formulated pastes are screen-printed (silk-screening) onto the suitable substrates and the wet films are subsequently fired at sufficiently high temperature^{146,147}.

There is not much literature on the preparation and properties of CdS thick films. Nicoll and Kazan⁴⁴ (1955) had earlier used the process of silk-screening to prepare powder-binder type layers of CdS. Micheletti and Mark¹⁵⁷ (1968) have demonstrated the consequences of the oxygen chemisorption on the equilibrium conductivity and the transient photoconductivity of sintered CdS layers prepared by silk-screening method. In these investigations, however, silk-screening was used only as a conventional tool/ technique for producing powdered or sintered layers of CdS without paying much attention to the optimisation of

TABLE - 1.6 B

SOME IMPORTANT RESULTS ON THE PHOTOCONDUCTING PROPERTIES OF THIN FILMS OF CdS PREPARED BY CHEMICAL BATH DEPOSITION AND OTHER TECHNIQUES

IMPORTANT METHODS / MODIFICATIONS	CRYSTAL STRUCTURE	ACTIVATION BY	PHOTOSENSITIVITY	SPECTRAL RESPONSE	RESPONSE TIME (RISE / DECAY)	LIGHT-INTENSITY DEPENDENCE OF RESISTANCE / CURRENT
(142) Nagao and Watanabe (1968)	Cubic	Cl compensated Cu	—	(i) $\lambda_{\max} \approx 470$ nm (for lightly doped films) (ii) $\lambda_{\max} \approx 570$ nm (for heavily doped films)	—	Linear variation
(143) Pavaskar et al (1977)	Cubic (90%) + Hexagonal (10%)	—	—	$\lambda_{\max} \approx 520$ nm (at 300° K) ≈ 480 nm (at 93° K)	—	—
(144) Sathaye and Sinha (1976)	Amorphous	I compensated Cu	$\frac{\sigma_L}{\sigma_D} \approx 50$	$\lambda_{\max} \approx 456$ nm (at 300° K) ≈ 460 nm (at 93° K)	—	—
(145) Croitoru and Jakobson (1979)	Cubic	—	—	$\lambda_{\max} \approx 430$ nm	Sudden rise and fast decay	(i) Sublinear variation ($n = 0.43$) for lower intensities (ii) Superlinear variation ($n = 1.33$) for higher intensities
	—	—	$\frac{\rho_D}{\rho_L} \approx 10^4$	$\lambda_{\max} = 490$ nm	1.5×10^{-4} sec (with additional illumination) 2.5×10^{-3} sec (without additional illumination)	—

typical thick film parameters. Recently, Moriwaki⁹² (1975) has filed a patent on the preparation of the screen-printed films of photoconducting CdS. Porada and Schabowska¹⁰⁷ (1980) have obtained thick films of CdS by silk-screening process. They have used a low alkali content glaze as a binder in the form of a fine-grained powder with the addition of solvents like terpinol and amyl alcohol. They have reported higher magnitude of growth and decay times of photoconductivity for such films in comparison to that of vacuum-evaporated films of CdS and explained it on the basis of high trap-density in screen-printed films. But the details of the preparation technique, particularly about the firing process, are not adequately presented by them and some ambiguity, therefore, remains in their interpretation.

1.6. SUMMARY AND CONCLUSIONS

With this background we can summarise as follows:

- (1) For most of the investigations dealing with the basic photoconductivity processes, single crystals of CdS have been preferred because of the relative ease of defining the pertinent variables.
- (2) For most of the commercial applications, sintered layers of CdS have been preferred because of certain

advantages like large-area fabrication, uniformity, high mechanical strength and simplicity.

(3) Thin films have been used for both the purposes - the basic investigations of the phenomenon and the commercial applications.

After having done an extensive literature survey of CdS photoconductors in various forms, we can conclude that:

(1) CdS photoconductors prepared by different techniques generally show different behaviour.

(2) A slight variation of conditions in a method of preparation sometimes changes the properties considerably.

(3) A complete report on the preparation and properties of CdS thick films is not yet available.

In view of this current status, it has been felt necessary to prepare and characterise thick films of photoconducting CdS.

1.7. CHEMISORPTION OF OXYGEN ON CdS

Chemisorption is the formation of adsorbed ions by the exchange of electrons between an adsorbate and an adsorbent. It plays a significant role in the photoconductive processes of II-VI compounds. The presence of adsorbed ions is beneficial and in many cases essential to the appearance of the desired photoconducting properties. On the other hand, it is detrimental as it leads to instabilities and deterioration in the properties of photocells.

From an electronic view point, the adsorbate usually provides at least one electronic state within the band gap of the adsorbent at the surface. This surface state, induced due to chemisorption, strongly influences the electrical properties^{of} the adsorbent directly through new electronic transitions involving this state and also through changes in the surface potential of the adsorbent. The study of the chemisorption of various gases on the photoconducting material is, therefore, indispensable for a better understanding of the photoconductivity mechanism. As a matter of fact, chemisorption of oxygen on CdS has been the subject of an extensive research for the past two decades.

Mark¹⁴⁸⁻¹⁵⁰ (1964-65) has given a thorough report on the kinetics and energetics of the oxygen chemisorption on CdS crystals. He (1964) observed considerable reversible changes in photoconductive gain and response time of certain insulating CdS crystals as a result of the variation in oxygen partial pressure¹⁴⁸. It was further found that the rate of oxygen-adsorption follows the Elcovich rate equation. He (1965) also studied the dependence of photocurrent on the illumination intensity in attempting a closer examination of oxygen chemisorption and subsequently proposed a semi-quantitative model for photoinduced chemisorption¹⁴⁹. The thermal desorption time data and the activation energy data of his work offer a self-consistent substantiation of the earlier model¹⁵⁰. With these results, he has located the energy level associated with the chemisorbed oxygen at 0.91 eV below the conduction band in CdS.

Almost in the same period, Reed and Scott¹⁵¹ (1964) have investigated the effects of various ambient treatments on the surfaces of CdS single crystals by using photoconductivity measurements such as spectral response, decay rate of photoconductivity and thermally stimulated conductivity. From the temperature dependence of these effects, they have postulated the presence of two sets of surface states : (1) a set lying near the Fermi level

(intrinsic states) and (ii) a deeper lying set due to adsorbed oxygen (extrinsic states). They (1965) have also observed the variations in photoconducting properties of CdS single crystals with the changes in the light intensity and the ambient conditions¹⁵². These results were interpreted in terms of surface states and a surface barrier region. Sebenne and Balkanski¹⁵³ (1966) have done a quantitative evaluation of the donor densities near the surface and their distribution in the space-charge region by measuring conductivity changes of low resistivity single crystals of CdS under oxygen adsorption. They have used computerised calculations for this purpose.

Bube¹⁵⁴ (1966) set forth the basic significance of oxygen chemisorption in the photoelectronic behaviour of CdS single crystals. He insists that due to universal presence of oxygen chemisorption effects, every experiment in which the effect of heat, vacuum or photoexcitation are investigated towards understanding the nature of photochemical changes, must be interpreted in the light of the significant effects associated with the simple desorption of oxygen.

By various photoconductivity measurements, Shear et al.¹⁵⁵ (1965) have shown that the sintered layers of CdS are particularly sensitive to oxygen adsorption-desorption processes. According to them, the properties such as instability, non-reproducibility, variability through low

temperature annealing and long term drifts of sintered CdS-CdSe photoconductors may all be attributed to the effects of oxygen adsorption-desorption. In order to clarify the mechanism of the processes involved, Robinson and Bube¹⁵⁶ (1965) have performed photo-Hall measurements on such layers as a function of photoexcitation intensity, temperature and ambient atmosphere. They have observed a reduction in the electron density and the electron mobility of these layers by oxygen adsorption. They further reported that the change in electron mobility due to oxygen adsorption contributes significantly to the total photoconductivity change of such layers. An exhaustive treatment of the ambient sensitive photo-electronic behaviour of the sintered CdS layers is presented by Michelletti and Mark¹⁵⁷ (1968). They have demonstrated and explained the consequences of oxygen chemisorption on the equilibrium conductivity and on the transient photoconductivity of these layers.

Thin films are also sensitive to oxygen chemisorption. Michelletti and Mark¹⁵⁸ (1967) have reported that both the Hall-mobility and the conduction electron concentration of spray-deposited CdS films are reduced by chemisorbed oxygen, the former by a larger factor than the latter. The effects of oxygen adsorption and low-energy ion bombardment on the electrical properties of vacuum-

evaporated CdS films have been investigated by Hughes and Carter¹⁵⁹ (1968). The work of Legre and Martinuzzi¹⁶⁰ (1970) is also concerned with the effect of chemisorbed oxygen on the dark current and on an anomalous photovoltaic effect in evaporated layers of CdS. Thomas et al.¹⁶¹ (1970) have studied the influence of oxygen on the electrical properties of CdS thin films in the ultra high vacuum system where the samples had been prepared by evaporation. They have observed that upon oxygen admission, there is an increase in resistivity due to a decrease of both the free electron density and mobility. The decrease of the free electron density is shown to be associated with a surface trapping in deep oxygen acceptor levels. The mobility decrease is explained to be the result of an interaction between oxygen and the potential barriers at the grain boundaries.

In due course of time, oxygen chemisorption on CdS has been probed by a variety of experimental techniques such as field effect, oxygen partial pressure measurements, low-energy-electron diffraction (LEED), mass-spectrometry, surface photovoltage spectroscopy (SPS), Auger-electron spectroscopy (AES), electron spin resonance (ESR), etc. by many research workers.

Sawamoto¹⁶² (1965) studied the surface states in CdS single crystals by using transverse field effect method under

illumination. He estimated the energy levels of the surface states, the capture cross-section for free electrons and the densities of the surface states. However, a quantitative interpretation of the field-effect data under illumination is difficult because the light affects the occupation of the surface states as well as their interaction time with semiconducting bulk. Many et al.^{163, 164} (1967, 1969) have, therefore, performed field effect measurements in dark - at different ambient air pressures - to provide a deeper insight to the mechanism of oxygen chemisorption on CdS. Their analysis implied that at any given pressure the conduction electrons interact with a fixed density of physically adsorbed oxygen molecules throughout the relaxation process.

Williams¹⁶⁵ (1962) carried out surface photovoltage measurements on CdS single crystals and showed that there is a potential difference of 0.2 to 0.3 eV, at equilibrium, between the bulk and the surface. Haas et al.¹⁶⁶ (1965) have also employed surface photovoltage techniques to study the interactions of oxygen with surfaces of CdS single crystals. Shappir and Many¹⁶⁷ (1969) have presented the detail measurements on the surface photovoltage of CdS single crystals under different conditions of ambient pressure and light intensity. Their results support the conclusions drawn in the earlier work and, in addition,

shed further light on the oxygen adsorption-desorption processes. Many et al.^{163,164,167} (1967-69) have indicated that the combined measurements of the field-effect and the surface photovoltage provide a fairly detailed and self-consistent picture of oxygen adsorption-desorption processes in CdS.

Campbell and Farnsworth¹⁶⁸ (1968) have determined the effect of oxygen exposures on the work function and surface photovoltage of CdS single crystals. They have also made the direct observation of photoadsorption and desorption of oxygen by using the LEED technique.

Weber¹⁶⁹ (1968) developed a method to test the properties of space-charge layers at the surface of CdS. For this purpose, he assumed the direct capture of electrons and holes by the neutral and negatively charged oxygen as the rate limiting steps for the chemisorption and desorption processes respectively. Theoretical calculations based on this model exhibited qualitative agreement with the experimental results. In an excellent article, Weber¹⁷⁰ (1970) reported the room temperature chemisorption mechanism of oxygen at CdS surfaces. He established kinetics of photoconductivity during chemisorption at various oxygen pressures. His results suggest that (i) oxygen does not dissociate into atoms upon physical adsorption, (ii) chemisorption is a two-step process involving a precursor state,

(iii) photodesorption is also a two-step process consisting of a normal photodesorption followed by a thermally activated step and (iv) oxygen in the reversible low temperature chemisorption participates as O_2^- .

Schubert and Böer¹⁷¹ (1971) have detected the thermally stimulated desorption of oxygen in ultra high vacuum utilising Joule's heating of CdS crystal and monitoring the desorption with a mass-spectrometer.

There are numerous experiments which provide indirect evidence for the oxygen chemisorption through changes in electronic properties¹⁴⁸⁻¹⁷¹ as investigated by many authors in various ways. The first direct measurement of the adsorbed ambient species is presented by Baidyaroy et al.¹⁷² (1971). They have done the mass-spectrometric analysis of the ambient-surrounding the powdered samples of CdS - to elucidate the mechanism underlying photodesorption. From the illumination intensity and the wavelength dependence of desorption, they have concluded that the neutralization of the negative surface charge by photoexcited holes is the dominant photodesorption mechanism in CdS. In a separate study, Baidyaroy et al.¹⁷³ (1972) have found that atomically ordered surfaces of CdS single crystals are relatively insensitive to oxygen chemisorption. An analytical and experimental investigation of the effects of oxygen chemisorption on the electrical conductivity of CdS thin films is also reported by Baidyaroy and Mark¹⁷⁴ (1972).

Weitzel and Monteith¹⁷⁵ (1973) have studied the effect of oxygen chemisorption on the photocurrent flowing parallel to the surface in the sputtered thin films of CdS. They have used a model based on Wolkensteins theory of "weak" and "strong" chemisorption to derive an expression for the variation in the photocurrent as a function of time and oxygen partial pressures.

The chemisorption of oxygen on n-type CdS is critically reviewed by Many¹⁷⁶ (1974). Peshev¹⁷⁷ (1978) reinterpreted the available experimental data on oxygen-adsorption in case of CdS to avoid the necessity of dealing with low values of the capture cross-section for electrons of neutrally adsorbed oxygen. In another article, he (1978) has discussed the coexistence of physical and chemical adsorption on semiconductors by considering the example of $O_2/n\text{-CdS}$ system¹⁷⁸.

A thorough study of the mechanism and kinetics of oxygen chemisorption on thin evaporated films of CdS is done by Bhide et al.¹⁷⁹ (1977).

The entire range of the experimental observations of the well-known phenomenon of oxygen chemisorption on CdS suggests that the existence and distribution of surface states are strongly influenced by the chemical composition of the CdS surface. In most of the experiments, however, the chemical composition of the CdS surface was never monitored

until Brillson^{180,181} (1975) who carried out the surface photovoltage and Auger electron spectroscopic (SPS and AES) studies of (11 $\bar{2}$ 0) CdS surface. In his work, modifications of the electronic structure of (11 $\bar{2}$ 0) CdS surfaces (as determined by SPS) are shown to be associated with changes in their atomic compositions (as monitored by AES). He employed AES and LEED techniques to separate the effects of chemical contamination, non-stoichiometry and lattice disorder on the surface electronic properties of air-exposed, ion-bombarded, annealed, cleaved and adsorbate-covered surfaces.

Lagowski et al.¹⁸² (1979) have noted that electron beam irradiation in AES causes a significant decrease in surface concentration of oxygen chemisorbed on CdS. They have indicated that this electron beam induced desorption exhibits a logarithmic dependence on time and can be explained on the basis of the interaction of excess holes, generated by electron beam, with chemisorbed oxygen species. He and his coworkers¹⁸³ (1980) have also reported XPS and AES studies of surface compositional changes involved in electron stimulated adsorption which occurs on clean CdS surfaces under UHV conditions. It has been shown that the electron stimulated adsorption on CdS occurs due to a local activation of the surface rather than the dissociation of previously adsorbed species assumed in earlier studies.

Sootha et al.¹⁸⁴ (1980) have studied the ESR absorption in CdS powder after grinding single crystals at room temperature in air. ESR studies have also been made after heating these powders in different atmospheres. Different types of oxygen radicals have been detected in these powders under different experimental conditions.

REFERENCES

1. R. H. Bube;
"Photoconductivity of Solids", John Wiley and Son
Inc., New York (1960).
2. R. Frerichs;
Phy. Rev., 72, p. 594 (1947).
3. D. C. Reynolds et al.;
J. Appl. Phys., 23, p. 932 (1952).
J. Chem. Phys., 29, p. 1375 (1958).
4. a: R. H. Bube and S. M. Thomsen;
J. Chem. Phys., 23, p. 15 (1955).
b: R. H. Bube;
J. Chem. Phys., 23, p. 18 (1955).
5. R. H. Bube;
Phy. Rev., 99, p. 1105 (1955).
6. R. H. Bube;
J. Appl. Phys., 27, p. 1237 (1956).
7. D. C. Reynolds, S. J. Czyzak, R. C. Allen and
C. C. Reynolds;
J. Opt. Soc. Am., 45, p. 136 (1955).
8. J. Woods;
J. Electronics and Control, 3, p. 225 (1957).
9. J. Woods;
J. Electronics and Control, 5, p. 417 (1958).
10. S. Kitamura;
J. Phys. Soc. Jap., 16, p. 2430 (1961).
11. R. H. Bube and L. A. Barton;
RCA Review, 20, p. 564, (1959).
12. R. H. Bube;
J. Chem. Phys., 30, p. 266 (1959).
13. R. H. Bube;
J. Appl. Phys., 31, p. 1301 (1960).
14. J. A. Beun, R. Nitsche and H. U. Bolsterli,
Physica, 28, p. 184 (1962).

15. R. H. Bube;
J. Appl. Phys., 32, p. 1621 (1961).
16. R. H. Bube, E. L. Lind and A. B. Dreeben;
Phy. Rev., 128, p. 532 (1962).
17. R. H. Bube and B. Young;
J. Appl. Phys., 35, p. 462 (1964).
18. S. O. Hemila and R. H. Bube;
J. Appl. Phys., 38, p. 5258 (1967).
19. F. Cardon and R. H. Bube;
J. Appl. Phys., 35, p. 3344 (1964).
20. R. Crandall;
J. Appl. Phys., 38, p. 5425 (1967).
21. D. Dutton;
Phy. Rev., 112, p. 785 (1958).
22. M. Balkanski and R. D. Waldron;
Phy. Rev., 112, p. 123 (1958).
23. A. P. Trofimenko, G. A. Fedorus and A. K. Razmadze;
Sov. Phys. Sol. State, 2, p. 1033 (1960).
24. R. H. Bube;
J. Appl. Phys., 34, p. 3309 (1963).
25. K. H. Nicholas and J. Woods;
Brit. J. Appl. Phys., 15, p. 783 (1964).
26. J. Woods and K. H. Nicholas;
Brit. J. Appl. Phys., 15, p. 1361 (1964).
27. E. Tscholl;
Philips Res. Repts. (Suppl.) No. 6, p.1 (1968).
28. H. B. Im, H. E. Matthews and R. H. Bube;
J. Appl. Phys., 41, p. 2581 (1970).
29. R. H. Bube and H. E. Mac-Donald;
Phy. Rev., 121, p. 473 (1961).
30. V. Birkholz, W. Heering and F. Stockmann,
Phys. Stat. Sol., 27, K-69, (1968).
31. F. U. Weichman, R. K. Lomnes and S. Zukotynski;
Phys. Stat. Sol., 25, p. 583 (1968).

32. H. B. Kwok and R. H. Bube;
J. Appl. Phys., 44, p. 138 (1973).
33. V. A. Tyagai, V. N. Bondarenko and O. V. Snitko;
Sov. Phys. Solid State, 8, p. 2492 (1967).
34. K. Sawamoto;
Jap. J. Appl. Phys., 4, p. 173 (1965).
35. E. H. Weber;
Phys. Stat. Sol., 36, p. 175 (1969).
36. L. Clark and J. Woods;
Brit. J. Appl. Phys., 17, p. 319 (1966).
37. L. Clark and J. Woods;
J. Cryst. Growth, 3, p. 126 (1968).
38. S. G. Patil;
J. Phys. D, 5, p. 1692 (1972).
39. M. A. Carter and J. Woods;
J. Phys. D, 6, p. 337 (1973).
40. M. A. Salehi Manshadi and J. Woods;
Phys. Stat. Sol. (a), 40, K43 (1977).
41. B. T. Kolomiets;
Doklady Akad. Nauk SSSR, 83, p. 561 (1952).
42. S. Rothschild;
Brit. Pat., 566, 278 (1943).
43. S. M. Thomsen and R. H. Bube;
Rev. Sci. Instr., 26, p. 664 (1955).
44. F. H. Nicoll and B. Kazan;
J. Opt. Soc. Am., 45, p. 647 (1955).
45. P. W. Kruse;
Bull. Am. Phy. Soc., 1, p. 205 (1956).
46. S. Rothschild;
J. Opt. Soc. Am., 46, p. 662 (1956).
47. R. H. Bube and A. B. Dreeben;
Phy. Rev., 115, p. 1578 (1959).
48. R. H. Bube;
J. Appl. Phys., 31, p. 2239 (1960).

49. E. L. Lind and R. H. Bube;
J. Chem. Phys., 37, p. 2499 (1962).
50. M. Smith and A. J. Behringer;
J. Appl. Phys., 36, p. 3475 (1965).
51. T. Miyake;
Jap. J. Appl. Phys., 10, p. 427 (1971).
52. S. C. K. Misra, S. K. Agarwal, H. K. Sehgal and
R. C. Tyagi,
Ind. J. Pure Appl. Phys., 9, p. 369 (1971).
53. A. Angelov and M. Milyashev;
God. Sofii. Univ., Fiz. Fak [1970-1972], p.219.
C. A. 83:20440k.
54. M. J. B. Thomas and E. J. Zdanuk;
J. Electrochem. Soc., 106, p. 964 (1959).
55. R.R. Billups, W. L. Gardner and M. D. Zimmerman;
U. S. Dept. Com. Office Tech. Serv.,
PB Report 147, O10 (1959).
C.A. 56:15038i.
56. S. Kitamura, T. Kubo, T. Yamashita and Y. Amano;
Oyo Butsuri (Jap.), 29, p. 636 (1960).
C.A. 55:2289b.
57. S. Kitamura;
J. Phys. Soc. Japan, 15, p. 1697 and 2343 (1960).
58. S. Kitamura, T. Kubo, T. Yamashita and Y. Amano;
Natl. Tech. Report; 6, p. 11 (1960).
C.A. 54:19184f.
59. M. Zollei;
Acta Phys. Chem. Szeged (Hungari),
12, p. 21 (1966).
60. A. Baczynski and M. Czajkowski;
Acta Phys. Polon., 22, p. 151 (1962).
C.A. 59:4647c.
61. E. M. Denga, V. I. Bugrienko and A. L. Rvachev;
Ukr. Fiz. Zh., 11, p. 507 (1966).
C. A. 65:6479a.
62. G. Goldbach,
Expt. Tech. Phys. 16, p. 108 (1968),
C.A. 71:106643t.

63. T. Yamashita, M. Yoshida, T. Ohtani, T. Kotake, N. Nada and S. Kitamura;
Natl. Tech. Rep.(Japan), 15, p. 145 (1969).
C. A. 75:12039f.
64. G. I. Glukhova, Goldenveizer and I. M. Davydkin, I. N. Pavlova and K. B. Fedotova;
Opt. Mekh. Prom., 39, p. 45 (1972).
C.A. 77:170187y.
65. A. M. Pavelets, G. A. Fedorus and M. K. Sheinkman;
Poluprov. Tekh. Mikroelektron, 12, p. 71 (1973),
C.A. 79:156670p.
66. A. M. Pavelets, I. B. Ermolovich, G. A. Fedorus and M. K. Sheinkman;
Ukr. Fiz. Zh., 19, p. 406 (1974).
C.A. 81:7974b.
67. Q. T. Islam, S. Ahmed, M. D. Mia and M. A. Subhan;
J. Bangladesh Acad. Sci., 1, p. 37 (1977).
C.A. 87:192612s.
68. M. Zollei;
Acta Phys. Chem., 17, p. 29 (1971).
C.A. 76:2000ly.
69. M. Chockalingam, K. N. Rao, N. Rangarajan and C.V. Suryanarayana;
Ind. J. Pure Appl. Phys., 8, p. 744 (1970).
70. J. Jakimavicius, A. Alisauskas, A. Sirvaitis;
Liet. Fiz. Rinkinys, 11, p. 493 (1971),
C.A. 76:38400n.
71. J. Jakimavicius, A. Alisauskas, A. K. Duoba and A. Sirvaitis;
Liet. Fiz. Rinkinys, 14, p. 1019 (1974).
C.A. 83:89570v.
72. J. Jakimavicius, A. Saidkhanov, A. Alisauskas and A. Sirvaitis;
Liet. Fiz. Rinkinys, 16, p. 453 (1976).
C.A. 85:170474e.
73. J. Jakimavicius, A. Alisauskas and A. Sirvaitis;
Liet. Fiz. Rinkinys, 18, p. 211 (1978).
C.A. 89:15513f.
74. S. Yoshimatsu, C. Kanzaki, S. Ibuki and N. Murai;
J. Phys. Soc. Japan, 10, p. 493 (1955).

75. J. Bissinger;
Prace Przemyslowego Inst. Elektron., 3, p.119 (1962).
C.A. 59:13437a.
76. P. H. Wendland;
Rev. Sci. Instru., 33, p. 337 (1962).
77. Ya. V. Khiie and Yu. A. Varvas,
Tr. Tallin. Politekh. Inst., Ser. A, No. 217,
p. 137 (1965). C.A. 64:16793b.
78. J. Varvas et al;
Tr. Tallin. Politekh. Inst., Ser. A, No. 262,
p. 49 and 59 (1968). C.A. 71:16889y and 71:16888x.
79. R. E. Ott;
Tr. Tallin. Politekh. Inst., Ser. A, No. 263, p.93
(1968). C.A. 70:119340w.
80. I. Bunget, M.R. Leonovici, V. Mihai, M. Popescu,
H. Alexandru, M. Steflea and A. Ioanid;
Rev. Roum. Phys., 24, p. 57 (1979).
81. A. Z. Czipott and A. L. Floyd;
U.S. 2,884,507 (28 April 1949).
C.A. 53:13801a.
82. S. M. Thomsen;
U. S. 2,765,385 (2 Oct. 1956).
C.A. 51:1740h.
83. J. G. van Santen and H. J. M. Joormann;
Neth. 106,419 (15 Nov. 1963).
C.A. 60:15298f.
84. Rank Xerox Ltd;
Brit. 1,079,065 (Cl H Olc) (9 Aug. 1967).
C.A. 68:109199b.
85. J. G. van Santen, H. Esvelt and H. J. M. Joormann;
U. S. 3,284,235 (Cl. 117-201) (8 Nov. 1966).
C.A. 66:15060F
86. C. V. Suryanarayana, N. Rangarajan, K. N. Rao and
M. J. Mangalam,
Indian 115,347 (11 Jul. 1970).
C.A. 76:9827b.
87. T. Yamashita, T. Ohtani, M. Yoshida, S. Kitamura
and H. Murakami;
Brit. 1,177,462 (Cl. H Olc) (14 Jan. 1970).
C.A. 72:72372g.

88. T. Yamashita, T. Ohtani, M. Yoshida, S. Kitamura and H. Murakami;
Ger. 1,764,809 (Cl. H01c) (25 March 1971).
C.A. 75:12285h.
89. H. A. Hodes, J. Sobieski and M.C. Zerner;
U.S. 3,598,643 [Cl.117-201; G 03g (C9d, H 011)]
(10 Aug. 1971), C. A. 75:146254f.
90. H. Nakatsui;
Japan Kokai, 73,52,187 [Cl 99(5) J42] (21 July 1973).
C.A. 79:109616n
91. G. A. Marlor and J. B. Mooney;
U.S. 3,754,985 [Cl.117/201;C 23c] (28 Aug. 1973).
C.A. 79:130608w.
92. Y. Moriwaki;
Japan Kokai 75,51,286 (Cl.H 01) (8 May 1975).
C.A. 83:156842a.
93. E. Schwarz;
Nature, 162, p. 614 (1948).
Proc. Phys. Soc., 62A, p. 530 (1949).
94. W. Veith;
Compt. Rend., 230, p. 947 (1950).
95. W. Veith;
Z. Angew Physik. 7, p. 1 (1955).
96. R. E. Aitchison;
Nature, 167, p. 812 (1951).
97. R. C. Nelson;
J. Opt. Soc. Am., 45, p. 774 (1955).
98. A. Bramley;
Phy. Rev., 98, p. 246 (1955).
99. G. Kuwabara;
J. Phys. Soc. Jap., 9, p. 97 (1954).
100. G. Wlerick;
Compt. Rend., 239, p. 257 (1954).
101. R. Lawrance;
Brit. J. Appl. Phys., 10, p. 298 (1959).
102. K. V. Shalimova, T. S. Travina and R. R. Rezvyi;
Sov. Phys. Docklady, 6, p. 404 (1961).

103. E. B. Kaganovich, A. V. Lyubchenko and S. V. Svechnikov;
Fiz. Tekn. Poluprov., 2, p. 1392 (1968).
P.A. 72: 10068
104. a: J.I.B. Wilson and J. Woods;
J. Phys. Chem. Solids, 34, p. 171 (1973).
b: R. W. Buckley and J. Woods;
J. Phys. D, 6, p. 1084 (1973).
105. Z. Porada, E. Schabowska and J. Turczak;
Thin Sol. Films, 65, p. 137 (1980).
106. Z. Porada and E. Schabowska;
Thin Sol. Films, 69, p. 165 (1980).
107. Z. Porada and E. Schabowska;
Thin Sol. Films, 66, 455 (1980).
108. J. Gottesman and W. F. C. Ferguson;
J. Opt. Soc. Am., 44, p. 368 (1954).
109. J. F. Hall and W. F. C. Ferguson;
J. Opt. Soc. Am., 45, p. 714 (1955).
110. K. V. Shalimova, T. S. Travina and L. L. Golik;
Sov. Phys. Doklady, 6, p. 396 (1961).
111. M. Bujatti and F. Marcelja;
Thin Sol. Films, 11, p. 249 (1972).
112. E. Khawaja and S. G. Tomlin;
J. Phys. D, 8, p. 581 (1975).
113. J. H. Wohlgenuth, D. E. Brodie and P. C. Eastman,
Can. J. Phys., 54, p. 785 (1976).
114. R. K. Cook and R. W. Christy;
J. Appl. Phys., 51, p. 668 (1980).
115. J. M. Gilles and J. van Cakenberghe;
Nature, 182, p. 862 (1958).
116. P. H. Wendland;
J. Opt. Soc. Am., 52, p. 581 (1962).
117. J. Dresner and F. V. Shallcross;
J. Appl. Phys., 34, p. 2390 (1963).

118. A. J. Behringer and L. Corrsin;
J. Electrochem.Soc., 110, p. 1083 (1963).
119. J. Sakai and H. Okimura;
Jap. J. Appl. Phys., 3, p. 144 (1964).
120. F. Aramu, P. Manca and C. Muntoni;
Phys. Lett., 19, p. 638 (1965).
121. F. I. Vergunas, T. A. Mingazin, E. M. Smirnova
and S. Abdiev;
Sov. Phys. Crystallography, 11, p. 420 (1966).
122. R. C. Tyagi and R. Kumar;
Thin Sol. Films, 25, S-21 (1975).
123. A. Waxman, V. E. Henrich, F. V. Shallcross,
H. Borkan and P. K. Weimer;
J. Appl. Phys., 36, p. 168 (1965).
124. A. Leviadi, B. Melchiorri, F. Melchiorri
and G. Moreno;
Nuovo-Cimeta-B (Italy), 56b, p. 239 (1968).
125. M. A. Giraev, I. A. Karpovich and B.N. Zvonkov;
Sov. Phys. Solid State, 6, p. 1738 (1965).
126. G. Helwig and M. Konig;
Z. Angew Physik, 7, p. 323 (1955).
127. I. Lagnado and M. Lichtensteiger;
J. Val Sci. Technol., 7, p. 318 (1970).
128. D.B. Fraser and H. Melchior;
J. Appl. Phys., 43, p. 3120 (1972).
129. W. H. Leighton;
J. Appl. Phys., 44, p. 5011, (1973).
130. N. Takagi, H. Yamada, M. Tanaka and K. Tasai;
Jap. J. Appl. Phys., 17, p. 1155 (1978).
131. R. R. Chamberlin and J. S. Skarman;
J. Electrochem. Soc., 113, p. 86 (1966).
132. C. H. Wu and R. H. Bube;
J. Appl. Phys., 45, p. 648 (1974).
133. Y. Y. Ma and R. H. Bube;
J. Electrochem. Soc., 124, p. 1430 (1977).

134. P. K. Gogna, L. K. Malhotra and K. L. Chopra;
Res. and Ind., 22, p. 74 (1977).
135. B. K. Gupta, O. P. Agnihotri and A. Raza;
Thin Sol. Films, 48, p. 153 (1978).
136. B. K. Gupta and O. P. Agnihotri;
Sol. State Commun., 23, p. 295 (1977).
137. B. K. Gupta and O. P. Agnihotri;
Phil. Mag. B, 37, p. 631 (1978).
138. R. S. Berg, R.D. Nasby and C. Lampkin;
J. Vac. Sci. Technol., 15, p. 359 (1978).
139. M. S. Alaei and M. D. Rouhani;
J. Electron. Mat., 8, p. 289 (1979).
140. L. W. Chow, Y. C. Lee and H. L. Kwok;
Thin Sol. Films, 81, p. 307 (1981).
141. S. G. Mokrushin and Yu. D. Tkachev;
Kolloidn. Zh., 23, p. 438 (1961).
142. M. Nagao and S. Watanabe;
Jap. J. Appl. Phys., 7, p. 684 (1968).
143. N. R. Pavaskar, C.A. Menezes and A. P. B. Sinha;
J. Electrochem. Soc., 124, p. 743 (1977).
144. S. D. Sathaye and A. P. B. Sinha;
Thin Sol. Films, 37, p. 15 (1976).
145. N. Croitoru and S. Jakobson;
Thin Sol. Films, 56, L5, (1979).
146. C. A. Harper;
"Handbook of Thick Film Hybrid Microelectronics",
McGraw-Hill Book Company, New York (1974).
147. M. L. Topfer;
"Thick-Film Microelectronics",
Van Nostrand Reinhold Company, New York (1971).
148. P. Mark;
J. Phys. Chem. Solids, 25, p. 911 (1964).
149. P. Mark;
J. Phys. Chem. Solids, 26, p. 959 (1965).

150. P. Mark;
J. Phys. Chem. Solids, 26, p. 1767 (1965).
151. C. E. Reed and C. G. Scott;
Brit. J. Appl. Phys., 15, p. 1045 (1964).
152. C. E. Reed and C. G. Scott;
Brit. J. Appl. Phys., 16, p. 471 (1965).
153. C. Sebenne and M. Balkanski;
Surf. Sci., 5, p. 410 and 434 (1966).
154. R. H. Bube;
J. Electrochem. Soc., 113, p. 793 (1966).
155. H. Shear, E.A. Hilton and R. H. Bube;
J. Electrochem. Soc., 112, p. 997 (1965).
156. A. L. Robinson and R. H. Bube;
J. Electrochem. Soc., 112, p. 1002 (1965).
157. F. B. Micheletti and P. Mark;
J. Appl. Phys., 39, p. 5274 (1968).
158. F. B. Micheletti and P. Mark;
Appl. Phys. Letters, 10, p. 136 (1967).
159. D. M. Hughes and G. Carter;
Phys. Stat. Sol., 25, p. 449 (1968).
160. J. P. Legre and S. Martinuzzi;
Phys. Stat. Sol. (a), 1, p. 689 (1970).
161. P. A. Thomas, C. Sebenne and M. Balkanski;
Rev. Phys. Appl., 5, p. 683 (1970).
162. K. Sawamoto;
Jap. J. Appl. Phys., 4, p. 173 (1965).
163. A. Many and A. Katzir;
Surf. Sci., 6, p. 279 (1967).
164. A. Many, J. Shappir and U. Shaked;
Surf. Sci., 14, p. 156 (1969).
165. R.W. Williams;
J. Phys. Chem., Solids, 23, p. 1057 (1962).
166. K. J. Haas, D.C. Fox and M. J. Katz;
J. Phys. Chem. Solids, 26, p. 1779 (1965).
167. J. Shappir and A. Many;
Surf. Sci., 14, p. 169 (1969).

168. B. D. Campbell and H. E. Farnsworth;
Surf. Sci., 10, p. 197 (1968).
169. E. H. Weber;
Phys. Stat. Sol., 28, p. 649 (1968).
170. E. H. Weber;
Phys. Stat. Sol. (a), 1, p. 665 (1970).
171. R. Schubert and K. W. Boer;
J. Phys. Chem. Solids, 32, p. 77 (1971).
172. S. Baidyaroy, W. R. Bottoms and F. Mark;
Surf. Sci., 28, p. 517 (1971).
173. S. Baidyaroy, W. R. Bottoms and F. Mark;
Surf. Sci., 29, p. 165 (1972).
174. S. Baidyaroy and P. Mark;
Surf. Sci., 30, p. 53 (1972).
175. C. E. Weitzel and L. K. Monteith;
Surf. Sci., 40, p. 555 (1973).
176. A. Many;
Crit. Revs. on Solid State Sci., 4, p. 515 (1974).
177. O. Peshev;
Rev. Roum. Chim., 23, p. 1003 (1978).
178. O. Peshev;
Z. Phys. Chem., 113, p. 91 (1978).
179. V.G. Bhide, S. Jatar and A.C. Rastogi;
Pramana, 9, p. 399 (1977).
180. L. J. Brillson;
J. Vac. Sci. Technol., 12, p. 249 (1975).
181. L. J. Brillson;
Surf. Sci., 51, p. 45 (1975).
182. J. Lagowski, M. Lichtensteiger and P. M. Williams;
Surf. Sci., 84, L 223, (1979).
183. M. Lichtensteiger, C. Webb and J. Lagowski;
Surf. Sci., 97, L 375 (1980).
184. G. D. Sootha, G. K. Padam and S. K. Gupta;
Phys. Stat. Sol. (a), 58, p. 615 (1980).

CHAPTER – 2
EXPERIMENTAL

2.1. PREPARATION

General procedure for the preparation of thick films of photoconducting CdS can be described in four steps:

(1) Activation or doping of pure CdS

Highly pure CdS made by Koch-Light and Co., U.K., was used as the starting material for this work. For activation, the mixtures tabulated below (Table 2.1) were prepared.

TABLE 2.1
MIXTURES FOR ACTIVATION

<u>Sr.No.</u>	<u>Material</u>	<u>Function</u>	<u>Quality</u>	<u>Quantity</u> <u>parts by wt.</u>
1.	CdS	Basic photo-conductor matrix	99.999% pure	100
2.	$\text{CdCl}_2 \cdot 2.5\text{H}_2\text{O}$	Flux	A.R. grade	10
3.	$\text{CuCl}_2 \cdot 2\text{H}_2\text{O}$	Activator	A.R. grade	0.05-1

Mixtures containing the above mentioned components were ballmilled in acetone for two hours and subjected to initial bulk-firing at 500°C for two hours in air. This initial firing achieves the preliminary incorporation of activator components into the CdS matrix. The resulting mass in the form of lumps was thoroughly powdered by using double distilled acetone to ensure a sufficiently fine particle size. The activated powders thus obtained (the colour of which varies from yellow to blackish-brown

depending upon the activator concentration) were kept ready for the paste formulations.

(2) Formulation of the paste

The paste was prepared by mixing the activated CdS:Cu:Cl powder with a solution of ethyl cellulose in a mixture of solvents consisting of butyl cellosolve, butyl carbitol acetate and terpineol in the proportion 30:30:40. The mixing was carried out in a clean agate mortar pestle.

Fluidity of the paste depends upon the extent of organic part which goes in its formulation, i.e., on solid to liquid ratio. Pastes must exhibit a certain degree of yield such that after the flow occurs under squeegee pressure, it should stiffen and remain in position. In other words, it should exhibit thixotropic properties. Too much flow gives rise to smearing and poor line-definition of the prints; too little flow results in the retention of screen-pattern on the prints. Several formulations with different ratios were tried, the results of which are presented in Table 2.2.

TABLE 2.2

EFFECT OF DIFFERENT RATIOS FOR PASTE
FORMULATION ON SCREEN-PRINTING

Sr.No.	Ratio of activated CdS powder to the solution of a binder in a solvent mixture	Effect on screen-printing
1.	80:20	1) Very thick paste. 2) Screen-clogging. 3) Poor adhesion to the substrates.
2.	75:25	1) Paint-like in consistency. 2) Easy to print. 3) Good line definition. 4) Good adhesion to the substrate.
3.	70:30	1) Very fluid paste. 2) Poor line definition. 3) Smearing of the substrates with the paste.

In the light of these observations, the ratio was kept at 75:25 in formulating the pastes. A typical 75:25 formulation is given in Table 2.3.

TABLE 2.3

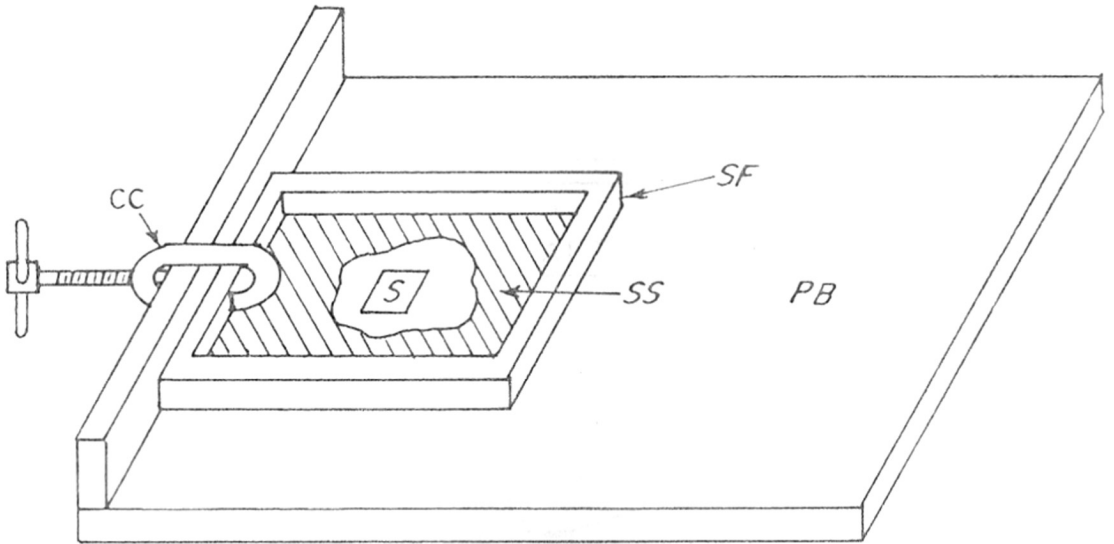
A TYPICAL 75:25 FORMULATION OF THE PASTE

Sr. No.	Material	Function	Quantity
1.	CdS:Cu:Cl (activated)	Basic paste ingredient	1 gm
2.	Ethyl cellulose	Filler i.e. temporary binder	0.0266 gm
3.	A mixture of solvents (butyl cellosolve + butyl carbitol acetate + terpineol)	Vehicle	0.32 ml

(3) Screen-printing

Silk-bolting cloth (160 mesh), with appropriate apertures blocked to form the desired pattern, mounted on a rigid frame was used as the screen (Fig. 2.1). Screen-printing was accomplished by a flexible squeegee stroking the paste across the screen surface onto ceramic alumina substrates (Fig. 2.2). The substrates (M/s. Electronic Slicing and Dicing Inc., USA) had the following specifications:

Material	: 96% Al_2O_3 as fired
Length and width tolerance	: $\pm 1\%$ NLT ± 0.005 in
Thickness tolerance:	$\pm 12\%$ NLT ± 0.0015 in
Camber	: 0.004 in/in



CC — 'C' CLAMP
S — SUBSTRATE
SF — SCREEN FRAME
SS — SCREEN STENCIL
PB — PRINTING BASE

FIG. 2.1 SCREEN-PRINTING BOARD

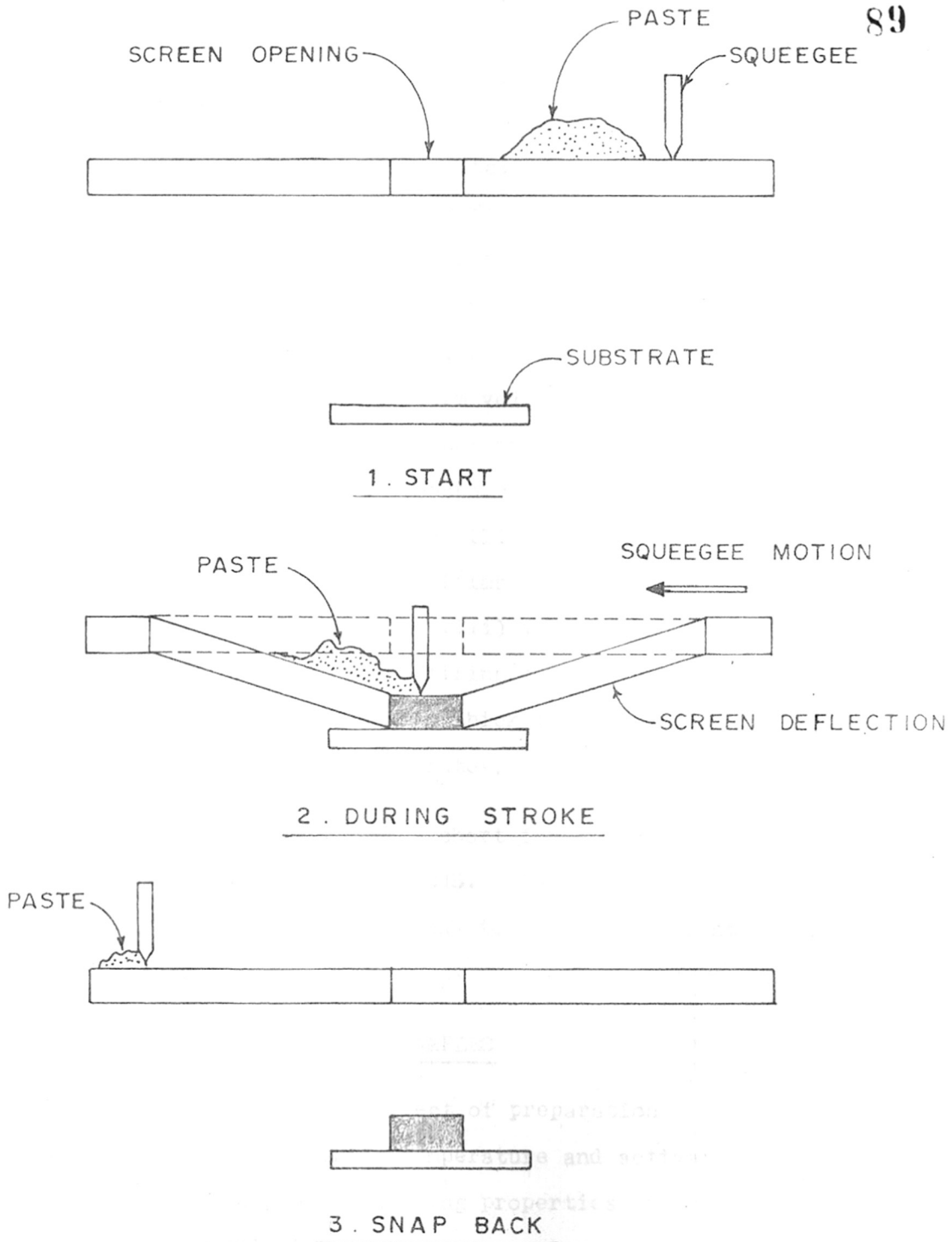


FIG. 2-2 SCREEN - PRINTING CYCLE

(4) Drying and firing

The 'wet' or 'green' films obtained by the screen-printing process were dried at 100°C for 20 minutes, preferably under IR radiations. IR radiations penetrate the films and permit drying without entrapping the vehicle due to crust formation over the surface which would subsequently blister during firing to form voids. Dry films were fired afterwards at the desired temperature for 10 minutes in nearly oxygen-free nitrogen atmosphere. Firing was carried out in a specially designed silica container with the provisions: (i) to hold sample films, (ii) to maintain dynamic atmosphere of nitrogen and (iii) to position thermocouple junction for recording the firing temperature. This high temperature firing matures the thick film elements and bonds them integrally to the substrates.

Fig. 2.3 presents the flow chart for the preparation of thick films of photoconducting CdS. Thick films of CdS, prepared in this way, were found to be well-adherent to the substrates.

2.2. PREPARATION OF THE TEST SAMPLES

For investigating the effect of preparation conditions, particularly firing temperature and activator concentration, on the photoconducting properties of these films; a stepwise variation of these parameters was

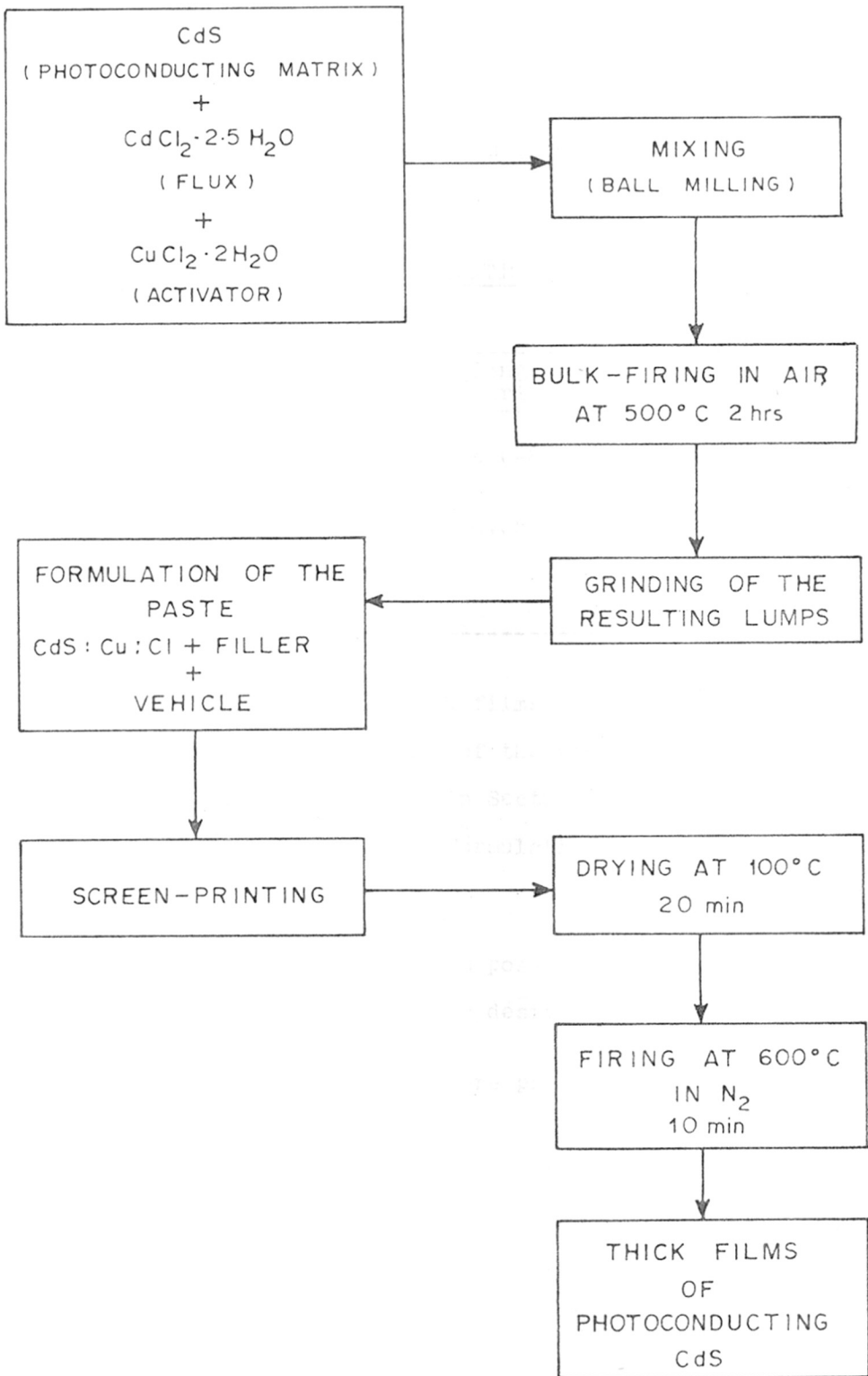


FIG. 2.3 FLOW CHART FOR THE PREPARATION OF THE THICK FILMS OF PHOTOCONDUCTING CdS

conducted at each part of the process (see Table 2.4).

TABLE 2.4

VARIATION IN THE PREPARATION PARAMETERS

Sr. No.	Variable parameter	Range of variation	Fixed parameter
1.	Firing temperature($^{\circ}\text{C}$)	400-800	Cu concentration.
2.	Concentration of Cu added as CuCl_2 (% by wt of CdS)	0.05-1	Firing temperature.

In addition to this, thick films of pure i.e. undoped CdS were also processed. Details of the preparation were, by and large, the same as described in Section 2.1. except some minor modifications of the paste-formulation composition whenever needed.

Using this technique, it is possible to prepare photoconducting films of CdS of any desirable dimensions.

Films of particular size were preferably used for specific investigations (see Table 2.5). Criteria for this was based on the sample holder and instrumental prerequisites.

TABLE 2.5
SIZE OF THE THICK FILMS FOR DIFFERENT
INVESTIGATIONS

Sr. No.	Particulars	Size cm x cm
1.	Physical properties	Surface morphology 0.8 x 0.4
		Structure 2.5 x 2.5
2.	Electrical and photoconducting properties	0.8 x 0.4
3.	ESCA studies	1 x 0.5

2.3. SURFACE MORPHOLOGY

The surface morphology of these films was examined by Scanning Electron Microscope (SEM - Model Cambridge Stereo Scan 150). Prior to scanning, samples were coated with thin metallic films to prevent the charging effects.

2.4. S T R U C T U R E

Structural investigations were performed on the thick film samples by employing X-ray powder diffraction techniques. Diffractograms (i.e. intensity versus 2θ curves) were recorded on a X-ray diffractometer (Model-Philips PW 1730) using Cu-K α radiation.

2.5. ELECTRICAL CONTACTS

For the measurements of the electrical properties, an ideal contact to the photoconductor surface is absolutely necessary having the following properties:

- (a) It should be highly conducting.
- (b) Contact material should not react with the photoconducting material.
- (c) Contact properties should not change with variations in temperature, illumination, electrical field and ambient conditions.

Barriers at the contact between a metal and a photoconductor generally arise due to (i) either, improper matching of the work functions between the metal and the photoconductor, (ii) or, the presence of surface states, (iii) or, the presence of a thin layer of oxide. A contact between a metal and a photoconductor will be proper when no such barriers exist. The ohmic contact satisfies most of the needs of an ideal contact.

It is reported that indium, gallium and indium-gallium eutectic mixtures make good ohmic contacts to CdS. Indium was, therefore, evaporated in vacuum (10^{-5} mm of Hg) onto the masked (interelectrode spacing $\simeq 1$ mm) thick film samples. Silver was then vacuum-deposited over indium to enable easy soldering of the lead wires.

Leads of 46 gauge silver-copper wires were soldered directly to the silver deposit. The ohmic nature of contacts was checked by measuring current-voltage characteristics (for a number of samples) in the dark as well as in the light.

2.6. MEASUREMENTS ON ELECTRICAL AND PHOTOCONDUCTING PROPERTIES

In this section, the description of sample-holders, the list of instruments used and the particulars of the experimentation are given.

2.6.1. Sample holders

Two types of sample holders were used to perform the measurements:

(1) Thermally insulated and shielded dark box with lid.

(2) A specially constructed all-metal vacuum cryostat (Fig. 2.4). This metal cryostat consists of two parts (A and B) made up of nickel plated copper. Part A is made up of two concentric cylinders 1 and 2, which are brazed at one end. The other end of the outer cylinder 1 has a flange in which holes are provided for bolting. The inner cylinder 2 is closed at the lower end and has a flat portion to mount the sample. A mini-heater (H), for heating the sample, is fixed at the base of inner cylinder. Direct

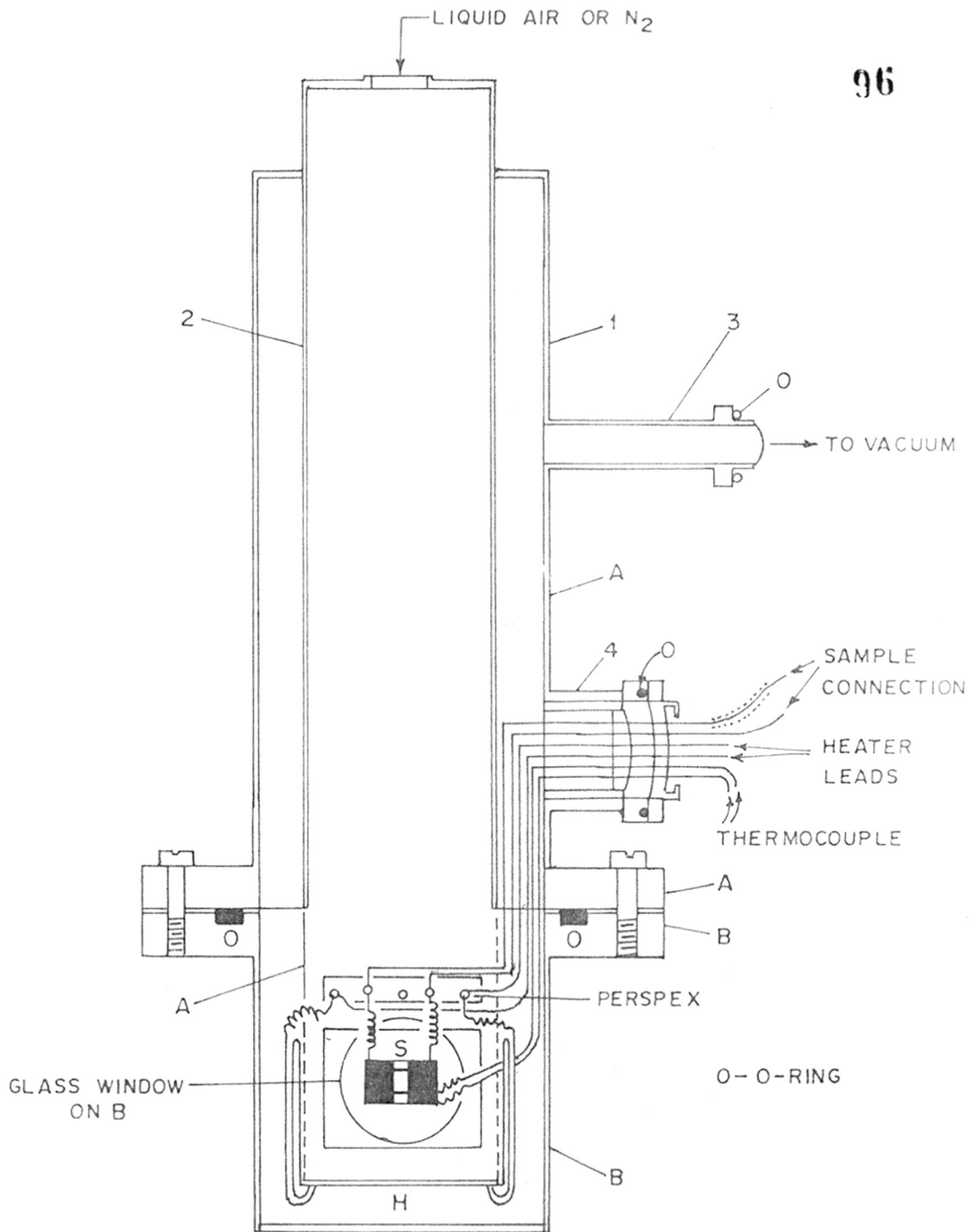


FIG. 2-4 SCHEMATIC DIAGRAM OF A METAL CRYOSTAT

cooling may be achieved by pouring liquid nitrogen in the cylinder 2. The cryostat can be evacuated through tube 3 (vacuum 10^{-5} mm of Hg). Heater leads, thermocouple and shielded measuring leads are brought out through a 9-pin-glass-metal-vacuum-lead-through sealed in tube 4.

Part B consists of a tube closed at one end and a flange fixed to this tube. A glass window is provided to this tube for illuminating the sample. Parts A and B, when bolted together, form the vacuum cryostat.

The temperature gradient between the metal base and the sample as well as thermocouple is minimised by means of a silicone based thermal compound which acts as a heat sink.

In view of the very high dark resistance of these films, special precautions were taken in earthing the equipment to avoid pick-up of a.c. signals leading to spurious measurements.

2.6.2. Instruments used

Instruments involved in these measurements are enlisted in Table 2.6.

TABLE 2.6INSTRUMENTS USED FOR THE MEASUREMENTS

Sr. No.	Measurements	Instrument/s used	Model
1.	Current	Electrometer amplifier Electrometer amplifier Philips VTVM	Trombay EA 810 EA 814 of ECIL (India) GM 6009/90
2.	Voltage	D.C. regulated variable voltage power supply	Aplab Model 7122
3.	Intensity of illumination	Lux-meter	Aplab type ML 4420.

2.6.3 Particulars of the experimentation

Particulars of the experimentation pertaining to the electrical and photoconducting properties of these films are presented in Table 2.7.

2.7. CHEMISORPTION OF OXYGEN

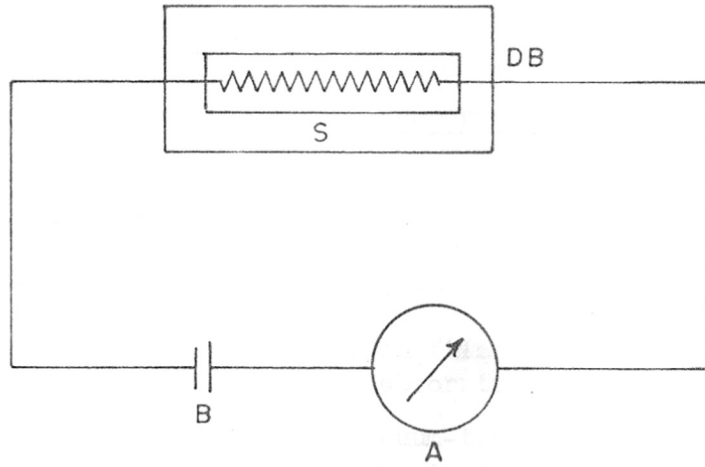
As indicated in Chapter 1, chemisorption of oxygen is of fundamental importance in understanding the photoconductivity processes in CdS. It was, therefore, imperative to examine oxygen-chemisorption on thick films of photoconducting CdS. We studied this phenomenon indirectly by dark current versus temperature measurements and directly by X-ray photoelectron spectroscopic examination.

TABLE - 2.7 .

PARTICULARS OF THE EXPERIMENTATION

Sr. NO.	PROPERTY STUDIED	SAMPLE HOLDER USED	TEMPERATURE/RANGE SELECTED °K	LIGHT SOURCE	RECORDING INSTRUMENTS			VOLTAGE APPLIED VOLTS
					FOR DARK CURRENT	FOR PHOTOCURRENT	FOR INT OF ILLUMINATION	
1	Dependence of photosensitivity on the preparation conditions	Dark box	300	500 W projection lamp	Electrometer amplifiers	VTVM	—	60
2	Current-voltage characteristics (in dark and light)	Dark box	300	Calibrated tungsten filament	Electrometer amplifiers	Electrometer amplifiers and VTVM	Luxmeter	0 - 60
3	Dark conductivity as a function of temperature.	Vacuum cryostat	130 - 375	—	Electrometer amplifiers	—	—	60
4	Dependence of photocurrent on the intensity of illumination.	Dark box	300	500 W projection lamp	—	VTVM and Trombay EA 810	Luxmeter	60
5	Spectral response	Vacuum cryostat	300 and 93	Hilger monochromator * equipped with 500 W projection lamp	—	Electrometer amplifiers and VTVM	—	30

* It was calibrated with vacuum thermopile (Hilger model FT-10) and necessary correction was made.



A - AMMETER

B - BATTERY

S - SAMPLE

DB - DARK BOX

FIG. 2.5 A SIMPLE CIRCUIT DIAGRAM FOR THE MEASUREMENT OF THE DARK CONDUCTIVITY

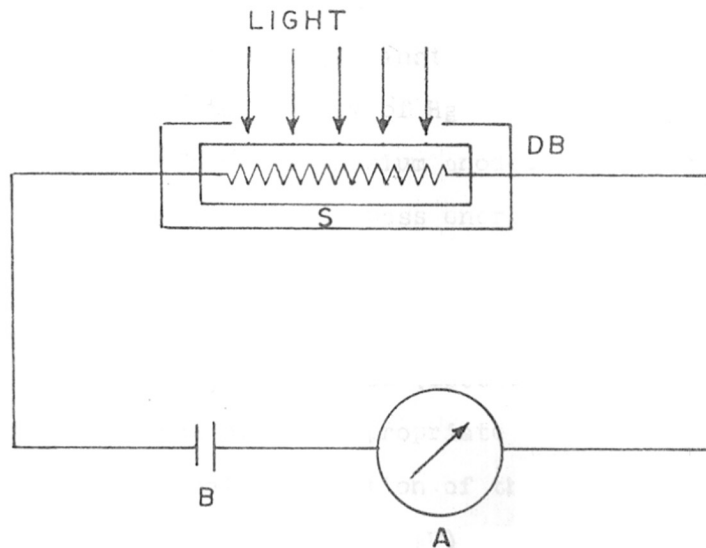


FIG. 2.6 A SIMPLE CIRCUIT DIAGRAM FOR THE MEASUREMENT OF THE PHOTOCONDUCTIVITY

2.7.1. Dark conductivity versus temperature

Dark conductivity of the samples was determined as a function of temperature during the oxygen adsorption-desorption cycles. These cycles include:

- (i) Heating of the virgin films upto 200°C in dark under vacuum (desorption).
- (ii) Heating of these vacuum-treated films upto 200°C in dark and in air (adsorption).

All these experiments were performed in the same vacuum-cryostat described earlier. Current measurements were carried out with electrometer amplifiers by applying a d.c. potential of 50 V.

2.7.2. X-ray photoelectron spectroscopy (XPS) studies

X-ray photoelectron spectra were recorded on ESCA-3Mk(II) [VG Scientific, UK] instrument operated at a base pressure of 10^{-8} to 10^{-9} mm of Hg. The photon beam used was the K_{α} line from a magnesium anode. All spectra were recorded at 50 eV analyser pass energy and 4 mm entrance slit width. The spectrometer was calibrated using a $Au4f_{7/2}$ line (84.0 eV) and Cls as an internal reference (285.0 eV). Initially, full scans (1000 eV) were recorded to ensure the presence of all appropriate peaks corresponding to the expected chemical composition of the surface. Subsequently, high resolution scans (30 eV) were acquired over a narrower energy scale to locate binding energies accurately.

CHAPTER - 3

RESULTS AND DISCUSSION

3.1. EFFECT OF PREPARATION CONDI- TIONS ON PHOTSENSITIVITY

It has been demonstrated that photosensitivity of CdS thick films can be greatly modified by preparation conditions particularly the firing temperature and impurity concentration.

3.1.1. Effect of firing temperature

The effect of firing temperature on the dark current and on the photocurrent is illustrated in Fig. 3.1. These two curves reveal that the dark current and the photocurrent increase with increase in firing temperature upto 600°C and decrease afterwards with further increase in the temperature. It is also noticed that adherence of the film to the substrate becomes poorer with an increase in firing temperature above 600°C . It is observed that photosensitivity is the highest for the films fired at 650°C . However, because of the adherence problem at this temperature, firing at 600°C is preferred.

The firing process proceeds through a complex mechanism in which:

- (i) The organic binder and solvents are burnt off, initially, below 300°C .

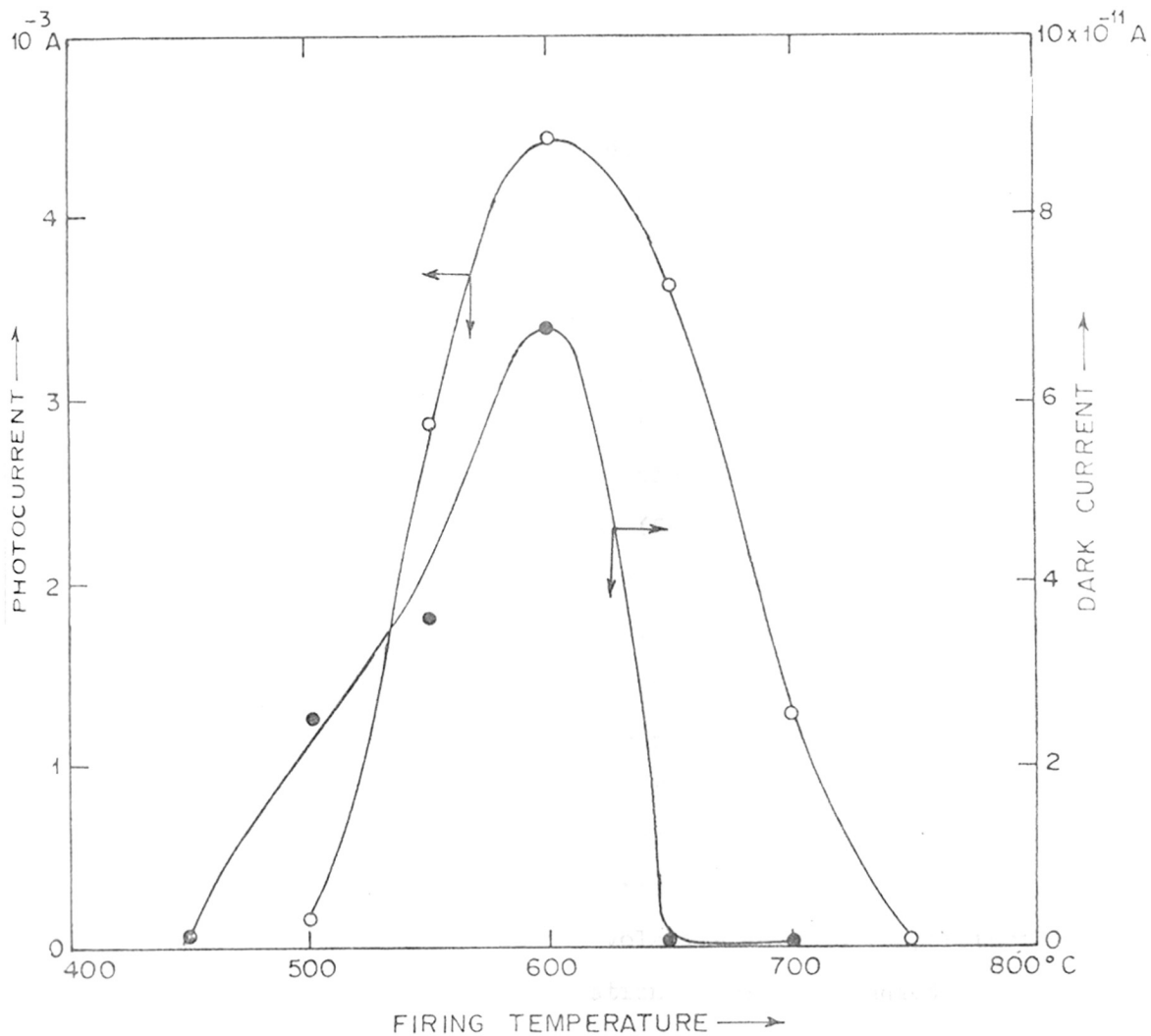


FIG. 3.1 EFFECT OF FIRING TEMPERATURE ON THE PHOTOCURRENT AND ON THE DARK CURRENT OF CdS THICK FILMS

(Cu CONCENTRATION = 0.05 % BY Wt)

(ii) Sintering, by which the intercrystallite barriers are reduced, is achieved. Sintering above 600°C is not advisable, as it leads to the poor adherence of the films.

(iii) Incorporation of chloride centers required for the charge compensation of copper centers in the CdS lattice is controlled¹. This is the consequence of volatilization of $\text{CdCl}_2 \cdot 2.5 \text{H}_2\text{O}$ which starts at a temperature just above its melting point (568°C) during the firing process. It becomes more significant at still higher firing temperatures which ultimately results in less number of chloride centers to compensate copper centers. However, because of the large amount of CdCl_2 added as a flux in the prefiring formulation and relatively short firing time, some concentration of chloride centers can be reasonably assumed to be present at all firing temperatures chosen for this study. Since $\text{CuCl}_2 \cdot 2\text{H}_2\text{O}$ is not volatile in this temperature range, its equilibrium concentration remains unchanged during this process. Thus difference in the relative concentration of chloride centers to compensate copper is established with the firing temperature which in turn, modifies the photosensitivity. From this discussion, it is clear that the maturity of the films is dominated by the effects (i) and (ii), while the photosensitivity of the films is dependent on the effect (iii).

3.1.2. Effect of copper concentration

The effect of Cu concentration on the photocurrent of the films is plotted in Fig. 3.2. The curve obtained shows a decrease in photocurrent with increase in Cu concentration. Further, it is found that these films do not show an appreciable change in the magnitude of dark current with the increase in Cu concentration.

It has been well established by Bube and Dreeben² that beyond a critical impurity concentration, the room temperature photosensitivity decreases rapidly. This desensitization effect can be explained on the basis of the mechanism originally offered by Bube and his coworkers³ while discussing high impurity concentration effects. According to them, it would be a direct result of the imperfection interactions that reduce the thermal hole-ionization energy of the sensitizing centers, either, through electrostatic interactions, or, by impurity banding. With the decreased hole-ionization energy, occupancy of the impurity states would be governed more by thermal behaviour (traps) than by recombination kinetics even at room temperature under the conditions of constant illumination. This condition as proposed by Rose⁴ is not favourable for photosensitivity.

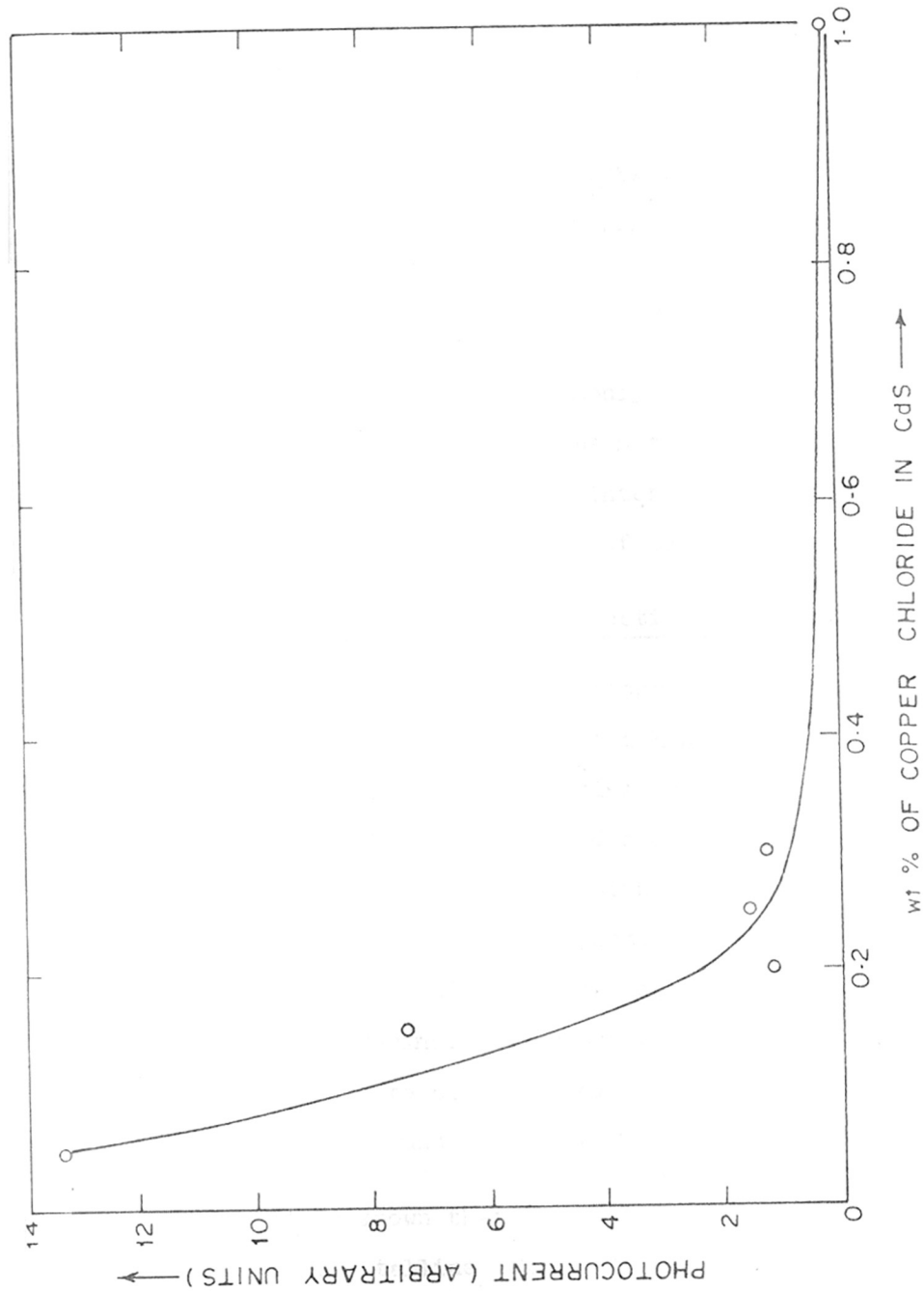


FIG. 3.2 EFFECT OF COPPER CONCENTRATION ON THE PHOTOCURRENT OF CdS THICK FILMS, AT ROOM TEMPERATURE AND UNDER CONSTANT ILLUMINATION
 (FIRING TEMPERATURE = 600°C)

All these observations have resulted in adopting (i) an optimum firing temperature of 600°C and (ii) an optimum copper concentration - 0.05% (added as CuCl₂ by wt. of CdS) to obtain the best and reproducible photosensitivity.

3.2. S T R U C T U R E

Since it has been commonly observed that the structure of CdS depends upon the method of preparation, it was thought that it would be of interest to examine the crystal structure of thick films of CdS.

3.2.1. Analysis of X-ray diffraction (XRD) data

A typical X-ray diffractogram of the undoped film is shown in Fig. 3.3. Corresponding XRD data i.e. the 'd' values and the relative intensities are presented in Table 3.1 along with the standard powder diffraction file data^{5,6} for the cubic and the hexagonal structures. A comparison between the observed and the reported data shows that **although** at a number of places the diffraction peaks due to the cubic and hexagonal phases overlap; there are some distinctive peaks to clearly indicate that both the phases are present in the undoped thick film of CdS.

It is known that in case of totally randomly oriented polycrystalline hexagonal CdS, (101) is the strongest diffraction whereas that in case of the cubic phase it is the

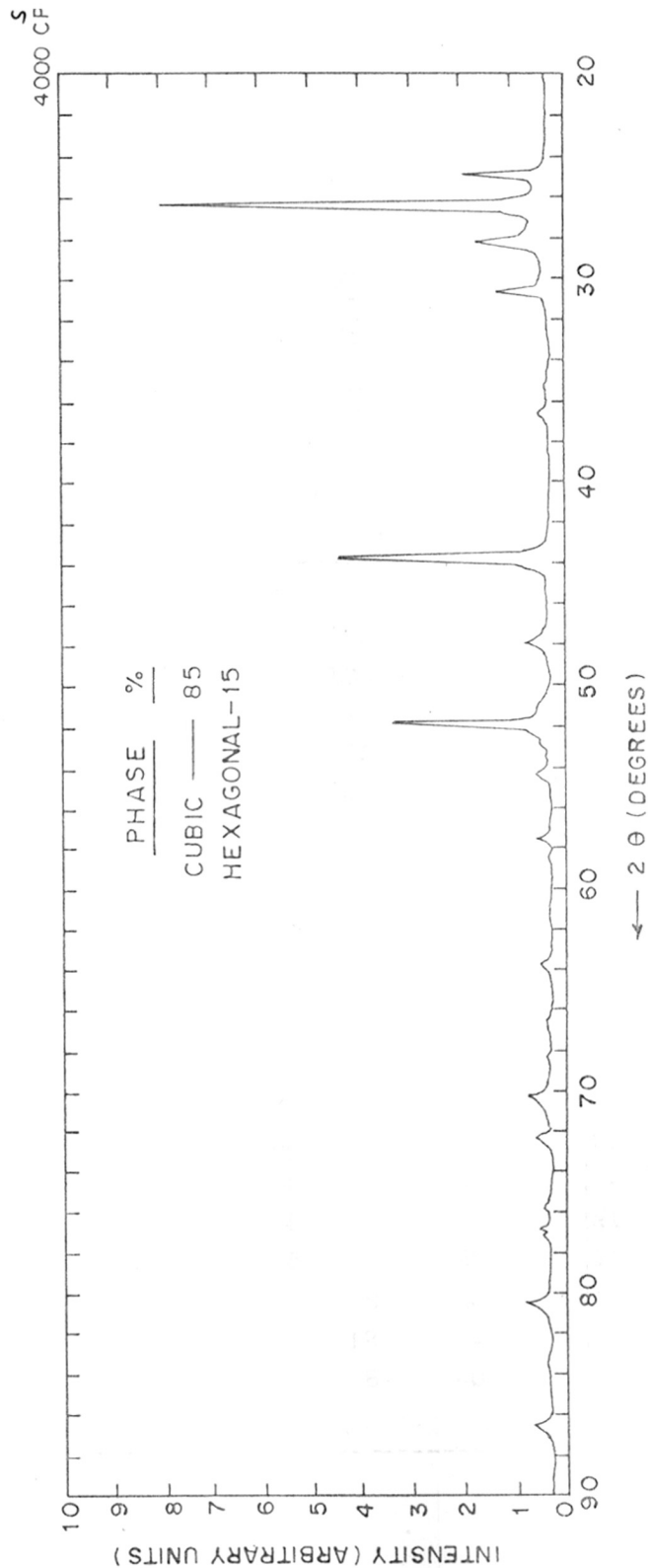


FIG. 3.3 X-RAY DIFFRACTOGRAM OF THE UNDOPED THICK FILM OF CdS

TABLE 3.1
X-RAY DIFFRACTION DATA FOR THE
UNDOPED THICK FILM OF CdS

d	Value \AA		Relative intensity			h k l	
	Observed	Reported	i.e. I/I _{max} .			Hex.	Cubic
	Hex.	Cubic	Observed	Reported		Hex.	Cubic
				Hex.	Cubic		
3.5728	3.583	-	22	75	-	100	-
3.3606	3.357	3.36	100	59	100	002	111
3.1563	3.160	-	20	100	-	101	-
2.9143	-	2.90	14	-	20	-	200
2.4466	2.450	-	4	25	-	102	-
2.0629	2.068	2.06	56	57	100	110	220
1.8974	1.898	-	7	42	-	103	-
1.7924	1.791	-	3	17	-	200	-
1.7602	1.761	1.76	40	45	90	112	311
1.7293	1.731	-	2	18	-	201	-
1.6851	1.679	1.68	4	4	10	004	222
1.5109	1.520	-	> 1	2	-	104	-
1.4596	-	1.45	3	-	10	-	400
1.3992	1.398	-	2	15	-	203	-
1.3739	1.3536	-	2	6	-	210	-
1.3387	-	1.340	6.5	-	30	-	331
1.3280	1.3271	-	2.5	11	-	211	-
1.3042	1.3032	1.30	4.5	7	20	114	420
1.1915	1.1940	1.19	7	8	40	300	422
1.1584	1.1585	-	3	12	-	213	-
1.1241	1.1249	1.12	5	8	40	302	333

(111) diffraction. In the present case the strongest diffraction peak is observed at $d = 3.36\overset{\circ}{\text{Å}}$ which ordinarily can be indexed as cubic (111). However, if the hexagonal phase is present with a strong basal plane orientation [i.e. (0001) plane parallel to the substrate] then the (002) diffraction from the hexagonal phase (at $d = 3.36\overset{\circ}{\text{Å}}$) can get substantially enhanced in intensity [the c-axis orientation pointed by Foster⁷ and Escoffery⁸]. In such a case, it is difficult to determine whether the crystallites are of cubic or hexagonal form. However, similar intensity pattern is also observed in the X-ray diffractogram of original CdS powder (to be presented afterwards) used as a starting material in the preparation of thick films. Since one cannot expect any degree of preferred orientation in the polycrystalline powder, the possibility of any preferred orientation in the thick film can also be ruled out. If that assumption is accepted, then the pattern can be taken to indicate a mixture with the cubic phase predominating.

Quantitative analysis of a mixture of cubic and hexagonal phases is not very easy, because the main XRD peaks of cubic phase overlap entirely on those of hexagonal phase^{5,6}. For the practical purposes, the ratio of the observed intensities of the peaks with 'd' values corresponding to cubic (111) and hexagonal (101) planes [i. e. $I_{\text{cub}}(111)/I_{\text{hex}}(101)$] in the same diffractogram can be

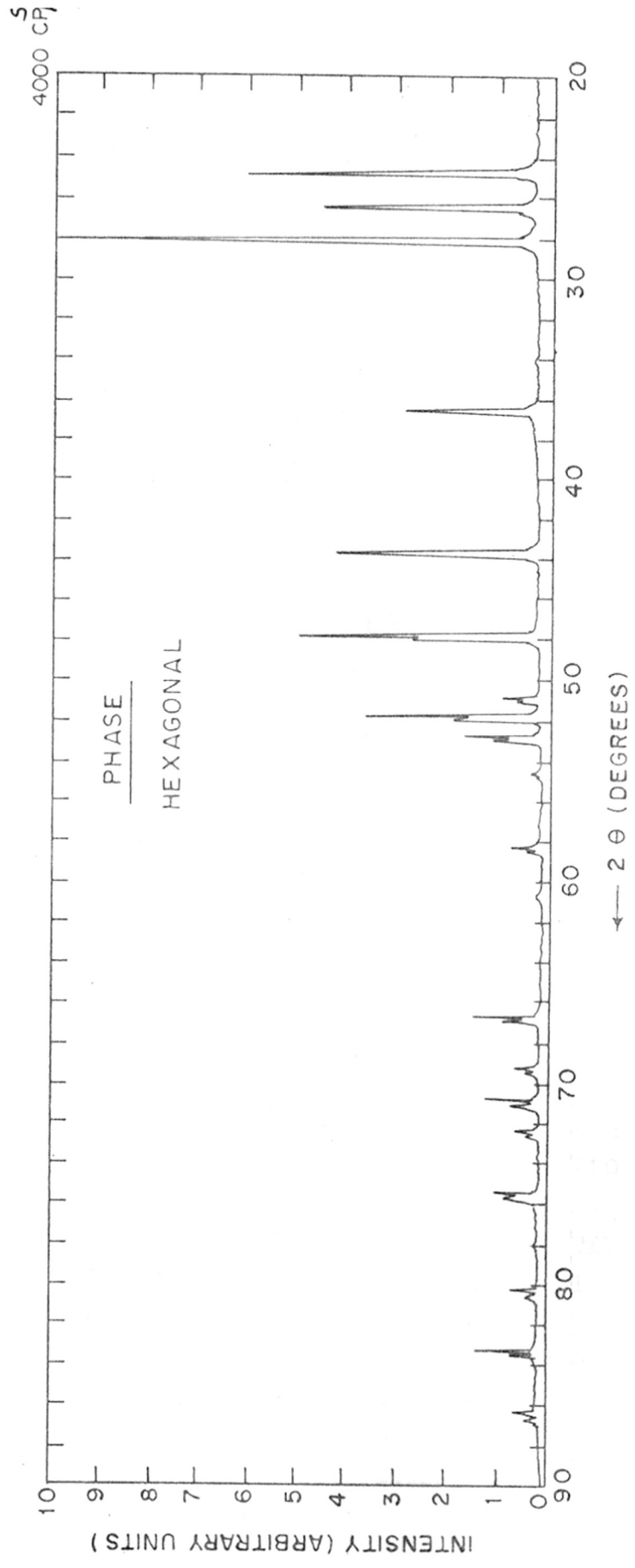
used as a rough measure to estimate the percentage of cubic and hexagonal phases in a given sample. This type of estimation shows that the undoped film consists of a mixture of approximately 85% cubic and 15% hexagonal form. A typical X-ray diffractogram of the doped film with optimum Cu concentration is shown in Fig. 3.4. Corresponding 'd' values, relative intensities and their literature values for the hexagonal and cubic structures are provided in Table 3.2. An examination of this data shows that:

(i) Observed 'd' values and relative intensities match with their literature values for the hexagonal structure.

(ii) The peaks with 'd' values corresponding to characteristically cubic (200), (400) and (331) planes are totally absent.

Owing to these observations, it is unlikely that the doped sample contains any notable percentage of cubic phase which can be detected by XRD. The doped film with optimum Cu concentration thus reveals the existence of only hexagonal phase. Similar studies of the doped samples with other Cu concentrations (viz. 0.1 to 1.00 % by wt. of CdS) also reveal the occurrence of only hexagonal phase.

The lattice parameters 'a' and 'c' for the hexagonal structure and 'a' for the cubic structure were



112
 FIG.3.4 X-RAY DIFFRACTOGRAM OF THE DOPED THICK FILM OF CdS (OPTIMUM Cu CONCENTRATION)

TABLE 3.2
X-RAY DIFFRACTION DATA FOR THE DOPED
THICK FILM OF CdS

<u>d Value Å</u>			<u>Relative intensity</u>				<u>hkl</u>	
<u>Observed</u>	<u>Reported</u>		<u>i.e. I/I_{max}.</u>				<u>Hex.</u>	<u>Cubic</u>
	<u>Hex.</u>	<u>Cubic</u>	<u>Observed</u>	<u>Reported</u>		<u>Hex.</u>	<u>Cubic</u>	
				<u>Hex.</u>	<u>Cubic</u>			
3.5870	3.583	-	60	75	-	100	-	
3.3668	3.357	3.36	44	59	100	002	111	
3.1639	3.160	-	100	100	-	101	-	
-	-	2.90	-	-	20	-	200	
2.4531	2.450	-	28	25	-	102	-	
2.0696	2.068	2.06	42	57	100	110	220	
1.8993	1.898	-	50	42	-	103	-	
1.7924	1.791	-	8	17	-	200	-	
1.7634	1.761	1.76	37	45	90	112	311	
1.7323	1.731	-	16.5	18	-	201	-	
1.6808	1.679	1.68	3	4	10	004	222	
1.5813	1.581	-	7	7	-	202	-	
1.5210	1.520	-	2.5	2	-	104	-	
-	-	1.45	-	-	10	-	400	
1.3992	1.398	-	15	15	-	203	-	
1.3547	1.3536	-	5	6	-	210	-	
-	-	1.340	-	-	30	-	331	
1.3280	1.3271	-	12	11	-	211	-	
1.3042	1.3032	1.30	5	7	20	114	420	
1.2581	1.2572	-	10	11	-	105	-	
1.1946	1.1940	1.19	6	8	40	300	422	
1.1590	1.1585	-	13	12	-	213	-	
1.1252	1.1249	1.12	5	8	40	302	333	

computed from the observed 'd' values by the method of successive refinements.

Formulae used were:

For the hexagonal system:

$$\frac{1}{d^2} = \frac{4}{3} \cdot \frac{h^2 + k^2 + hk}{a^2} + \frac{l^2}{c^2}$$

For the cubic system:

$$\frac{1}{d^2} = \frac{h^2 + k^2 + l^2}{a^2}$$

where, d = interplanar spacing, 'a' and 'c' = lattice parameters. Mean values of the lattice parameters are given in Table 3.3.

TABLE 3.3

LATTICE PARAMETERS FOR THE THICK FILMS OF CdS

Sr. No.	Sample	Concentration of CuCl ₂ (% by wt)	Structure	Lattice parameters Å			
				Cubic		Hexagonal	
			'a'	'a'	'c'	c/a	
1.	Undoped	-	Cubic (85%) + Hexagonal (15%)	5.8343	4.1295	6.7324	1.6303
2.	Doped	0.05	Hexagonal	-	4.1388	6.7237	1.6245
		0.15	Hexagonal	-	4.1388	6.7192	1.6234
		0.30	Hexagonal	-	4.1403	6.7257	1.6244
		1.00	Hexagonal	-	4.1441	6.7194	1.6214
3.	^{5,6} Reported	-	Cubic	5.82	-	-	-
		-	Hexagonal	-	4.136	6.713	1.6230
					4.142	6.724	1.6233

3.2.2. Predominance of cubic phase in undoped films

The cubic phase is less common in the single crystals, sintered layers and thin films of photoconducting CdS. For example, Lind and Bube⁹ have reported photoconductivity measurements on a cubic CdS powder-binder layer prepared by the precipitation of cadmium methyl mercaptide followed by sufficient heating to decompose the mercaptide. Nagao and Watanabe¹⁰ have produced cubic CdS films by chemical deposition technique. Escoffery⁸ observed the cubic phase in CdS films only under the controlled conditions of vapour deposition. Sathaye and Sinha¹¹ have investigated cubic phase in CdS films which were prepared by a novel method of chemical deposition. Favaskar et al.¹² have obtained a cubic dominated mixed phase [cubic (90%) + hexagonal (10%)] in the structural analysis of the undoped CdS films prepared by the chemical bath deposition technique. Ma and Bube¹³ have identified cubic dominated mixed phase in CdS layers spray-deposited at lower temperatures. Chopra and Khan¹⁴ have observed epitaxial growth of cubic CdS only in a limited range of substrate temperatures and film thickness and also under applied lateral electric field. Simov¹⁵ and many other workers have reported that epitaxially grown layers of CdS can contain the cubic phase, instead of, or together with the more common hexagonal phase. The preparation methods in most of these references, however, maintain the conditions in such a way that either no heating is involved or low-temperature heating is required.

Instability of the cubic phase at the temperatures sufficiently high to make single crystals or even photoconducting powders or layers by conventional techniques is the real hurdle in getting cubic CdS photoconductors. Recurrence of cubic phase in undoped films of CdS - presently being reported - is an interesting observation since these films undergo firing at 600°C for 10 minutes during preparation. It can perhaps be explained on the basis of the experiments in which powders were converted to hexagonal CdS leading to the conclusion that cubic CdS is metastable in the temperature range 20-900°C¹⁶.

3.2.3. Cubic to hexagonal phase transformation

An important feature of the structural investigations is the cubic (dominated) → hexagonal phase transformation which occurred as a result of doping (Figs. 3.3 and 3.4). Earlier, Jakimavicius et al.¹⁷ have reported cubic to hexagonal phase transformation in sintered CdS:Cu:Cl layers which occurred at 450-600°C. But the detailed experimental results and adequate explanations are not easily available.

By considering various stages of doping (see preparation section 2.1) certain XRD studies have been performed to pinpoint the origin of this phase transformation. The results so obtained are presented in Table 3.4.

TABLE 3.4

OBSERVATIONS TO PINPOINT THE ORIGIN OF
CUBIC → HEXAGONAL PHASE TRANSFORMATION

<u>Obs. No.</u>	<u>Description</u>	<u>Structure</u>	<u>Ref.</u>
1.	Pure CdS powder (99.999%) used as a starting material in the preparation of the thick films.	Cubic(90%) + Hexagonal (10%)	Fig.3.5(A)
2.	Pure CdS powder is heated at 500°C for 2 hours in air.	Cubic(87%) + Hexagonal (13%)	Fig.3.5(B)
3.	Pure CdS powder is mixed with CuCl ₂ (0.05% by wt) and the mixture is heated at 500°C for 2 hours in air.	Cubic(87%) + Hexagonal (13%)	Fig.3.5(C)
4.	Pure CdS powder is mixed with CdCl ₂ (10% by wt) and the mixture is heated at 500°C for 2 hours in air.	Hexagonal	Fig.3.5(D)

From these results, it is clear that such a phase transformation is aided by the action of CdCl₂. We have further used the differential thermal analysis (DTA) technique to provide deeper insight into the mechanism underlying CdCl₂ aided phase transformation. To countercheck the earlier results, DTA studies were performed on cubic dominated CdS powder prepared in our laboratory. A thermal analyser (Netzsch Gerätebau GmbH) was used to record DTA and TG curves. A dynamic atmosphere of N₂

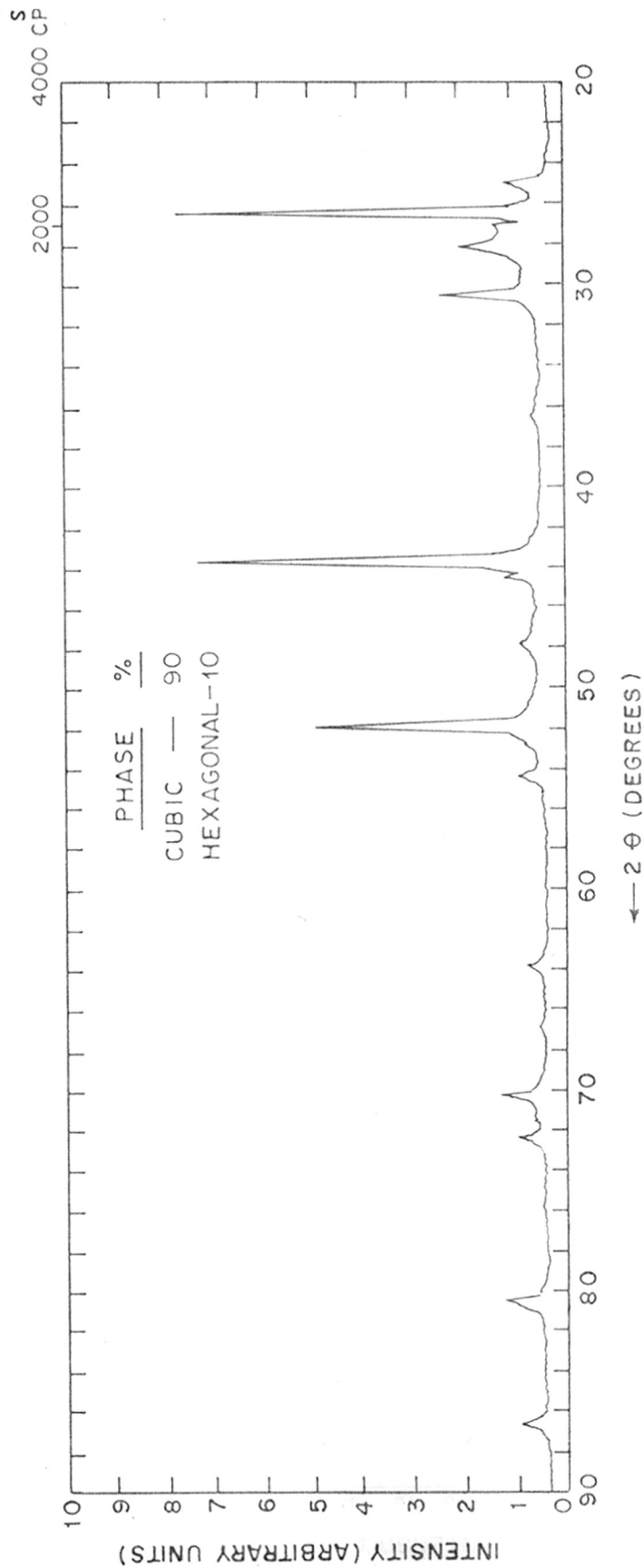


FIG. 3-5(A) X-RAY DIFFRACTOGRAM OF PURE CdS POWDER USED AS THE STARTING MATERIAL

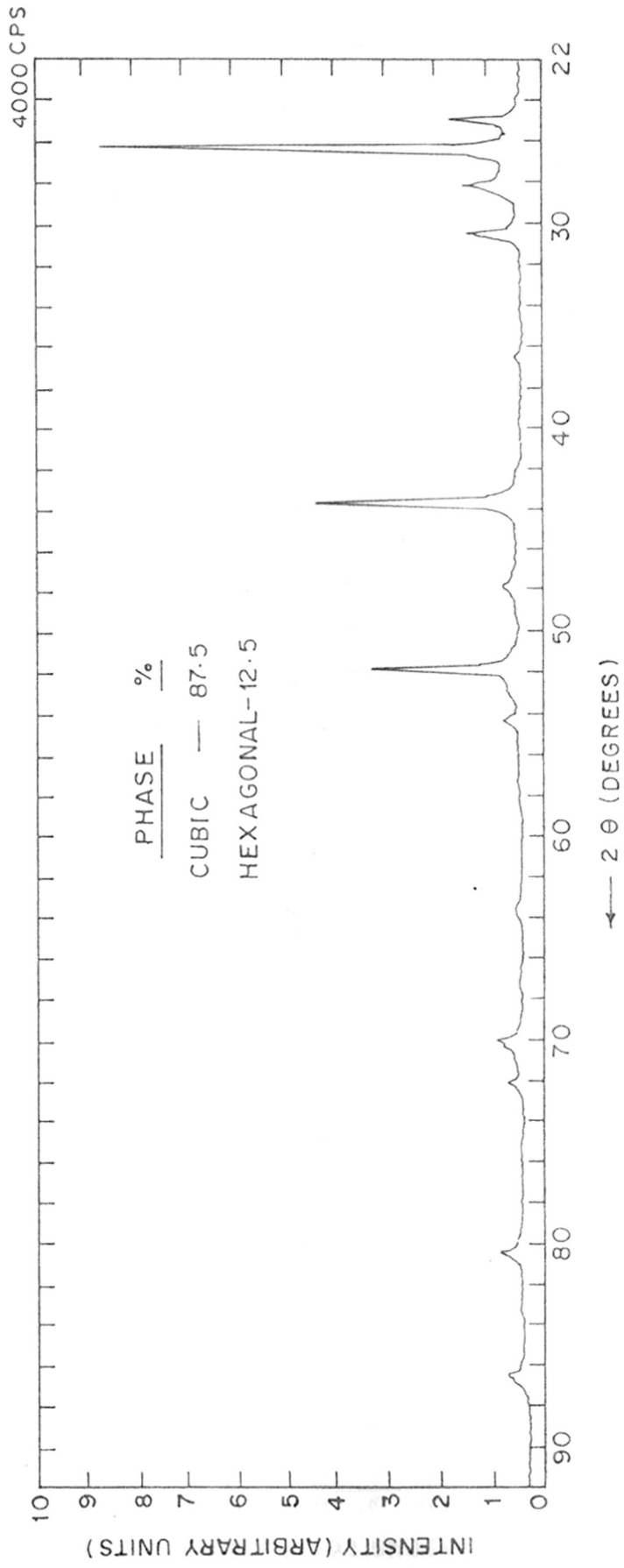


FIG. 3.5 (B) X-RAY DIFFRACTOGRAM OF PURE CdS POWDER HEATED IN AIR AT 500°C FOR 2 hrs

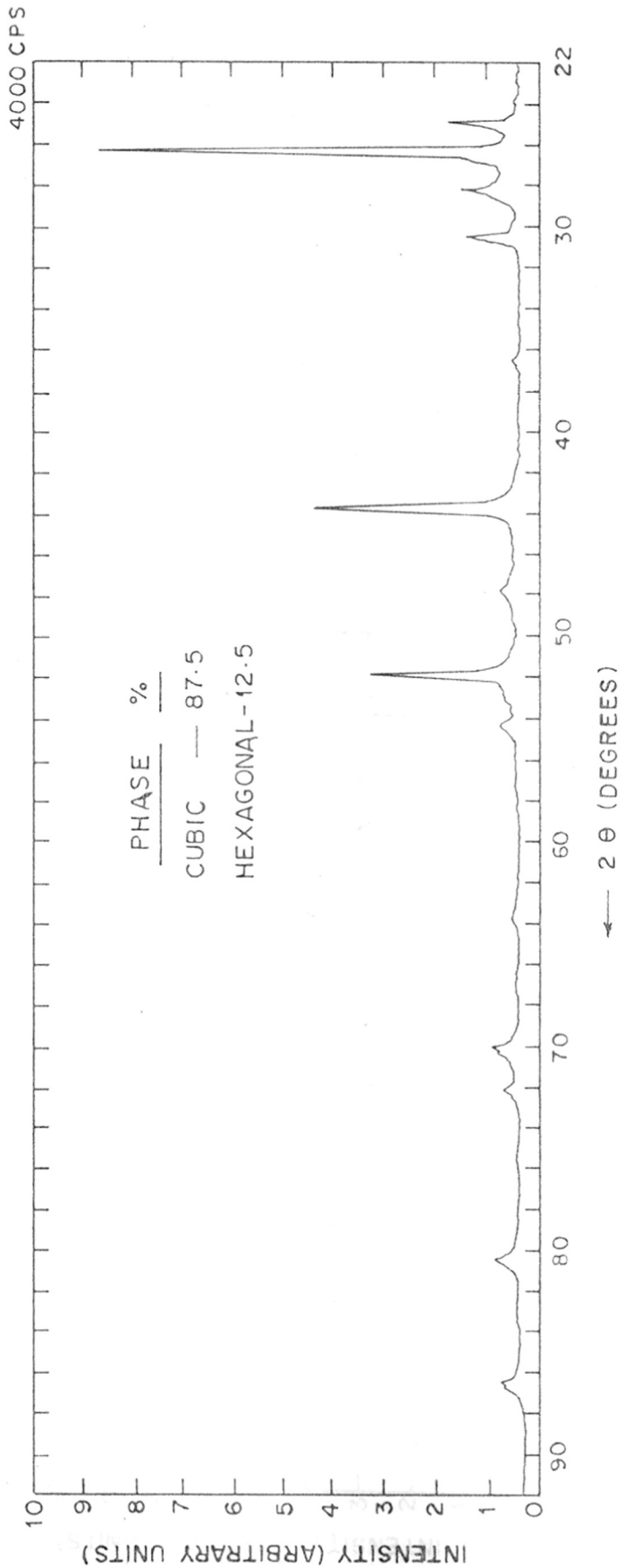


FIG. 3.5 (C) X-RAY DIFFRACTOGRAM OF A MIXTURE OF CdS + CuCl₂ (0.05% BY WT)
 HEATED IN AIR AT 500° C FOR 2 hrs

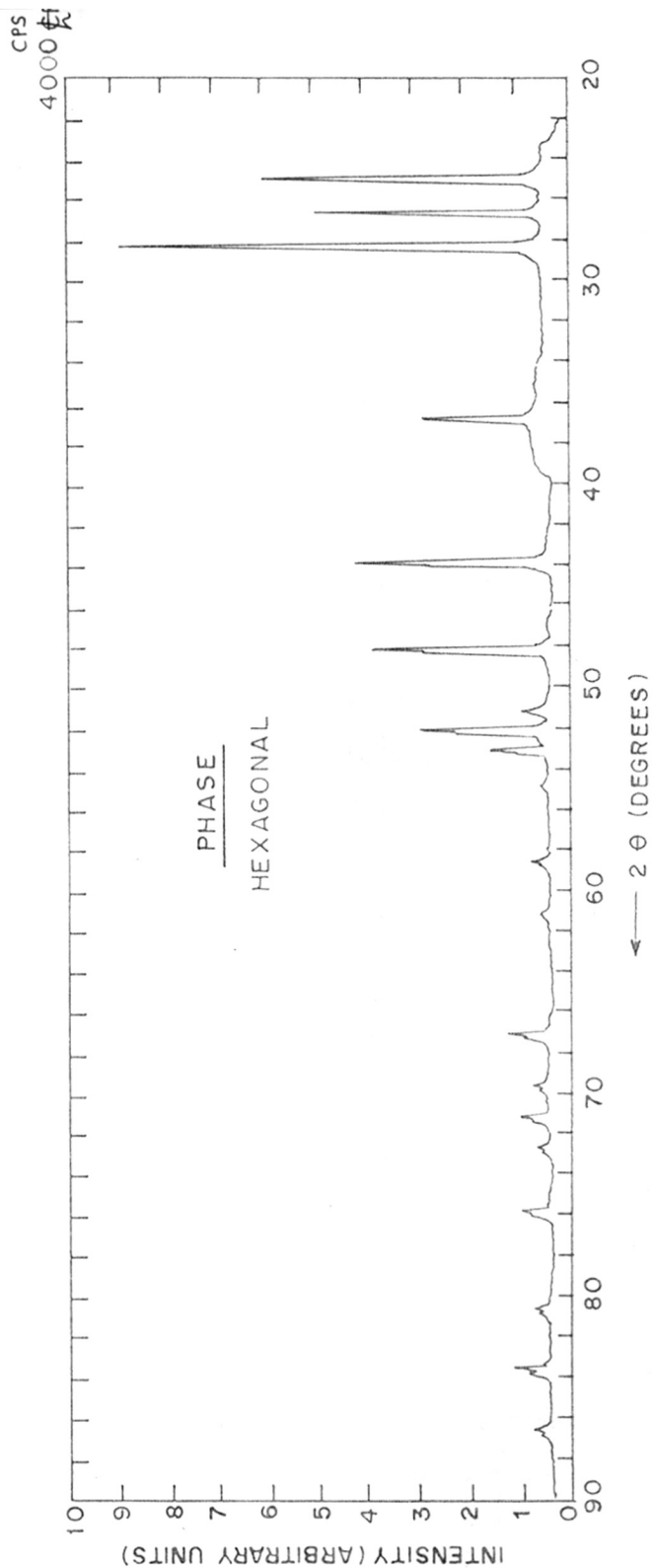


FIG. 3.5 (D) X-RAY DIFFRACTOGRAM OF A MIXTURE OF CdS + CdCl₂ (10 % BY WT) HEATED IN AIR AT 500 °C FOR 2 hrs 121

was maintained through the DTA furnace in order to avoid the possible oxidation of CdS at high temperatures. (Since a crystalline phase transformation of this type does not involve the evolution or absorption of a gaseous component, the shape of a DTA peak and its temperature will not be affected by the gas pressure of the system)¹⁸.

DTA curves and the corresponding thermograms (TG) are shown in Figs. 3.6 [(A), (B), (C) and (D)]. The important observations are as follows:

(1) DTA curve of pure CdS powder [Fig. 3.6(A)] gives an endothermic peak at 555°C (ΔT min.) and there is no weight loss in the corresponding TG. This endothermic peak, therefore, must have been caused by a cubic \rightarrow hexagonal phase transformation. The initial temperature of this change (i.e. ΔT_1) is about 400°C . This is in agreement with the XRD studies of Andrushko¹⁹ who showed that annealing in air at temperatures higher than 550°C converts all CdS powders into hexagonal form.

(2) DTA curve of pure $\text{CdCl}_2 \cdot 2.5 \text{H}_2\text{O}$ [Fig. 3.6(B)] indicates the melting transition at 568°C (ΔT min.).

(3) DTA curve of pure CdS powder mixed with CdCl_2 (10% by wt) and heated at 500°C for some time shows a small peak corresponding to the melting transition at 568°C [Fig. 3.6(C)]. It can be ascribed to a small amount of CdCl_2

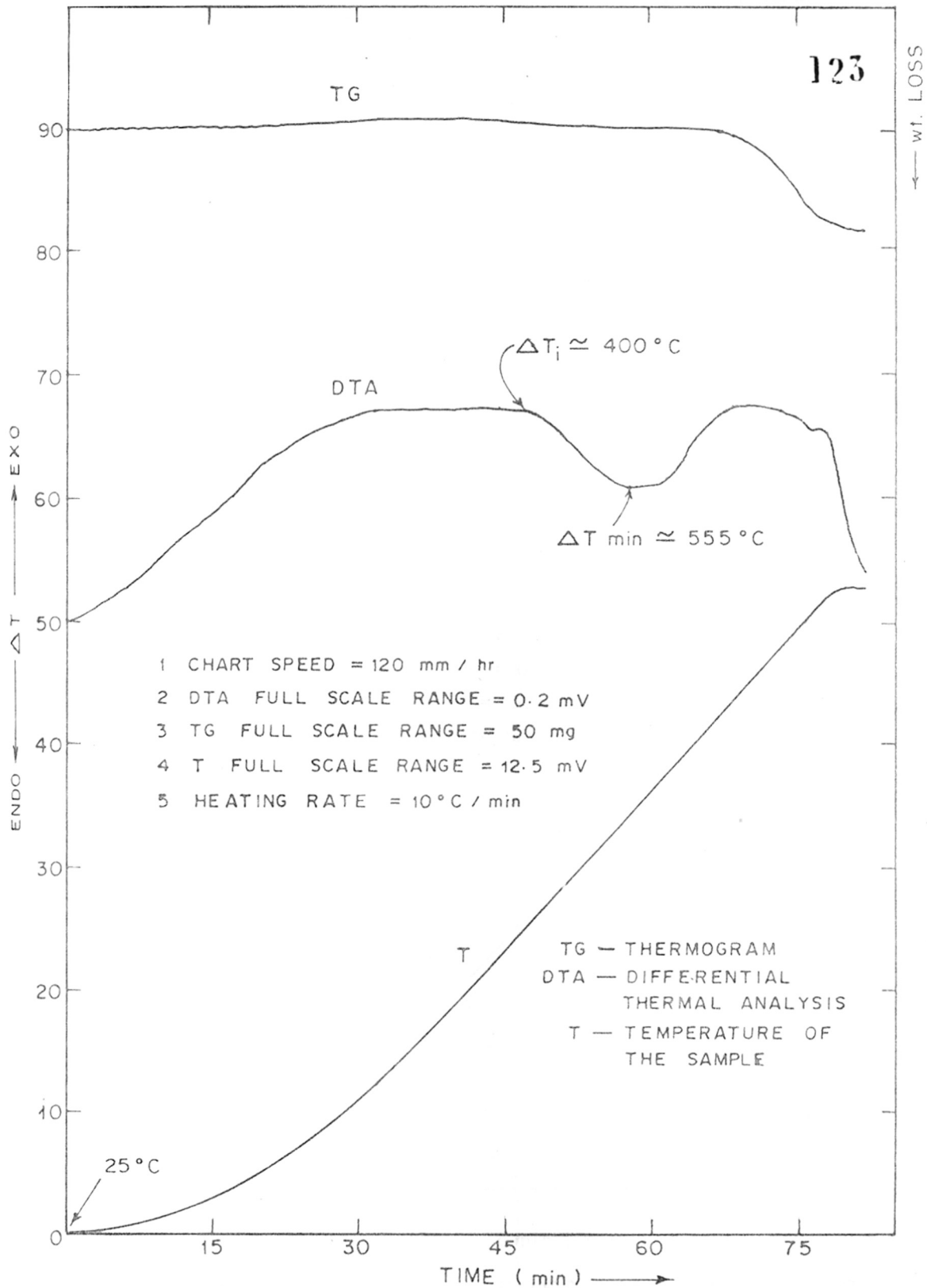


FIG. 3-6 (A) DTA AND TG CURVES FOR PURE CdS POWDER

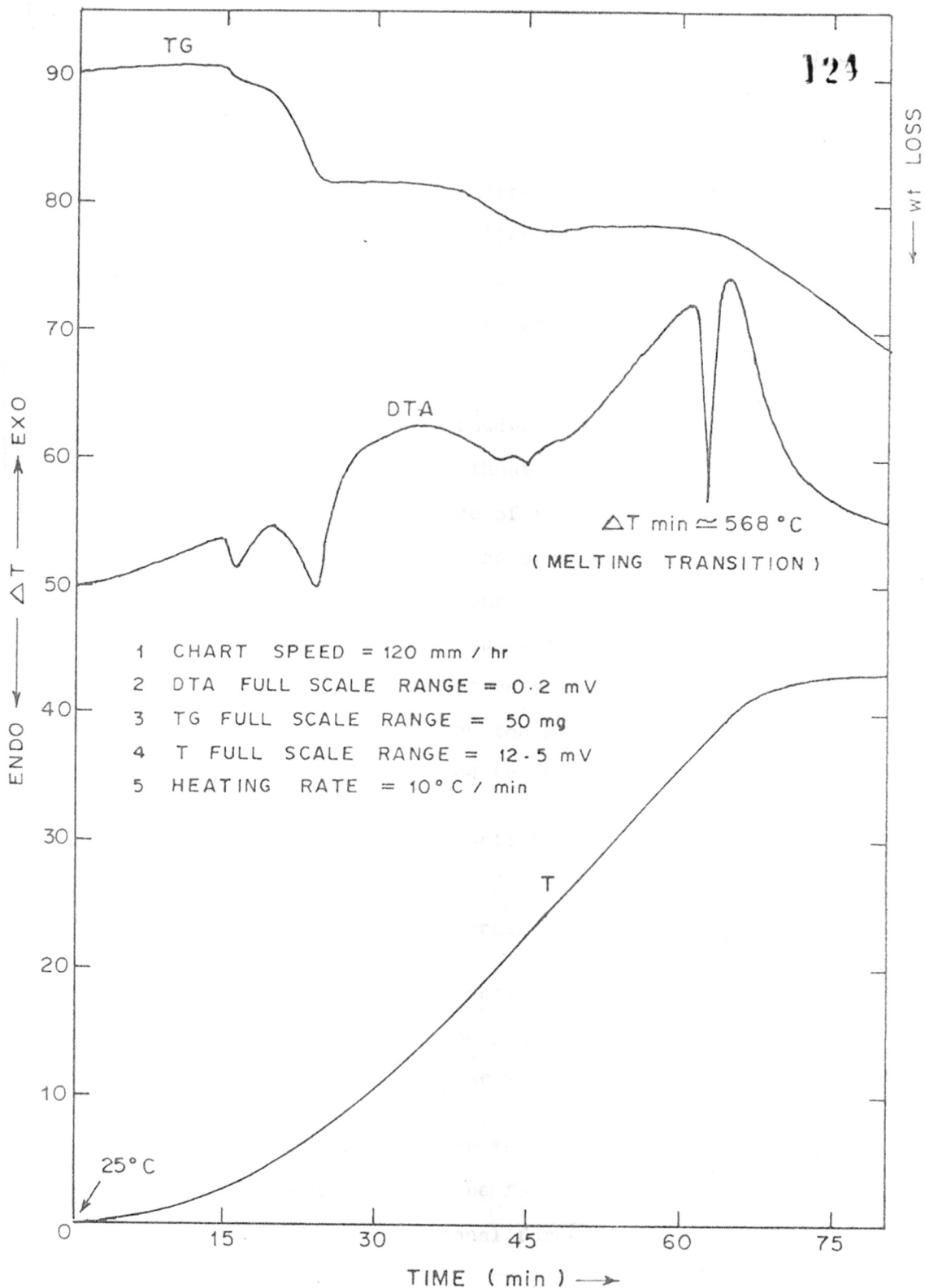


FIG. 3.6 (B) DTA AND TG CURVES FOR PURE $\text{CdCl}_2 \cdot 2.5 \text{H}_2\text{O}$ POWDER

which is still present as a result of incomplete volatilization. The absence of a peak corresponding to crystalline phase transformation clearly implies the presence of only one phase in the mixture and it is hexagonal as can be identified from the X-ray diffractogram of a similar mixture [Fig. 3.5(D)].

(4) DTA of the CdS powder which is mechanically mixed with CdCl_2 (10% by wt) without any prefiring shows a shift in the initial temperature of phase transformation (ΔT_1) to 330°C , although it covers approximately the same area under the peak as that of pure CdS [Fig. 3.6(D)]. This type of thermal behaviour suggests that the process of CdCl_2 aided phase transformation starts at a temperature which is considerably lower than the melting point of CdCl_2 . This result is further confirmed by the following observations:

(i) X-ray diffractogram of the mixture of CdS and CdCl_2 which is heated at 300°C for 2 hours reveals a significant increase in the percentage of hexagonal phase.

(ii) X-ray diffractogram of only CdS powder which is heated at 300°C for the same time could not show any increase in the percentage of hexagonal phase.

It was thought earlier that during the flux-action of CdCl_2 ; its molten mass might be facilitating the recrystallisation of cubic CdS in hexagonal form²⁰. But our DTA results

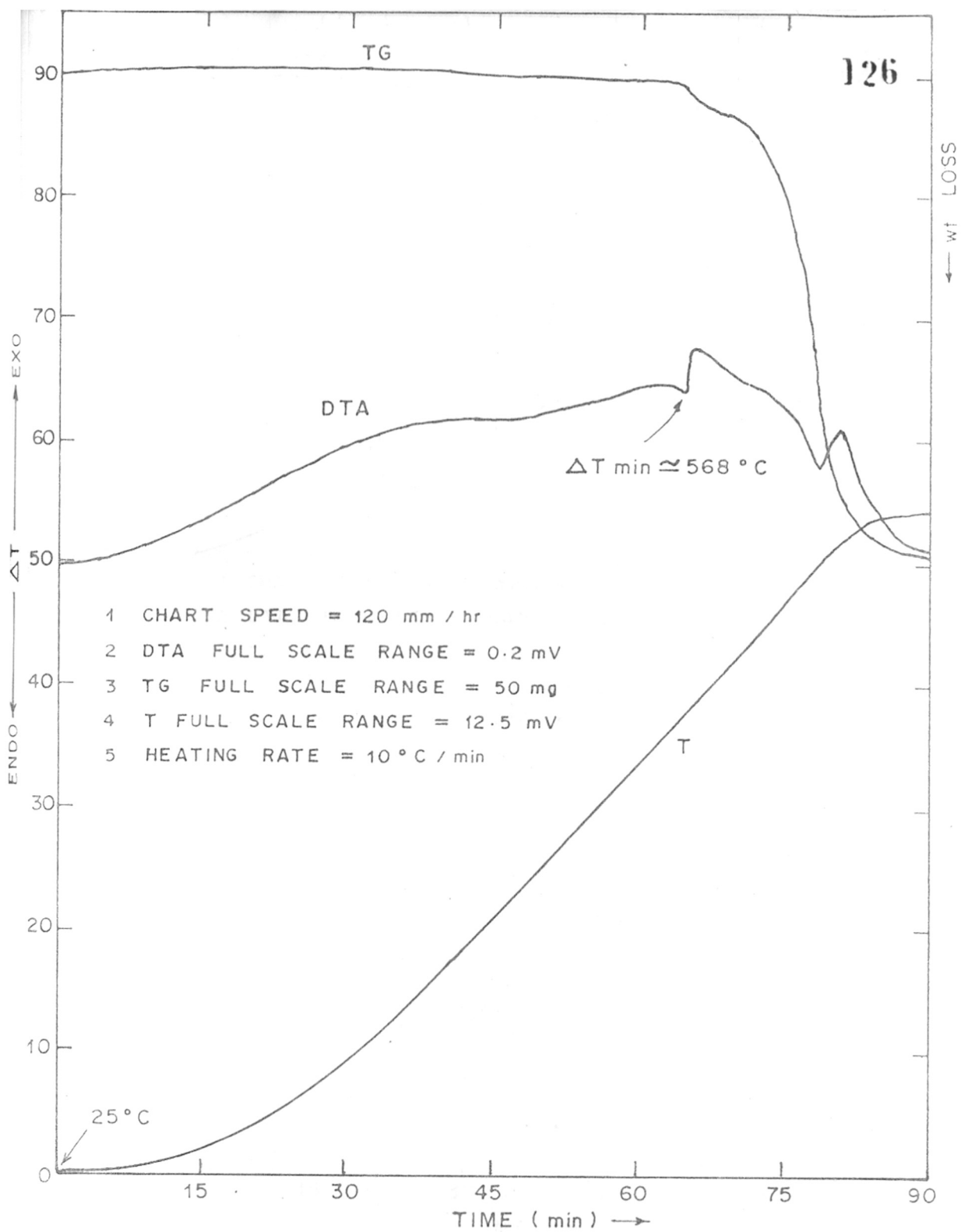


FIG. 3·6 (C) DTA AND TG CURVES FOR A MIXTURE OF CdS + CdCl₂ (10 % by wt) HEATED IN AIR AT 500 °C

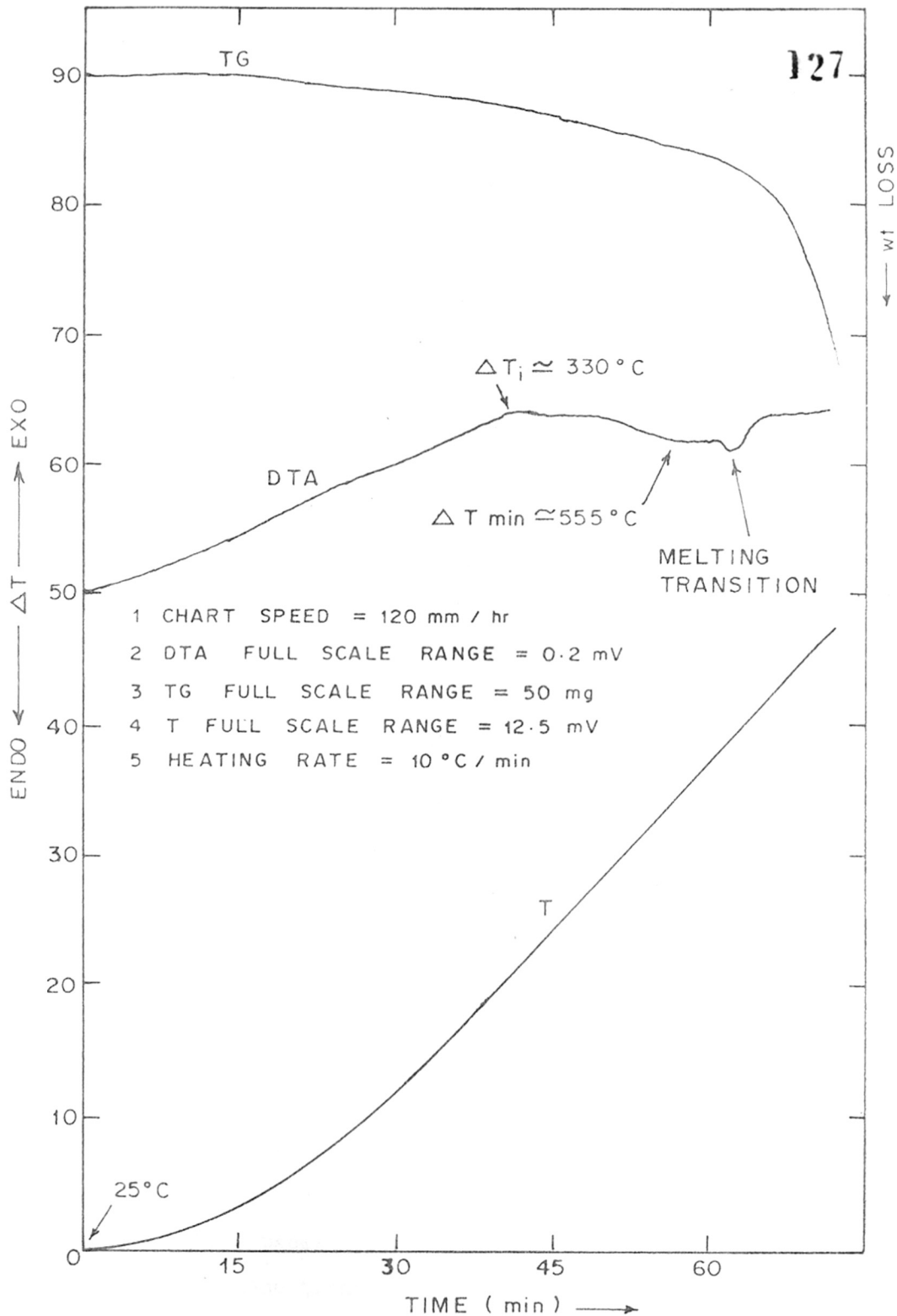


FIG. 3.6 (D) DTA AND TG CURVES FOR A MECHANICAL MIXTURE OF $\text{CdS} + \text{CdCl}_2$ (10% by wt)

(particularly 4) are not in favour of this flux-action mechanism. Such a phase transformation perhaps could be attributed to the incorporation of Cl^- ions in CdS matrix in the process of doping. Experiments with $\text{ZnS}^{21,22}$ powders have shown that both the rate and temperature for the hexagonal/cubic phase transformation can be greatly affected by impurities such as iron and chloride. It is interesting to note that Kremheller²² observed cubic to hexagonal phase transition of ZnS at 975°C in presence of chlorides but no transformation even at 1175°C in the absence of chlorides. Observations made by Behringer and Corrsin²³ in their XRD study of evaporated CdS films are also interesting. They have shown that the pyrolytic treatment to the films in contact with CdCl_2 containing CdS powder modifies the orientation from preferred to random.

To understand the role of chloride ions in bringing about the phase transformation, it would be appropriate to consider the difference between these two polymorphs of CdS. Actually both in cubic and hexagonal modifications of CdS, Cd atoms (also S atoms) are related one to other as are lattice points of close packed structures and a Cd atom is tetrahedrally surrounded by four S atoms and vice-versa. The only difference exists in the stacking sequences of close packed planes of Cd and S sub-lattices (Fig. 3.7). The phase transformation would therefore be

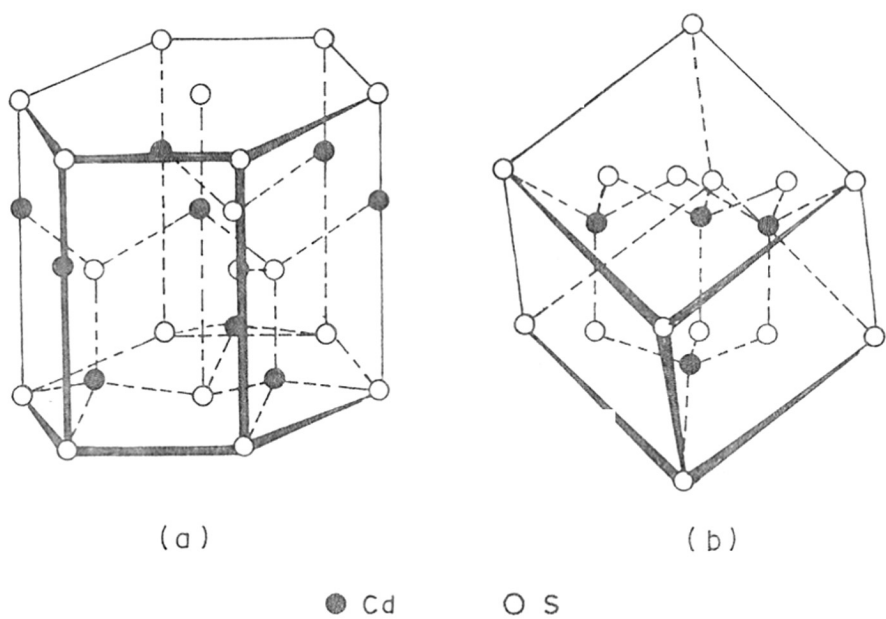
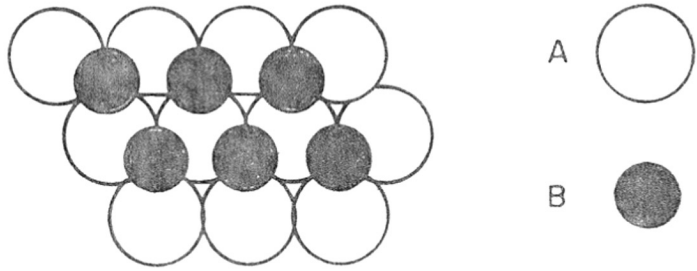
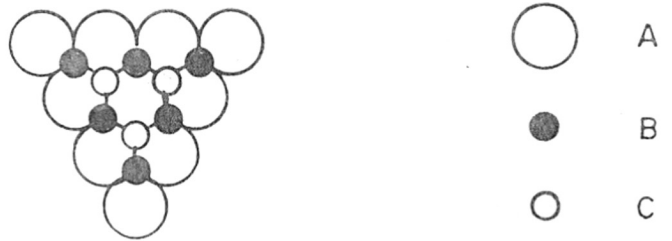


FIG. 3.7 (A) THE CRYSTAL STRUCTURES OF
(a) HEXAGONAL AND (b) CUBIC CdS



(a)



(b)

FIG. 3-7 (B) THE STACKING SEQUENCE :

(a) ABABA ----- OF HEXAGONAL CLOSE
PACKING

(b) ABCABCA ----- OF FACE-CENTERED CUBIC
STRUCTURE

possible only when there is a change in the stacking sequence by atomic rearrangements which may advance through certain vacancies.

It is well-known that there is a creation of Cd vacancies by the incorporation of Cl^- ions in CdS lattice in order to maintain the overall charge neutrality. These vacancies may bring about rearrangements of atoms in such a way that the stacking sequence ABCABCA ... of the face-centered cubic structure changes to more stable stacking sequence ABABA ... of hexagonal close-packing [Fig. 3.7(B)]. Atomic rearrangements in the absence of vacancies may not be easily possible in the close packed structure, if we consider atoms as hard spheres touching each other.

3.3. SURFACE MORPHOLOGY

Scanning Electron Micrographs (SEM photographs) of the undoped and doped (Cu concentration = 0.05 by wt) thick films of CdS are presented in Figs. 3.8 (A) and 3.8(B) respectively. It is clearly seen that:

(1) Undoped film consists of uniform grains of average grain size equal to $\sim 1 \mu$ [Fig. 3.8(A)]

(2) Doped film consists of large but non-uniform grains; size of which varies from $\sim 4 \mu$ to 10μ and all the crystallites are interconnected [Fig. 3.8(B)].

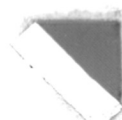
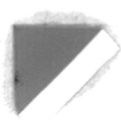


FIG. 3-8 (A) SCANNING ELECTRON MICROGRAPH
OF THE UNDOPED THICK FILM OF CdS

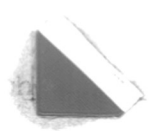
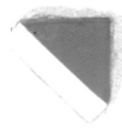


FIG. 3-8 (B) SCANNING ELECTRON MICROGRAPH
OF THE DOPED THICK FILM OF CdS
(.OPTIMUM Cu CONCENTRATION)

Scanning electron micrographs of the doped films with other Cu concentrations (e.g. 0.1 to 1% by wt of CdS) were also taken. These photomicrographs (not shown here) indicate that:

(1) Grain-size does not change appreciably with variation in Cu concentration.

(2) No systematic differences in the surface morphology of these films are observed.

By comparing the electron diffraction patterns of the evaporated CdS films to XRD patterns of the same samples, Shalimova et al.²⁴ and Galkin et al.²⁵ have discovered that the larger grains were hexagonal, whereas the smaller grains were a mixture of cubic and hexagonal phases. While investigating the properties of spray-deposited CdS films, Ma and Bube¹³ have actually pointed out the dependence of surface morphology on structure. Their observations are similar to those reported by Shalimova et al.²⁴ and Galkin et al.²⁵.

It has been already discussed that cubic dominated mixed phase exists in undoped thick films, whereas purely hexagonal phase exists in doped thick films of CdS (see previous section). In this way, our structural and surface morphological investigations confirm and provide an additional support to the results obtained by Shalimova et al.²⁴, Galkin et al.²⁵ and Ma and Bube¹³.

3.4. ELECTRICAL CONTACTS AND
CURRENT VOLTAGE CHARACTERISTICS

The performance of photoconductors in various devices depends upon an ohmic contact applied to the photoconductor. An ohmic contact is one that can replenish charge carriers drawn out of one electrode under the influence of the applied electric field in order to keep the electrical neutrality. The presence of ohmic contacts assures that flow of current initiated by photo-excitation will be terminated only by the recombination processes occurring in the photoconductor and not by the depletion of majority carriers by the applied field²⁶.

To verify the ohmic nature of the evaporated indium contacts made to these films, we have determined current-voltage [I-V] relationships for the d.c. applied field of 0-60 volts. I-V characteristics of undoped films, in dark and in light, are plotted in Fig. 3.9. These plots show a slight deviation from the linearity indicating a departure from the perfect ohmic behaviour.

I-V characteristics of the film doped with optimum Cu concentration are presented in Fig. 3.10. It is found that the dark current as well as photocurrent vary linearly [i.e. ohmically] with the applied voltage. This ohmic dependence of the current (dark and light) on the applied voltage is also confirmed for the doped films with other Cu

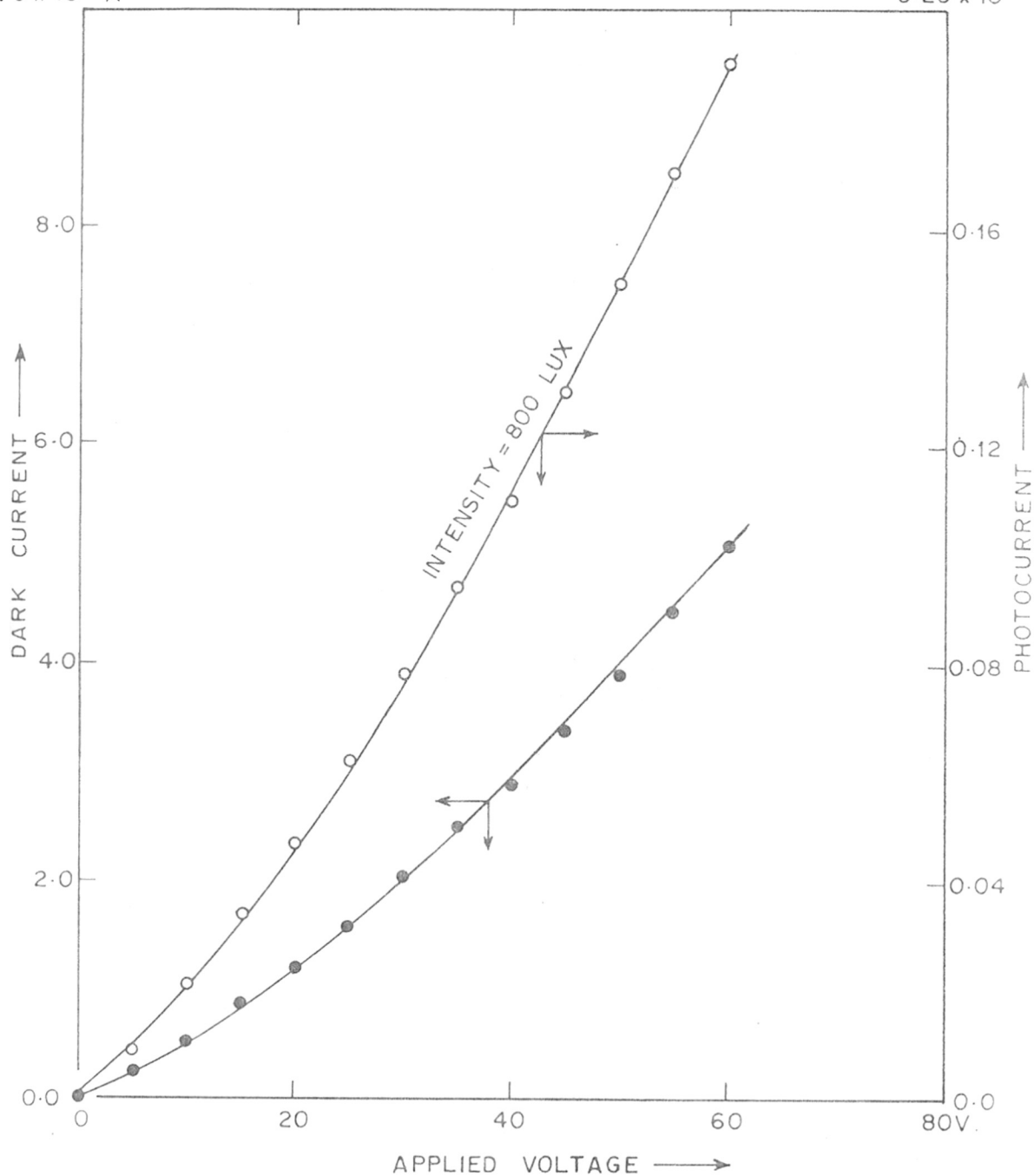
10.0×10^{-9} A 0.20×10^{-6} A

FIG. 3.9 CURRENT-VOLTAGE CHARACTERISTICS OF THE UNDOPED THICK FILM OF CdS (AT ROOM TEMPERATURE)

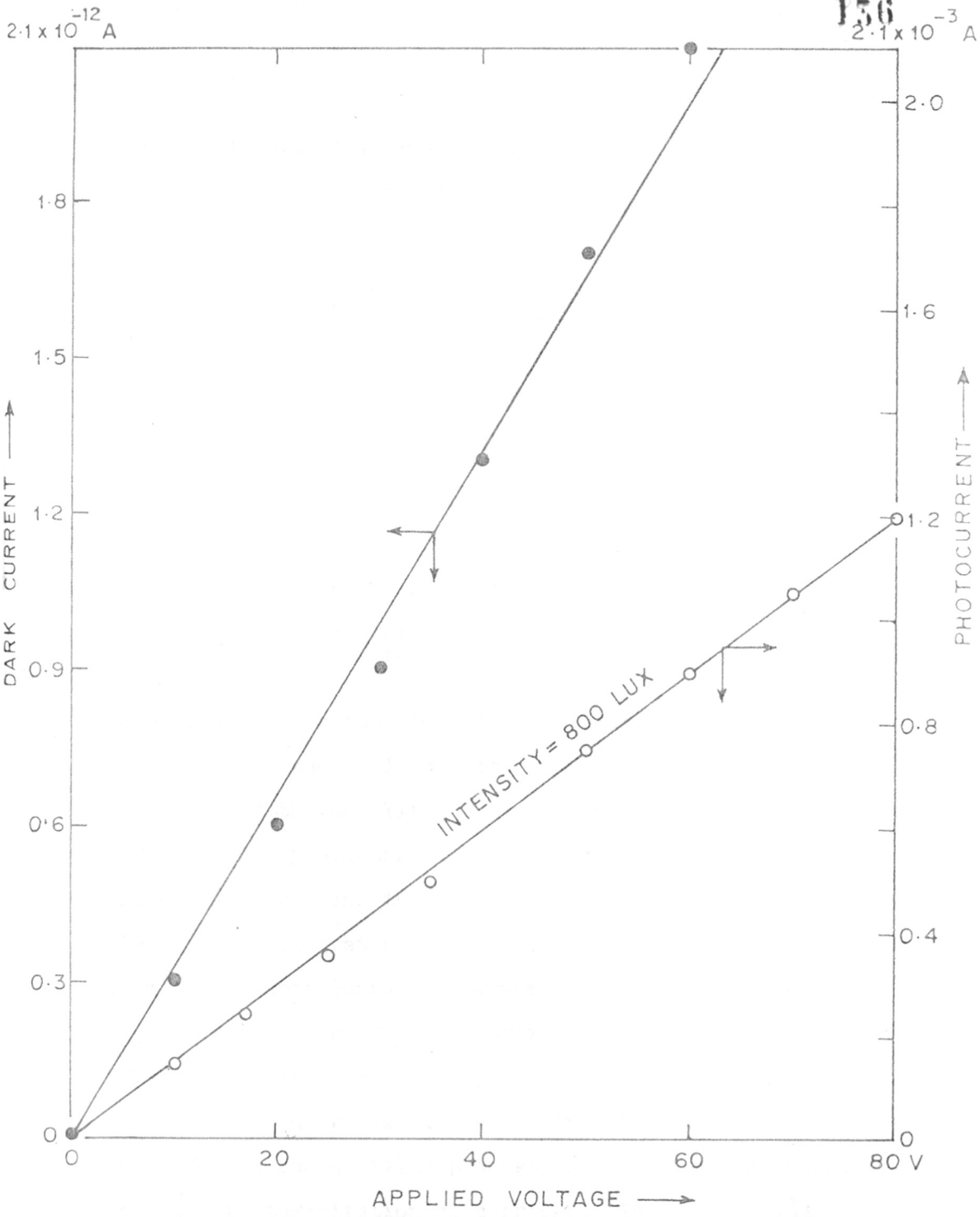


FIG. 3.10 CURRENT - VOLTAGE CHARACTERISTICS OF THE DOPED THICK FILM OF CdS (AT ROOM TEMPERATURE)

concentrations. All these results confirm an ohmic nature of the vacuum-evaporated indium contacts made to the thick films of CdS.

The linear behaviour of the photocurrent (I_p) with the applied voltage (V) is consistent with the relation²⁷,

$$I_p = \frac{e \mu \tau f}{L^2} \cdot V$$

where e = electron charge,

τ and μ = lifetime and mobility of free electrons,

L = interelectrode spacing,

f = rate at which free electrons are generated as a result of photoexcitation.

According to this equation, the photocurrent should increase linearly with the applied voltage assuming that neither the lifetime nor the mobility of electrons are voltage dependent. In principle, photocurrent can be made indefinitely large either by increasing the voltage or by decreasing the inter-electrode spacing at a specific illumination level. The need of an ohmic contact, however, sets an upper limit to the maximum electric field applicable to the photoconductor²⁶. If the field is increased beyond a critical value, the injection of charge carriers from the ohmic cathode will dominate the conductivity process in the material, rather than the photoexcitation of carriers. In view of this possible problem, all the electrical and photoconducting measurements have been carried out by applying a d.c. potential which falls in the ohmic range of variation.

3.6. DARK CONDUCTIVITY AS A FUNCTION OF TEMPERATURE

The deliberate incorporation of impurities in a photoconducting material (semiconductor or insulator) always affects its dark conductivity. For example, donor impurities in n-type material/acceptor impurities in p-type material increase the dark conductivity. Donor impurities in p-type material/acceptor impurities in n-type material decrease the dark conductivity.

Quantitatively the location and density of imperfection levels can be determined by several methods²⁸. Variation of the free carrier density with the temperature is the most convenient method often used for this purpose. Experimentally, it involves the measurement of dark conductivity as a function of temperature.

For the n-type of semiconductor, electrical conductivity (σ) can be expressed as

$$\sigma = n e \mu$$

where n and μ = density and mobility of free electrons respectively,

e = electronic charge.

The conductivity (σ) is generally controlled by thermal raising of electrons from the levels present in the forbidden gap to the conduction band and by the capture of

free electrons by these levels. It varies with temperature according to Wilson's expression:

$$\sigma = \sigma_0 \exp (-\Delta E/kT)$$

where σ_0 = pre-exponential factor (mho.cm⁻¹),
 ΔE = energy of activation (eV),
 k = Boltzman constant (eV/^ok),
 T = absolute temperature (^oK).

A plot of $\ln \sigma$ against $1/T$ yields a straightline having a negative slope of $-\Delta E/k$ and an intercept equal to $\ln \sigma_0$. Such a plot also takes into account of the variation in electron mobility (μ) with the temperature. However, since (i) μ is approximately proportional to $T^{-3/2}$ in CdS and (ii) the density of states term in the expression for electrical conductivity (σ) involves a factor $T^{3/2}$, σ should be directly proportional to the density of free electrons. Figs. 3.11 and 3.12 are the plots of $\log (I_d)$ versus $10^3/T$ (where I_d = the magnitude of dark current and T = absolute temperature) over the temperature range of 150-370^oK for the undoped and doped thick films of CdS respectively.

As perceptible from Fig. 3.11; I_d of the undoped film is such that:

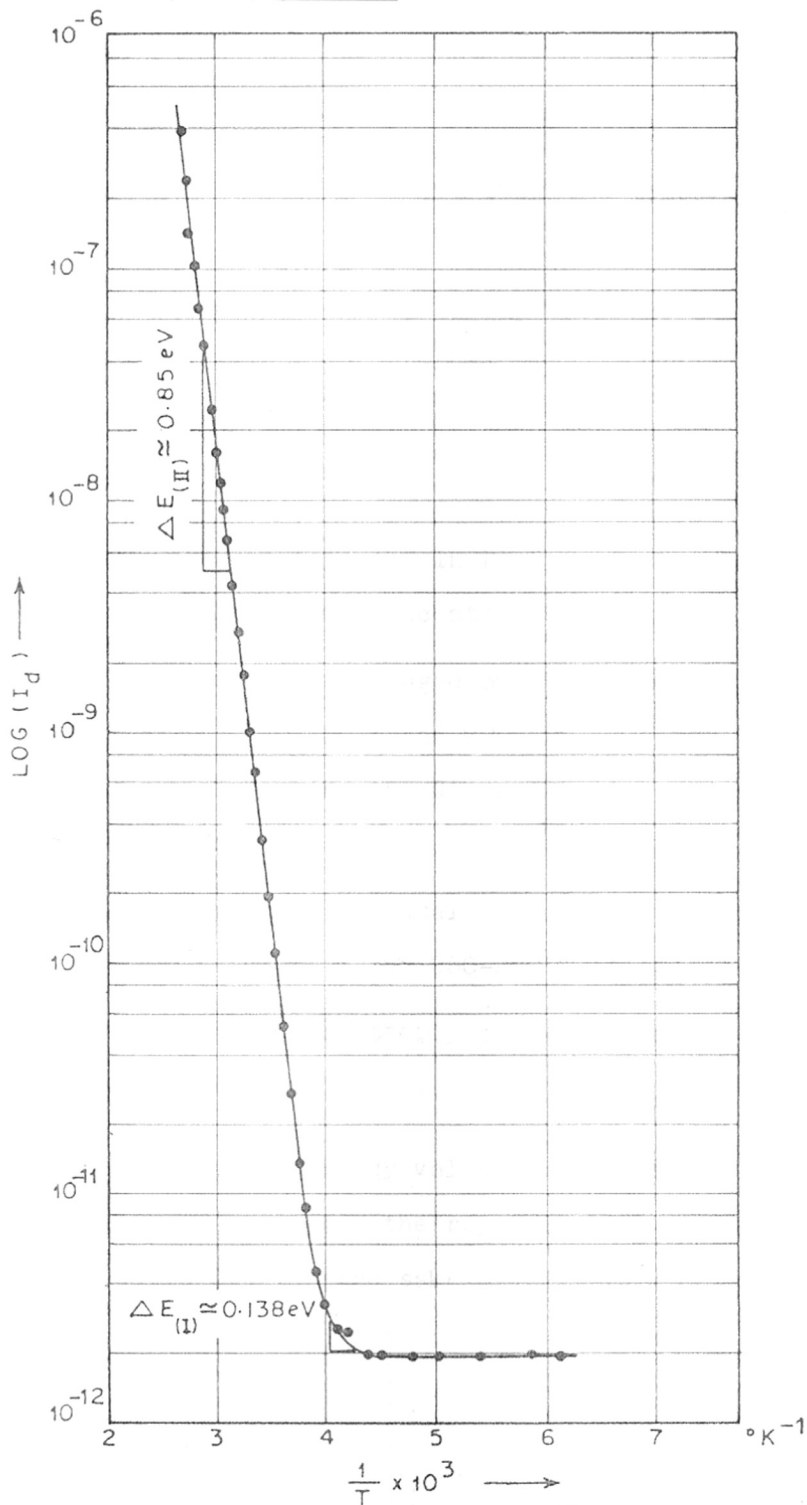


FIG. 3.11 PLOT OF $\text{LOG}(I_d)$ VS $\frac{10^3}{T}$ (WHERE I_d = DARK CURRENT AND T = ABSOLUTE TEMPERATURE) FOR THE UNDOPED THICK FILM OF CdS

(1) It remains unchanged over the temperature range of 150-230^oK.

(2) It increases very slowly over the temperature range of 230-260^oK (slope I).

(3) It increases steeply over the temperature range of 270-370^oK (slope II).

Similarly, as depicted in Fig. 3.12, I_d of the doped film (**with** optimum Cu concentration) is such that:

(1) It remains unchanged over the temperature ranges of 150-200^oK, 220-250^oK and 290-320^oK. (This is a typical behaviour suggesting the discrete nature of the imperfection centers).

(2) It increases gradually over the temperature ranges of 200-220^oK (slope I) and 250-290^oK (slope II).

(3) It increases steeply over the temperature range of 290-370^oK (slope III).

The activation energy values as determined from the slopes of these plots and the reported values are presented in Table 3.5 for the sake of comparison.

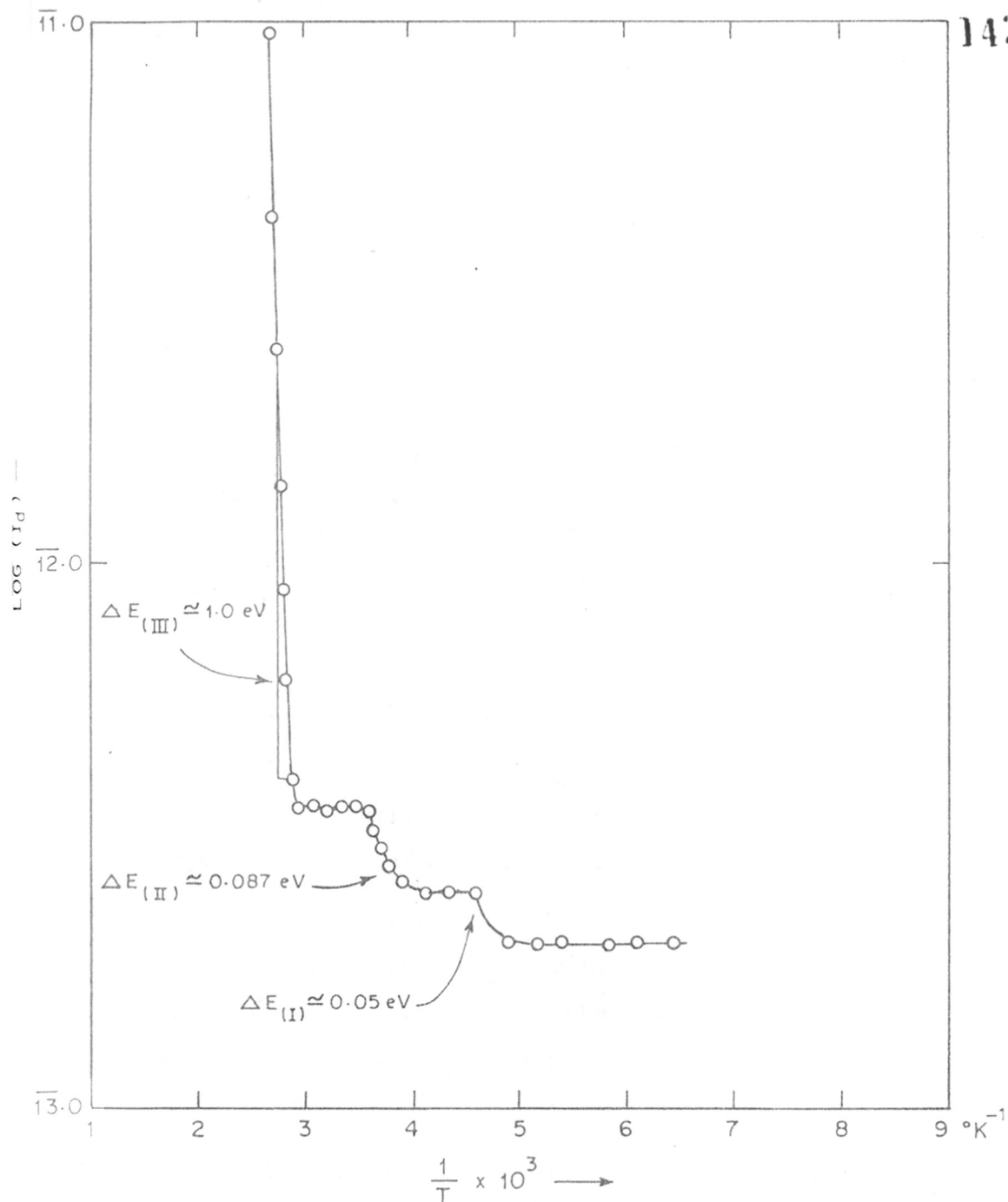


FIG. 3-12 PLOT OF $\text{LOG}(I_D)$ VS $\frac{10^3}{T}$ FOR THE DOPED THICK FILM OF CdS WITH OPTIMUM Cu CONCENTRATION

TABLE 3.5

ACTIVATION ENERGY VALUES AND NATURE
OF THE IMPERFECTION CENTERS

Sr. No.	Sample	Activation energy eV		Nature of the imperfection center
		Present study	Reported study	
1.	Undoped i.e. pure CdS film	0.138	0.14 ^a	Donor
		0.85	0.83 ^a	Acceptor
2.	Doped, i.e. CdS:Cu:Cl film	0.059	0.05 ^a	Donor
		0.087		Donor
		1.05	1.00 ^b	Acceptor

a = See references 29, 30.

b = See references 28, 31.

As indicated in Table 3.5, there are two principal ionization energies of imperfections for undoped films:

(1) A level at 0.138 eV may be the same shallow trap (0.14 eV) reported by Woods and Nicholas^{29,30}. Such a level is characteristic of Cd-rich crystals and has been attributed to individual S vacancies in the charge configuration³⁰.

(2) A level at 0.85 eV can be compared with the defect at 0.83 eV reported by Woods and Nicholas²⁹ in their conductivity glow curve measurements on CdS single crystals.

This trap center is generally formed by photochemical reactions. Since it is found in both S rich and Cd rich crystals, Woods and Nicholas³⁰ suggested that it may be a complex of Cd and S vacancies associated in nearest neighbour sites. A level at 0.85 eV, in the present case, can also be interpreted on similar lines.

There are three principal ionization energies of imperfections for doped thick films of CdS:

(1) A level at 0.059 eV, when compared with the reported data, appears to be a donor level associated with chloride centers^{28,30}.

(2) A level at 0.087 eV can be assumed to be an additional donor level formed by either chloride impurity, individual S vacancies or their complex association.

(3) In view of the known data for CdS crystals, a level at 1.05 eV may be attributed to a compensated acceptor type of sensitizing centers^{28,31}. The physical and chemical identity of such centers - which give rise to photosensitivity²⁷ - has not yet been rigorously determined. It can be associated with either Cu impurity or Cd vacancy/Cu impurity - Cd vacancy complex³².

3.6. PHOTSENSITIVITY

The representative values of photosensitivity of CdS photoconductors prepared by various techniques are presented in Table 3.6. It reveals the superior sensitivity of our films.

TABLE 3.6

PHOTSENSITIVITY VALUES OF CdS PHOTO-
CONDUCTORS PREPARED BY VARIOUS TECHNIQUES

Sr. No.	Method of preparation	Photosensitivity = $\frac{\text{Photocurrent}}{\text{Dark current}}$	Ref. No.
1.	Single crystal techniques	$10^5 - 10^6$	33
2.	Sintered layer techniques	$10^6 - 10^7$	1,34
3.	Thin film techniques		
	a: Evaporation in vacuum	$10^4 - 10^7$	35
	b: Sputtering	10^5	36
	c: Chemical bath deposition	50	12
	d: Chemical spray deposition (spray pyrolysis)	10^6	37,38
	e: Chemical printing*	10^4	39
4.	Thick film technique		
	a: Undoped*	10^2	Present investi- gation
	b: Doped with optimum Cu concentration	$10^8 - 10^9$	
	c: Heavily doped with Cu	10^4	

* These techniques do not involve any impurity incorporation for sensitization.

3.6.1. Photosensitivity and oxygen chemisorption

As reviewed in Chapter (1), the chemisorption of oxygen is of basic importance in understanding the photoconductivity processes in CdS. It was, therefore, anticipated that oxygen chemisorption could play an important role in the overall photoelectronic behaviour of our films. As described in Chapter (1), a variety of experimental techniques have been employed to probe oxygen chemisorption in CdS indirectly. The most convenient method used for this purpose involves the measurement of electrical conductivity (dark as well as light) as a function of temperature in the presence (adsorption) and absence (desorption) of oxygen.

We preferred to carry out dark conductivity measurements as a function of temperature during the oxygen adsorption-desorption cycles. Plots of dark current versus temperature data corresponding to a doped film with optimum Cu concentration are shown in Figs. 3.13 and 3.14.

The curve in Fig. 3.13 indicates the electrical conductivity behaviour of an as-prepared (virgin) film during the desorption run in which it is heated upto 200°C in the dark under vacuum. As evident from this curve:

(i) I_d (magnitude of the dark current) increases gradually

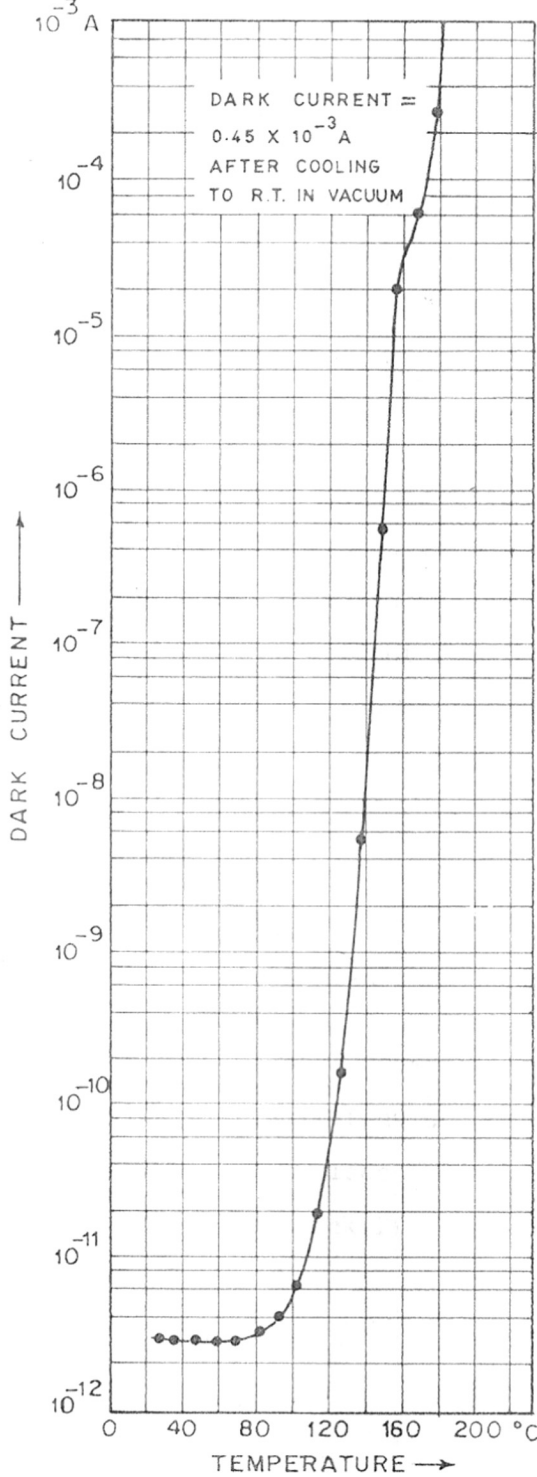


FIG. 3.13 VARIATION IN THE DARK CURRENT WITH THE TEMPERATURE FOR THE DOPED FILM WITH OPTIMUM Cu. CONCENTRATION WHILE HEATING IN VACUUM.

in the beginning upto 100°C , (ii) I_d rises steeply from 10^{-12} (at 100°C) to 10^{-3} A (at 200°C), (iii) on cooling the sample from 200°C to room temperature without breaking the vacuum, I_d observed is of the order of 10^{-4} A and sample exhibits no photosensitivity.

The curve in Fig. 3.14 illustrates the electrical conductivity behaviour of the same vacuum-treated film during the adsorption run in which it is heated upto 200°C in air and in the dark. As evident from this curve; (i) I_d increases gradually in the beginning from 10^{-4} A (at room temperature) to 10^{-3} A (at 110°C), (ii) I_d falls off rapidly above 110°C from 10^{-3} A to 10^{-6} A, (iii) on cooling the sample from 200°C to room temperature in air, I_d attains the value of the order of 10^{-12} A and the sample exhibits the original high photosensitivity.

Similar type of measurements were also performed on the doped samples with different Cu concentrations. The data given in Table 3.7 summarises the experimental results of oxygen chemisorption on thick films of CdS with various Cu concentrations.

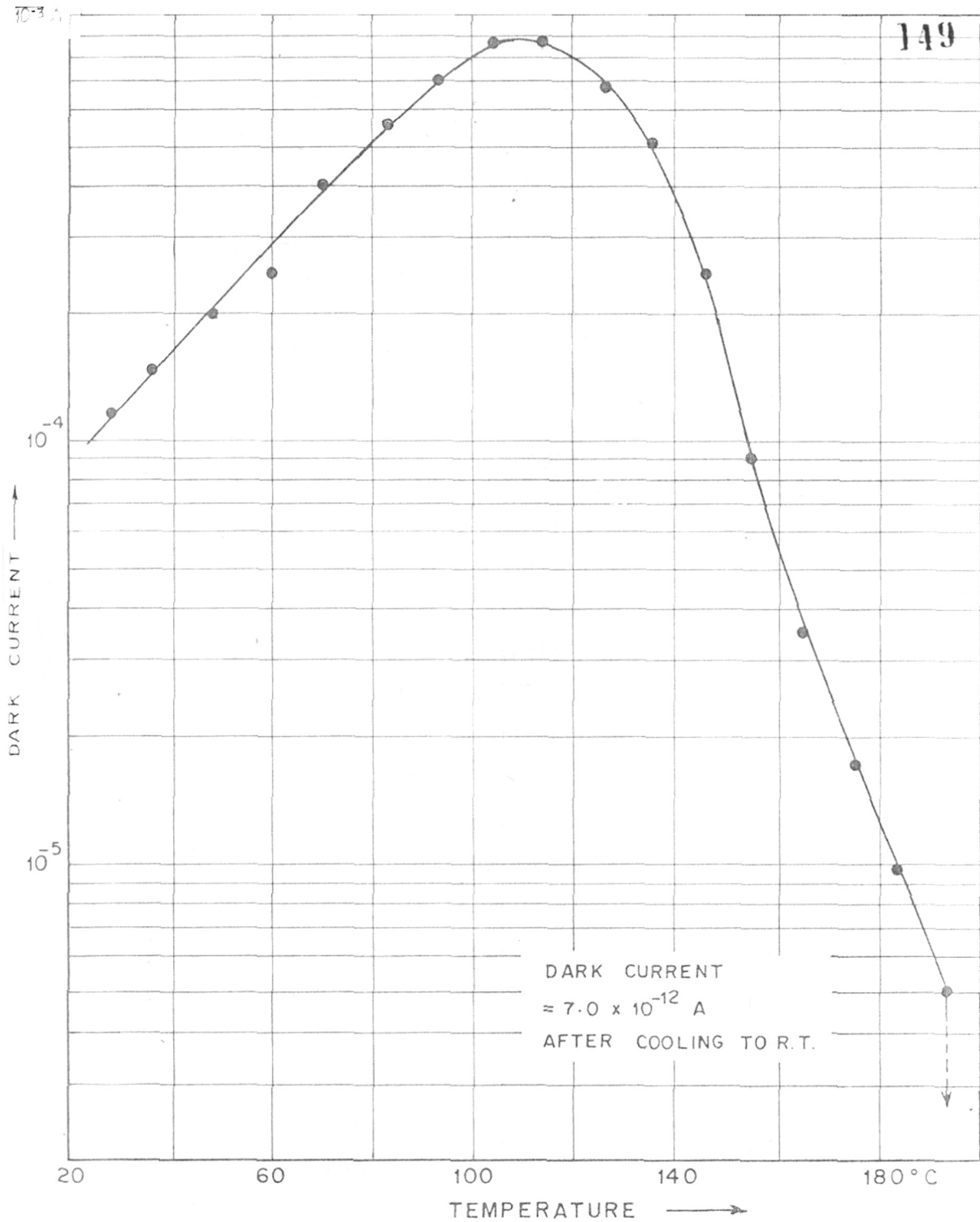


FIG. 3.14 VARIATION IN THE DARK CURRENT WITH THE TEMPERATURE FOR THE VACUUM-TREATED FILM WHILE HEATING IN AIR

TABLE 3.7

SUMMARY OF THE EXPERIMENTAL RESULTS OF
OXYGEN-CHEMISORPTION ON THE THICK FILMS
OF CdS

Sr. No.	Concentration of Cu added as CuCl ₂ (by wt of CdS)	Dark current at room temperature A		
		As prepared	On desorption	On re-adsorption
1.	0.05	3.0×10^{-12}	4.5×10^{-4}	7.0×10^{-12}
2.	0.10	4.0×10^{-12}	3.5×10^{-2}	5.0×10^{-12}
3.	0.20	4.5×10^{-12}	5.0×10^{-5}	6.0×10^{-12}
4.	0.30	3.0×10^{-12}	1.5×10^{-3}	2.0×10^{-9}
5.	1.00	4.0×10^{-12}	1.5×10^{-10}	4.0×10^{-12}

There are some quantitative discrepancies regarding the values of electrical conductivity of these films although subjected to similar ambient treatments. Since the data presented in Table 3.7 deals with a adsorption-desorption period of only 15-20 minutes; there is a lack of complete experimental data with respect to the kinetics of chemisorption (to be discussed afterwards) for each Cu concentration, which may apparently give rise to such discrepancies. The data presented in Table 3.7, however, satisfies the restricted intention of showing the complete reversibility of chemisorption effects on electrical conductivity.

Although it is difficult to separate true thermal changes in dark conductivity from chemisorption effects in case of semiconductors, we have drawn certain meaningful conclusions from these results:

[A] An initial gradual increase in I_d [observation (i) of Figs. 3.13 and 3.14] is attributed to the thermal ionization of impurity centers availing more number of free electrons for conduction (see Section 3.5).

[B] The high dark conductivity at 200°C [observation (ii) of Figs. 3.13 and 3.14] is consistent with the typical thermal behaviour of a semiconductor in which electrons are thermally excited from valence band to conduction band.

[C] The observations (iii) (of Figs. 3.13 and 3.14) indicate the phenomenal reversible variation (8 orders of magnitude) in the room temperature dark conductivity. Such variations in dark conductivity can be discussed on the basis of a following phenomenological model proposed earlier by Micheletti and Mark⁴⁰.

Fig. 3.15 is the band model for thin photoconductor under illumination. From an electronic view point, chemisorbed oxygen introduces extrinsic surface states in the principle band gap of CdS. These chemisorbate surface states of concentration N_t are shown to be acceptorlike state at 0.9 eV below the bottom-edge of the conduction band.

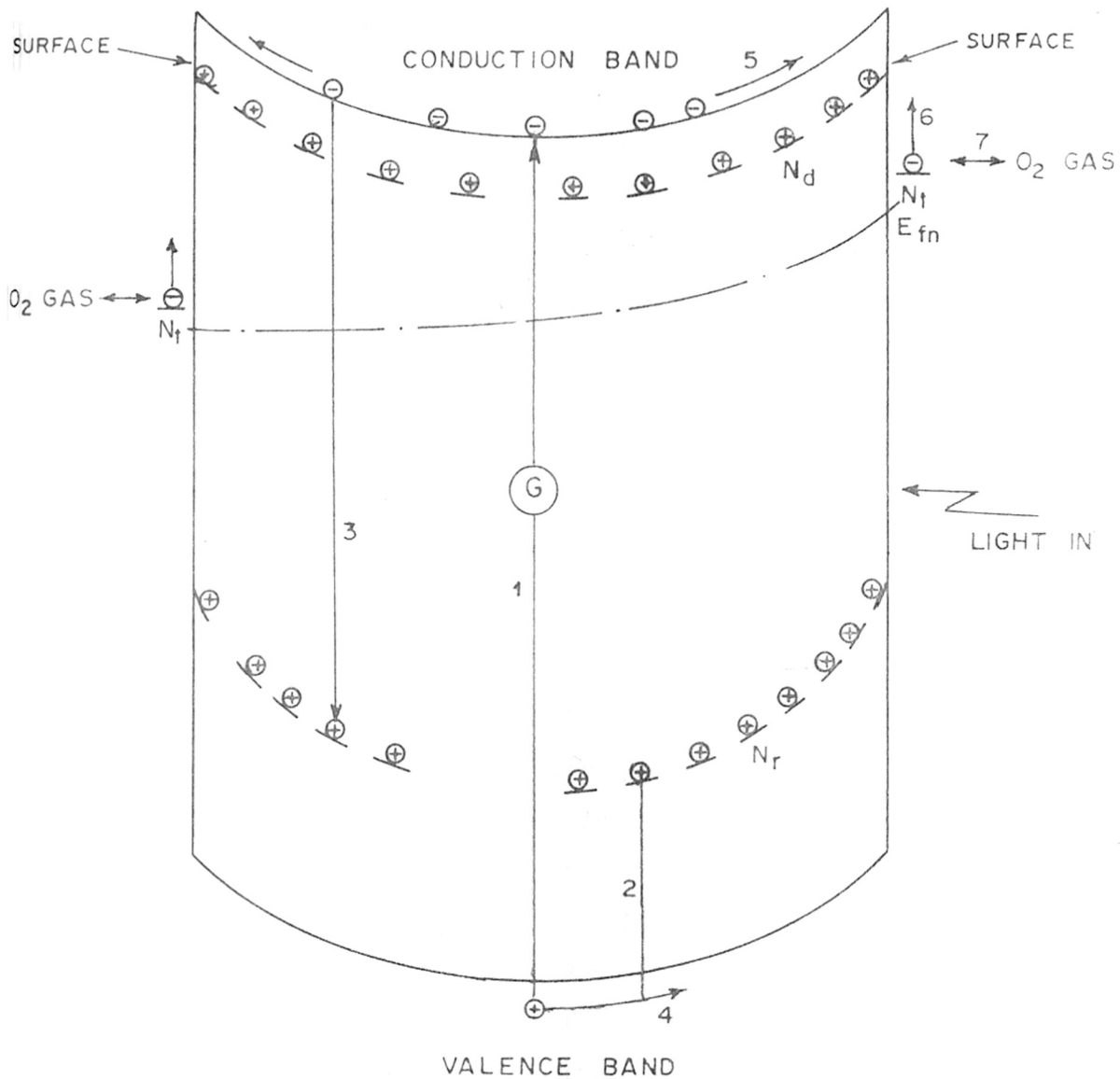


FIG. 3.15 BAND MODEL ILLUSTRATING OXYGEN CHEMISORPTION-DESORPTION ON CdS

In addition, there are donor levels of concentration N_d (probably due to chloride) and recombination centers of concentration N_r (probably due to copper). The quasi-Fermi level for electron, (E_{fn}) is raised at the right side of the figure which corresponds to illumination incident from the right. This is in accordance with a greater population of the surface states and consequently a larger electrostatic surface barrier on the illuminated surface compared to the unilluminated one. The processes to be considered are labelled in Fig. 3.15 as:

(1) Optical generation of carriers by band gap excitation, (2) capture of photoexcited holes by the recombination centers, (3) bulk-recombination, (4) photo-desorption in which photoexcited holes can recombine with electrons at the surface (i.e. with chemisorbed ions), if their transit time to the surface is shorter than their lifetime, (5) chemisorption in which electrons from the conduction band are captured by the physically adsorbed oxygen at the surface, (6) thermal desorption in which electrons are thermally released from the surface into the conduction band, (7) physical adsorption and desorption of uncharged oxygen between the surface and the ambient.

With this model, it is possible to explain 8 to 10 orders increase in I_d , the magnitude of room temperature dark current (Fig. 3.13) in terms of thermal desorption of

oxygen indicated by process (6). The thermally released electrons by process (6) contribute significantly to the electrical conductivity in the dark even at room temperature. Similarly, decrease in I_d by same orders of magnitude (Fig. 3.14) can be associated with the chemisorption of oxygen indicated by process (5). This process reduces the density of conduction electrons thereby causing decrease in dark conductivity.

As stated earlier, we report 8 to 9 orders change in the magnitude of room temperature dark conductivity as a result of adsorption-desorption ambient treatments. Micheletti and Mark⁴⁰ have reported 6 to 7 orders change in the magnitude of the same for the screen-printed films of CdS treated under similar ambient conditions. Our photoconductivity values, however, are quite comparable with their data. This leads to the conclusion that chemisorption of oxygen is more effective in lowering the dark current (while photocurrent remains unaltered) which ultimately increases photosensitivity in the present case. This strong oxygen-chemisorption perhaps could be related to the larger thickness ($\sim 20\mu$) and bigger grain size ($\sim 4-10 \mu$) of our doped samples, compared to the thickness ($\sim 3-5 \mu$) and grain size ($\sim 1 \mu$) of the films used by Micheletti and Mark⁴⁰. This along with the typical surface morphology of the films might have offered a high surface to volume ratio for the fused intergranular contacts or 'necks' which are supposed to be responsible for the chemisorption in the sintered films.

Finally, it should be noted that:

(1) In absence of chemisorbed oxygen, our films exhibit very high dark conductivity and with photoexcitation, they do not show any change in conductivity.

(2) In presence of chemisorbed oxygen, these films in contrast exhibit very low dark conductivity and with photoexcitation, they exhibit manyfold change in conductivity.

The high photosensitivity of the as-prepared thick films of CdS, therefore, indicates that these have already passed through a process of chemisorption in the preparation procedure.

We have used a mechanism proposed by Micheletti and Mark⁴⁰ (MM) to account for the key role of chemisorbed oxygen in enhancing the photosensitivity of CdS films. It is applicable to a case in which strongly absorbed light is used with a thicker sample so that the conducting channel is narrow and near the surface. According to MM model, chemisorbed oxygen induces the surface state in the bandgap of CdS. Like a bulk defect state, this extrinsic surface state may function either as a trap when it is in communication with only one band or a recombination center when it is in communication with both the bands. Unlike the bulk defect states, the surface states are usually associated with a space-charge layer that strongly influences the transition

rate of bulk carriers to surface. In this way, there are three dominant charge quantities open to consideration:

- (1) the negative charge at the surface in the adsorbate state,
- (2) compensating positive charge in the bulk consisting of ionised donors,
- (3) photoexcited holes captured by the recombination centers (Fig. . 3.15).

The accumulation of negative charge in the chemisorbate states exerts a considerable surface potential repulsive for electrons. Thus, the free electrons are concentrated in a channel through the center of the sample. On the other hand, the holes captured in the recombination centers get accumulated near the surface in the space-charge regions because of the small concentration of free electrons available for recombination in this region. The physical separation of the free electrons from the majority of the holes captured in the recombination centers causes the centers in the space-charge region to have a very small effective capture cross-section for electrons.

Referring to Fig. 3.15, the recombination centers now can be divided roughly into two classes:

(I) Those in space-charge region having a high concentration of holes and a small effective capture cross-section for electrons.

(II) Those in the center of the sample having high concentration of electrons but a small effective capture cross-section for holes.

A small capture cross-section for electrons of the class (I) centers leads to an increase in the lifetime of photoexcited electrons in the conduction band at the surface and hence to high surface photoconductivity^{4,40} (since photoconductivity \propto lifetime of majority carriers). Exactly reverse situation of the class (II) centers gives rise to small bulk photoconductivity^{4,40}.

3.6.2. Kinetics of oxygen-chemisorption

Curves in Fig. 3.16 illustrate the variation in dark conductivity as a function of time for a previously vacuum-treated sample (i.e. free from chemisorbed oxygen) exposed to air at six different temperatures. Since the measurements have to be performed on the same sample of a specific dopant concentration, it was necessary to heat the sample at 200°C under vacuum for some time after each readsorption treatment at a given temperature. The data plotted in Fig. 3.16 corresponds to a doped film with Cu concentration of 0.1% by wt of CdS. The important observations are:

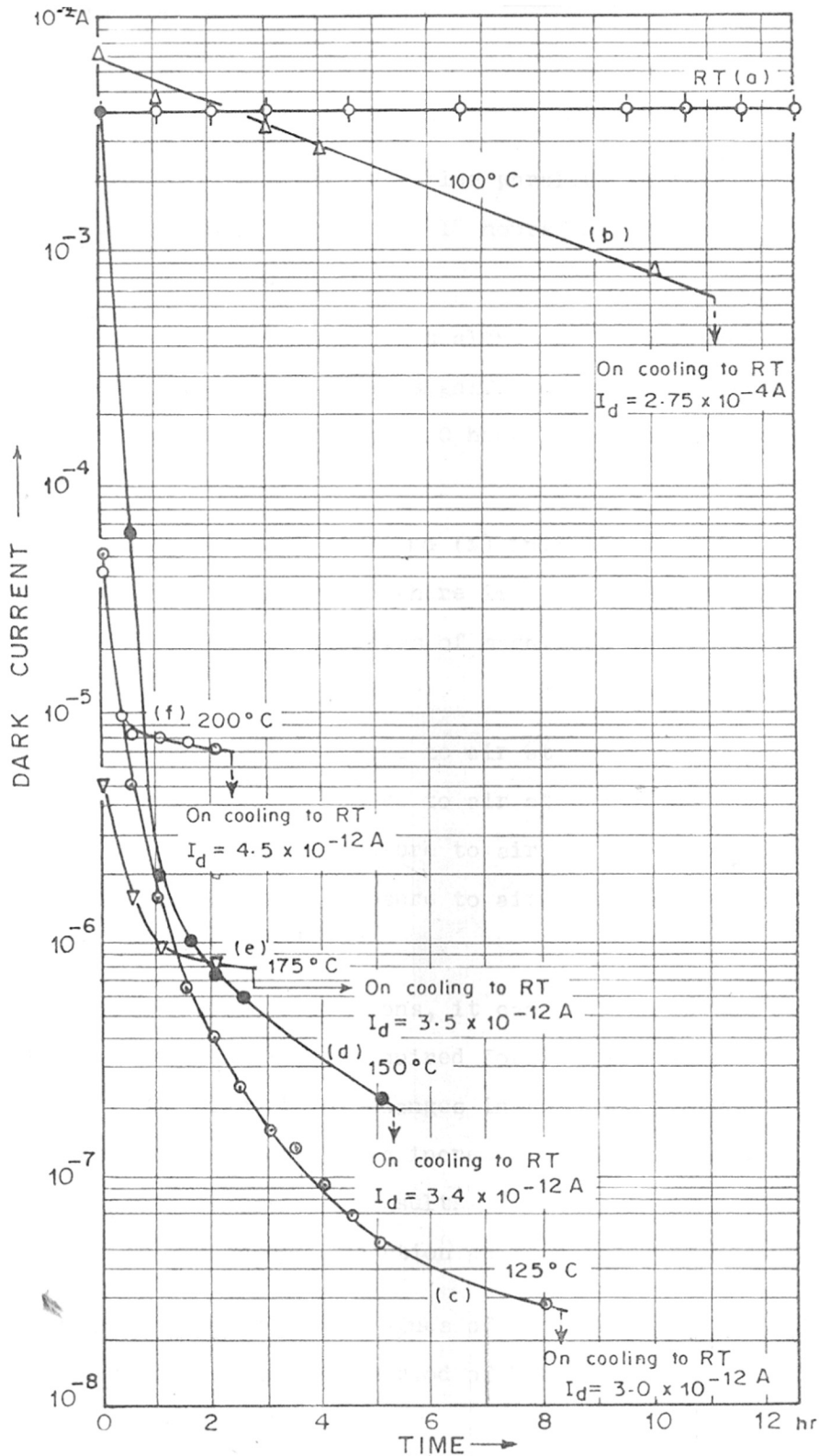


FIG. 3.16 VARIATION IN THE DARK CURRENT WITH THE TIME OF EXPOSURE TO AIR AT DIFFERENT TEMPERATURES FOR A VACUUM-TREATED FILM

(1) Plot (a) is a straight-line parallel to X-axis, showing no change in I_d even after 12 hours exposure to air at room temperature.

(2) Curve (b) indicates that although I_d decreases gradually with time, there is no significant change in its room temperature value even after 10 hours exposure to air at 100°C .

(3) Curves (c), (d), (e) and (f) indicate that I_d falls off rapidly with time and there is a decrease in its room temperature value by 9 orders of magnitude as a result of:

- (i) 8 hrs exposure to air at 125°C ,
- (ii) 5 hrs exposure to air at 150°C ,
- (iii) 2.5 hrs exposure to air at 175°C , and
- (iv) 1.5 hrs exposure to air at 200°C respectively.

With these observations, it can be pointed out that the characteristic time required for the chemisorption to cause significant changes in the room temperature dark conductivity decreases with increase in temperature. This is in agreement with the results of Bhide et al.⁴¹ on the kinetics of oxygen-chemisorption on thin films of CdS.

We have chosen the values of dark current (I_d) corresponding to a adsorption period of 2 hrs at the

temperatures 125°C, 150°C, 175°C and 200°C from the curves of Fig. 3.16. Corresponding values of $\log(I_d)$ are then plotted against $10^3/T$ (where, T = temperature in °K) in Fig. 3.17. The activation energy value as calculated from the slope of this plot is ~ 0.90 eV. It is in good agreement with the value 0.91 eV reported by Mark⁴² who associated it with an energy level induced by chemisorbed oxygen below the bottom edge of the conduction band in CdS.

Deeper insight could be provided into the kinetics of chemisorption only when it is studied with respect to various dopant concentrations, applied field and illumination intensities⁴¹ which has not been possible during this study. However, the data presented in Fig. 3.16 are useful to demonstrate that the changes due to chemisorption, which otherwise may require several days to take place at room temperature, can be brought about just by heating for few hours at elevated temperatures.

3.6.3. X-ray photoelectron spectroscopic (XPS) studies of oxygen-chemisorption

As the adsorption of oxygen on the surface of CdS is in the form of radicals⁴³, modern surface sensitive techniques such as XPS, AES, SIMS are expected to give some direct evidence in support of the formation of chemical bonds at the active sites on the surface of CdS.

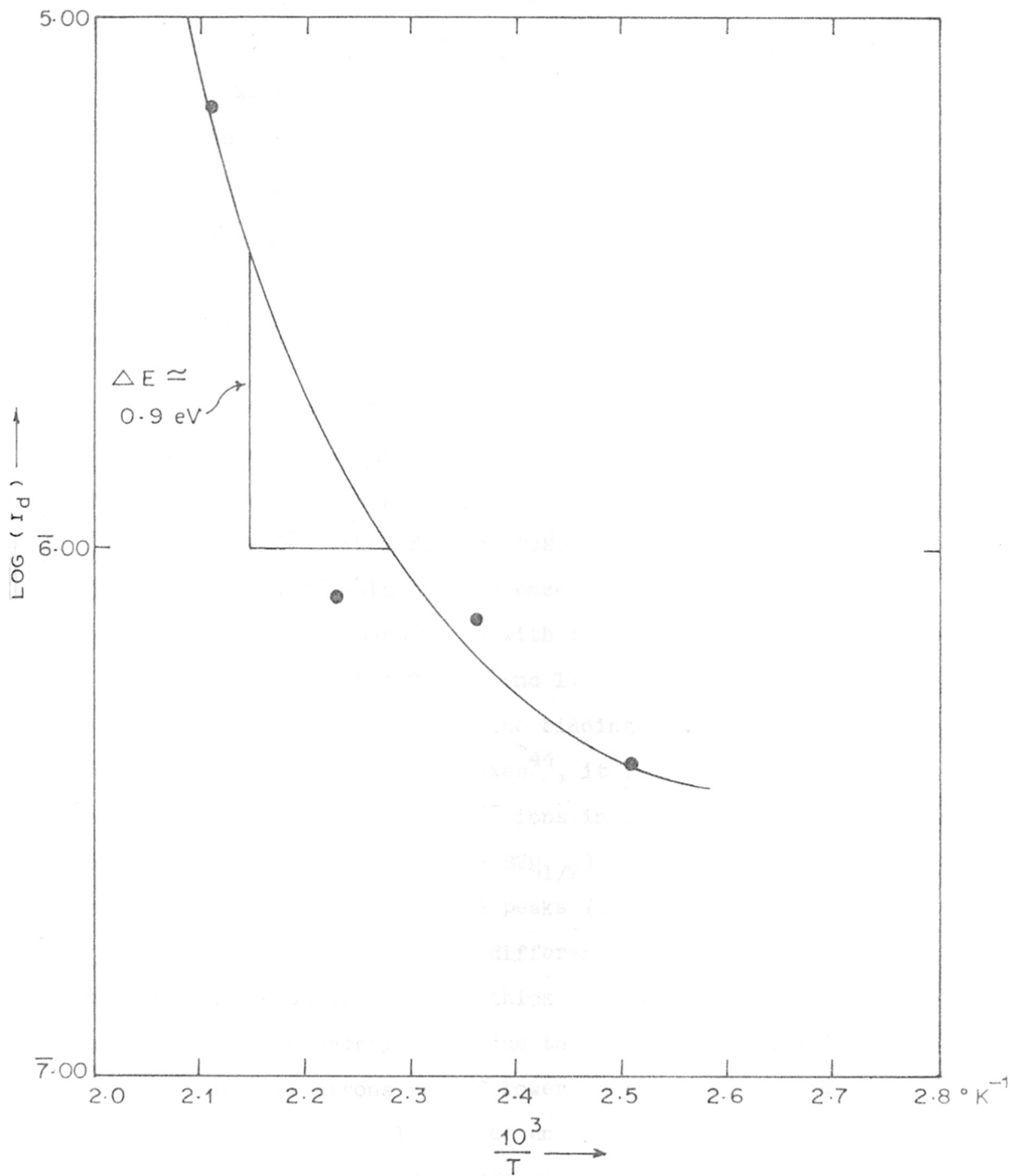


FIG. 3.17 PLOT OF $\text{LOG}(I_D)$ VS $10^3/T$

(DRAWN BY USING THE DATA OF FIG. 3.16)

We have carried out XPS examination of our films mainly with the objectives:

- (1) To monitor the chemical composition of the surface at a microscopic level,
- (2) To extract information regarding the chemical bonding of an adsorbate with the adsorbent.

Necessary XPS spectra have been reproduced in Figs. 3.18 and 3.19. Fig. 3.18 (a) presents the high resolution scan of an as-prepared highly photosensitive ($I_p/I_d = 10^8-10^9$) thick film of CdS. A careful examination of the spectrum reveals the presence of a triplet structure of S2p spread over about 20 eV with the peaks centered at 162.6 ± 0.2 eV, 172.8 ± 0.2 eV and 179.7 ± 0.2 eV. On comparing systematically with the binding energies reported on a variety of sulphur complexes⁴⁴, it is possible to assign the 162.6 eV peak to S²⁻ ions in CdS. As the spin-orbit splitting ($S2p_{3/2} \rightarrow S2p_{1/2}$) of S2p level is 2 eV, the higher binding energy (BE) peaks (172-179 eV) have to be assigned to the species of different chemical composition present on the surface of CdS thick films. The higher BE peaks are not secondary peaks due to Auger transitions because Auger electrons are of lower energy than the XPS electrons. This film also gives an O1s peak in the XPS high resolution scan thereby offering a direct evidence for the presence of chemisorbed oxygen [Fig. 3.19(a) - O1s level]

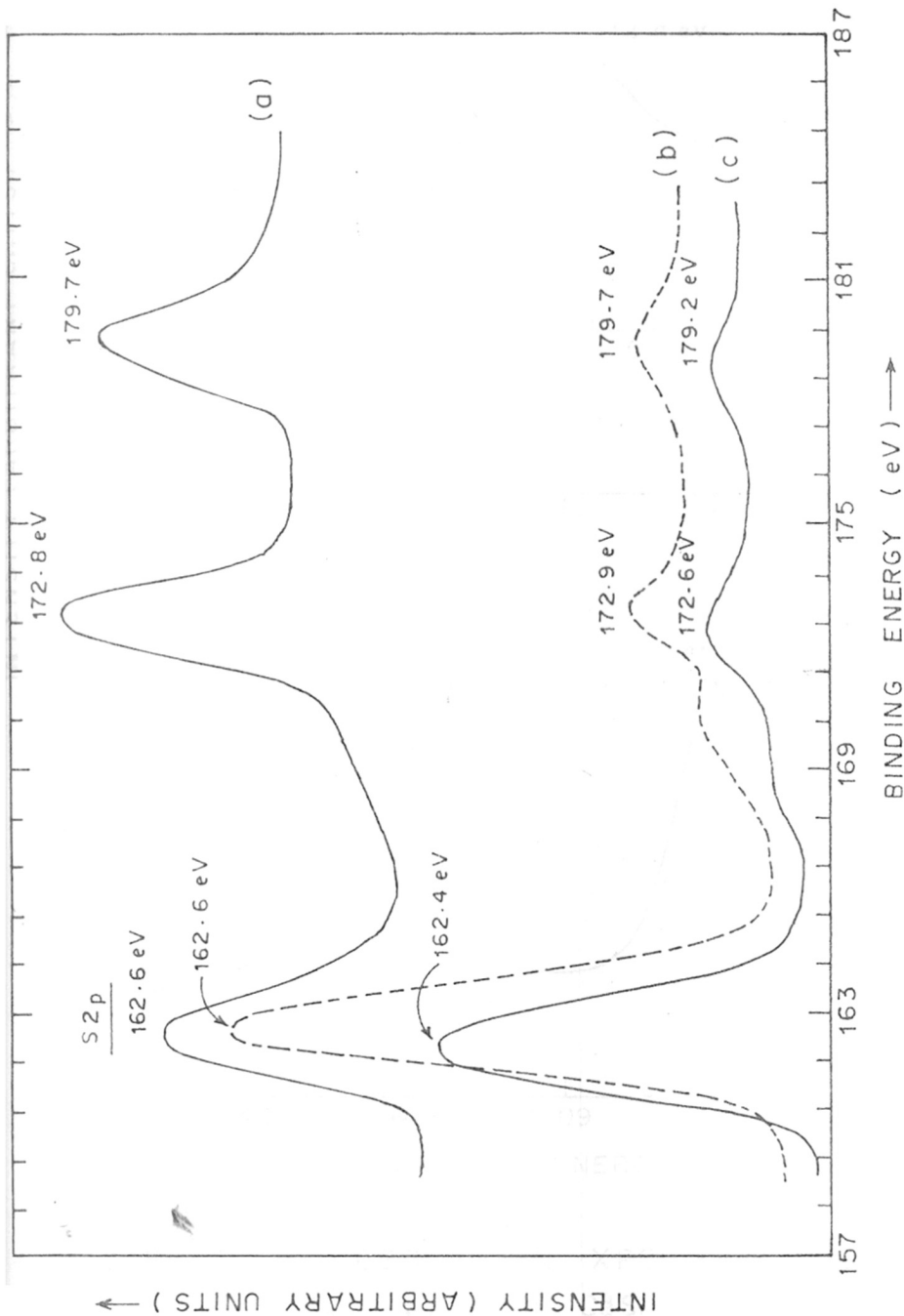


FIG. 3-18 HIGH RESOLUTION XPS SPECTRA (S_{2p}) OF CdS RECORDED WITH MgK α RADIATION: (a) AS-PREPARED FILM, (b) FILM HEATED AT 200 °C IN VACUUM IN DARK AND (c) PURE CdS POWDER USED IN THE PREPARATION

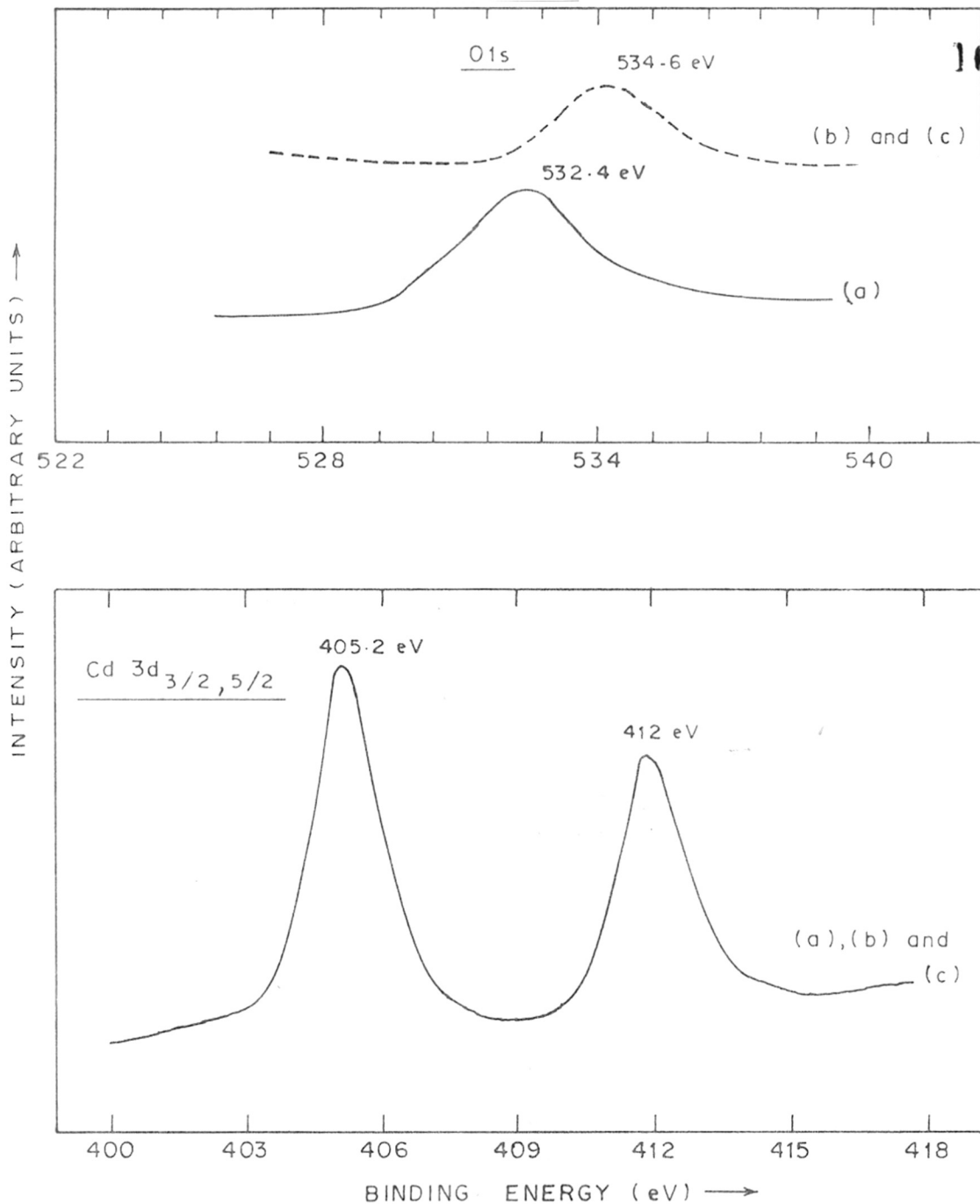


FIG. 3.19 HIGH RESOLUTION XPS SPECTRA [O1s AND Cd 3d_{3/2,5/2}] OF CdS RECORDED WITH MgK α RADIATION :

(a) AS-PREPARED FILM, (b) FILM HEATED AT 200°C IN VACUUM IN DARK AND (c) PURE CdS POWDER USED IN THE PREPARATION

discussed so far. It is broad and centered at 532.4 eV, indicating a change in chemical bonding and/or coordination for chemisorbed oxygen species on CdS thick film as the reported BE values for the adsorbed oxygen species on the metallic systems is around 530.0 eV⁴⁵.

It may be possible to identify these higher BE peaks of S2p level by using the finger-print analysis of the available XPS shifts data for a variety of S-O complexes⁴⁶⁻⁴⁹. Recently, Lichtensteiger et al.⁴⁷ have reported the presence of SO_4^{--} species (~ 169 eV) in their XPS studies of electron stimulated oxygen adsorption on single crystals of CdS. Their results also show the absence of the secondary peak around 169 eV from the clean surface of CdS, indicating that the adsorbed oxygen is totally responsible for the formation of SO_4^{--} like species on the surface. It is interesting to note that there is no ESR signal from the clean surface of CdS single crystals⁴³. Lichtman et al.⁴⁸ have also reported the formation of thin sulphate layer (peak at 169-170 eV) in their exhaustive XPS studies on twenty four sulphides. A peak at the very similar BE position (~ 172 eV) is observed for S2p level in polycrystalline CdSO_4 . Using these data, the second peak at 172.8 eV is attributed to the formation of SO_4^{--} like species by the preferential bonding of chemisorbed oxygen with 'S' sites on the surface of CdS thick film.

The appearance of the third peak (179.7 eV) is still striking. The S_{2p} BE has been found to decrease in the expected fashion in series such as $SF > S_2F_{10} > SOF_2 > SO_2 > SO_4^{--} > SO_3^{--} > S_8 > S^-$ [see reference 44, p. 184]. Since the peak at 172.8 eV is assigned to the formation of SO_4^{--} like species, the third peak on higher BE side may be attributed to the formation of SO_2 like species according to the reported BE series. Infact, Furuyama et al.⁴⁹ have observed a S_{2p} peak at 176.6 eV in their SO_2 adsorption studies and assigned it to SO_2 species in condensed state. The third peak at 179.7 eV in the present case may be indicative of bonding of chemisorbed oxygen with 'S' sites in SO_2 like configuration. However, these peaks are always present together in the XPS spectra of the as-prepared films. It is interesting to note that Barber et al.⁵⁰ have also reported SIMS studies of SO_2 adsorption on silver at 620°K and have found S, SO_4 and SO_2 species as SIMS clusters.

Significant appearance of these additional peaks with intensities almost equal to that of 162.6 eV peak in the XPS spectrum of an as-prepared film suggests a strong oxygen chemisorption; chemisorbed oxygen being preferentially bonded to S sites in SO_4^{--} and SO_2 like configurations. This interpretation is further substantiated by the appearance of a relatively strong peak at 162.6 ± 0.2 eV

(with considerable intensity reduction of other two peaks) in the XPS spectrum of vacuum-treated film [Fig. 3.18(b)] which exhibits no photosensitivity. This ^{is} in accordance with the thermal desorption during vacuum-heating which leaves hardly any oxygen to be chemisorbed on CdS to form SO_4^{--} and SO_2 like species. However, these additional peaks do not disappear even after prolonged thermal desorption treatment. Such a situation probably may not be encountered since the original CdS powder used to prepare thick films also shows similar triplet structure [Fig. 3.18 (c)].

The O1s peak centered at 534.6 eV is also present in the XPS spectrum of the vacuum-treated film [Fig. 3.19(b)]. This higher BE peak (shift = 2.3 eV) is assigned to the adsorption of water vapour⁴⁵ which is most likely to take place during the transfer of the vacuum-treated film to the UHV chamber of the spectrometer. Pure CdS powder used as a starting material also indicates similar adsorption of water vapour (Fig. 3.19(b) and (c) - O1s level].

It is evident from these XPS results that the strong chemisorption of oxygen on the surface of CdS thick film, exhibiting very high photosensitivity, leads to the formation of SO_4^{--} and SO_2 like species on the surface in addition to S^{--} configuration. After thermal desorption

treatment, the characteristic SO_4^{--} and SO_2 peak intensities decrease considerably and at the same time the film also loses its high photosensitivity.

3.7. DEPENDENCE OF PHOTOCURRENT ON THE INTENSITY OF ILLUMINATION

The dependence of photocurrent (I_p) on the intensity of illumination (f) can be expressed by a simple power law

$$I_p \propto f^n$$

where, n = an exponent of variation. It implies that if logarithmic values of photocurrent are plotted against logarithmic values of illumination intensities, a straight-line with slope equal to 'n' will be obtained.

Figs. 3.20 (A) and 3.20 (B) show the dependence of photocurrent on the intensity of illumination for the undoped and doped thick films of CdS respectively. Figs. 3.21 (A), 3.21 (B) and 3.21 (C) are the plots of corresponding $\log(I_p)$ versus $\log(f)$ data.

It is evident from these plots that:

- (1) Undoped film shows a square-root variation ($n \approx 0.5$) of the photocurrent with the intensity of illumination over the entire range of measurements [Figs. 3.20(A) and 3.21 (A)].

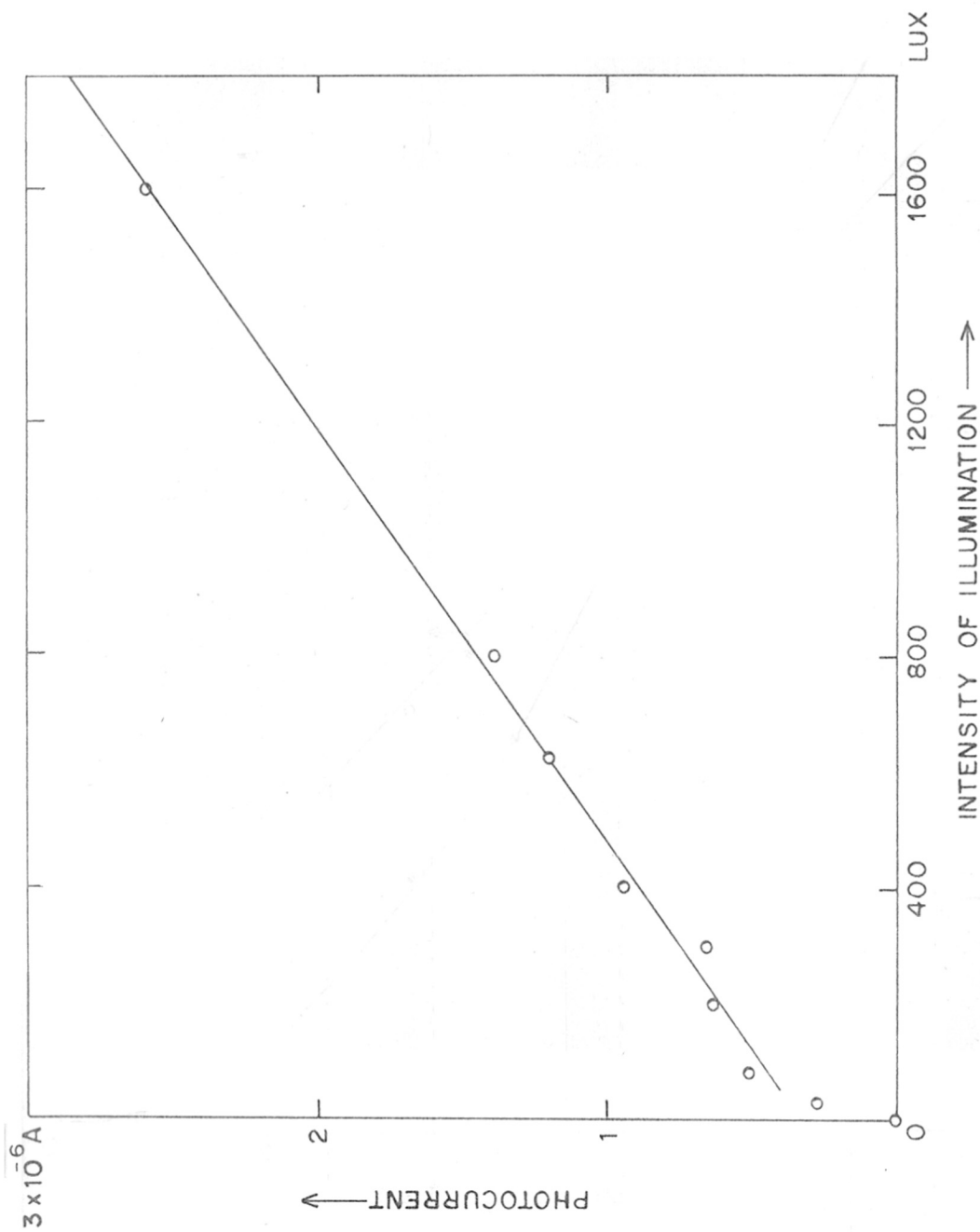


FIG.3.20(A) VARIATION IN THE PHOTOCURRENT WITH THE INTENSITY OF ILLUMINATION FOR UNDOPED THICK FILM OF CdS

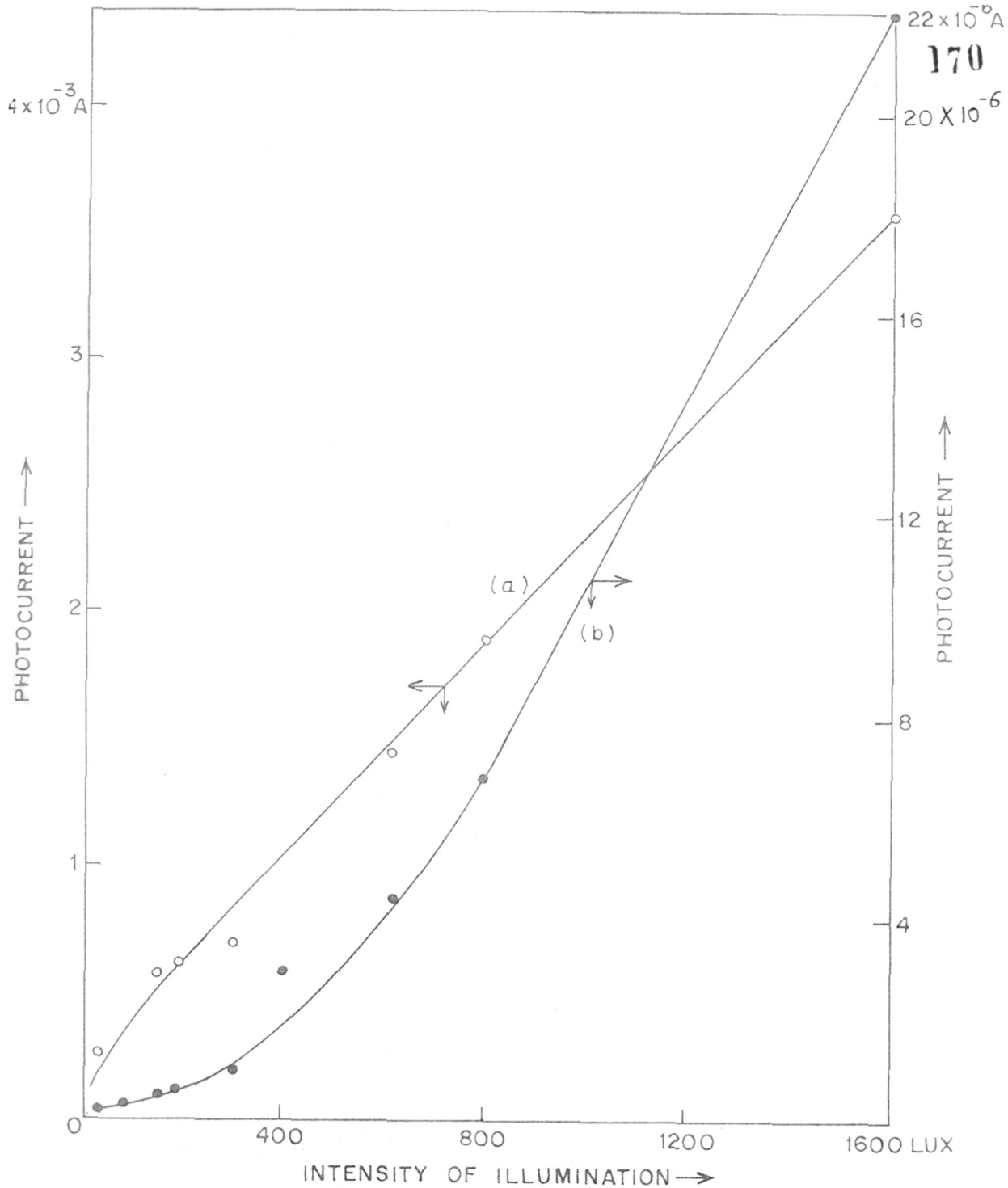


FIG. 3.20(B) VARIATION IN THE PHOTOCURRENT WITH THE INTENSITY OF ILLUMINATION FOR THE DOPED THICK FILMS OF CdS : (a) LOWER Cu CONC. (0.05% by wt) (b) HIGHER Cu CONC. (0.3% by wt)

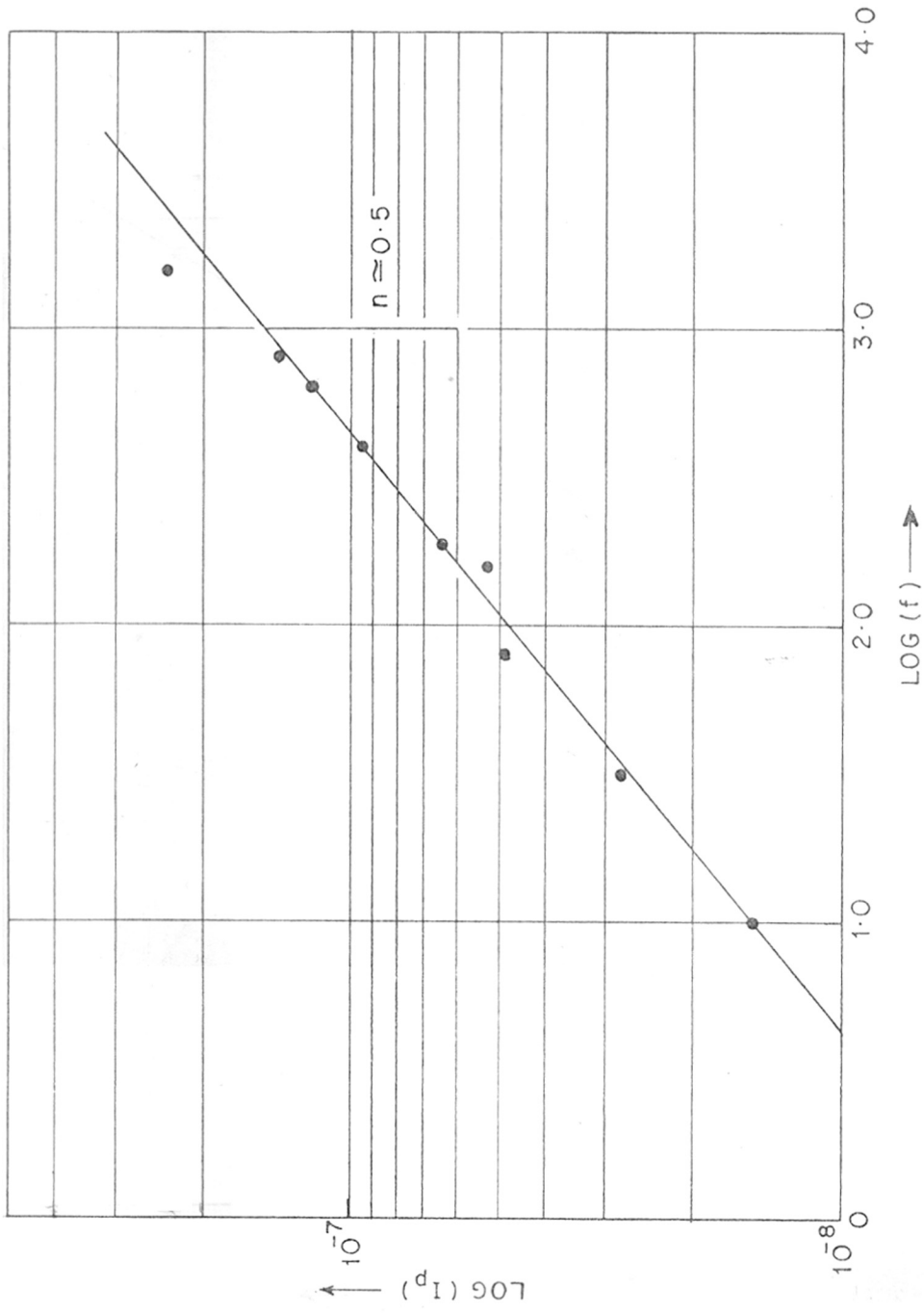


FIG. 3.21 (A) PLOT OF $\text{LOG}(I_p)$ Vs $\text{LOG}(f)$ [WHERE, I_p = PHOTOCURRENT AND f = INTENSITY OF ILLUMINATION] FOR THE UNDOPED THICK FILM OF CdS

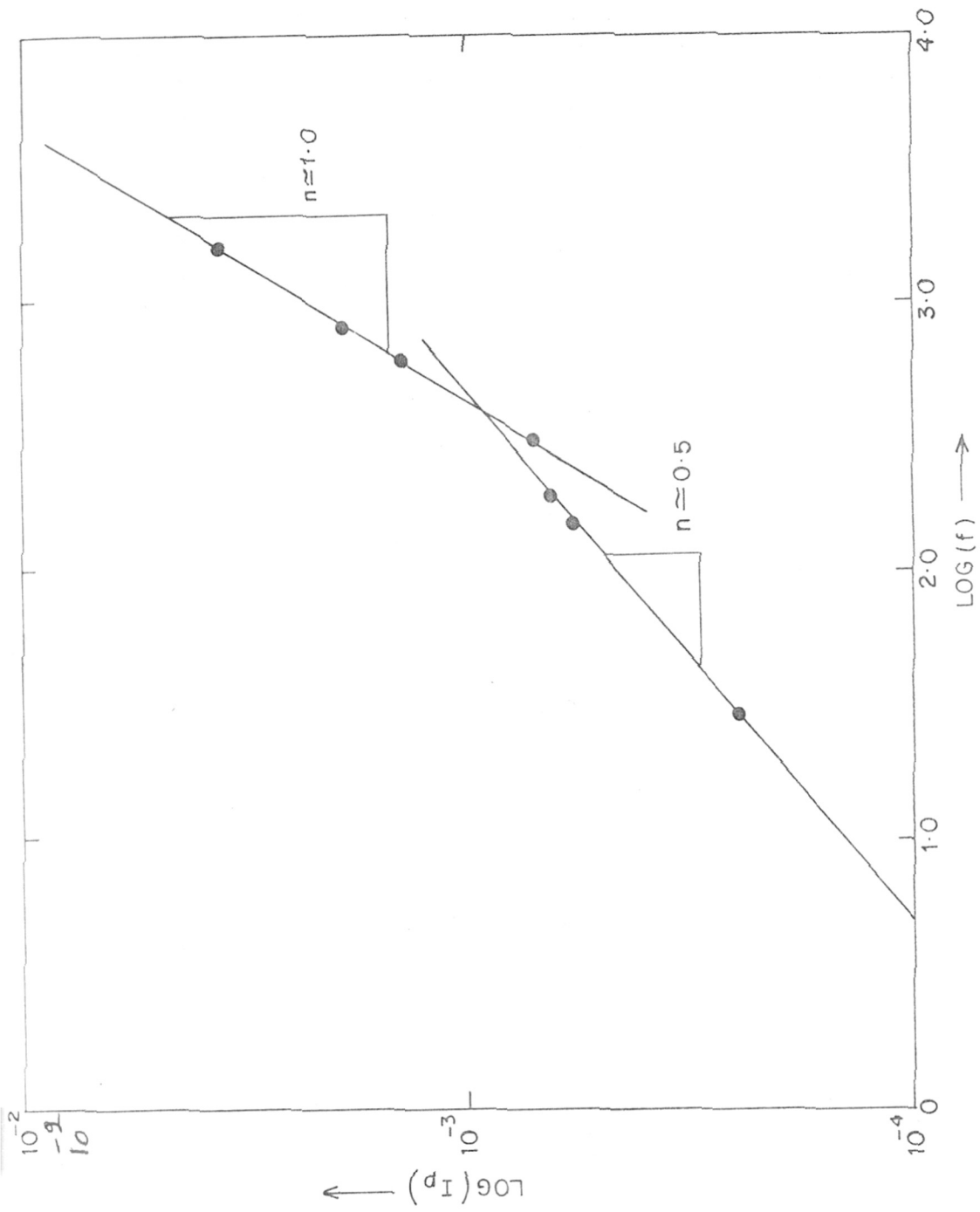


FIG. 3-21(B) PLOT OF LOG (I_p) Vs LOG (f) FOR THE DOPED THICK FILM OF CdS WITH LOW Cu CONCENTRATION (0.05 by wt)

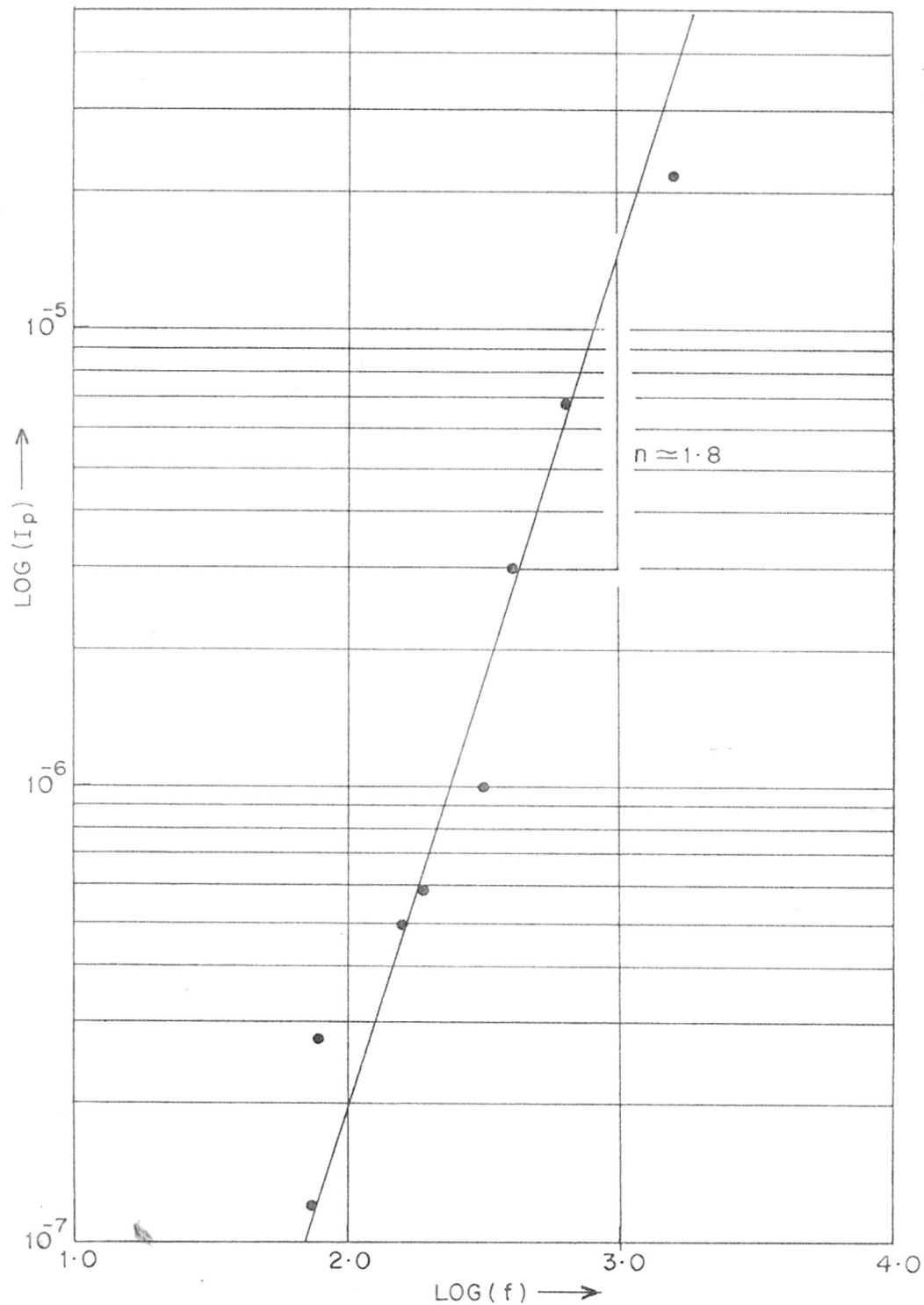


FIG. 3.21(C) PLOT OF $\text{LOG}(I_p)$ VS $\text{LOG}(f)$ FOR THE DOPED THICK FILM OF CdS WITH HIGH Cu CONCENTRATION (0.3% by wt)

(2) Doped films with lower Cu concentrations (viz. 0.05 to 0.1% by wt) exhibit (i) a square-root variation ($n \approx 0.5$) of the photocurrent with relatively lower illumination intensities and (ii) a linear variation ($n \approx 1.0$) of the photocurrent with higher illumination intensities [Figs. 3.20(B) - curve (a) and 3.21 (B)].

(3) Doped films with higher Cu concentration (viz. $> 0.3\%$ by wt) show a superlinear variation ($n \approx 1.8$) of the photocurrent with the intensity of illumination over the entire range of investigation [Figs. 3.20 (B) - curve (b) and 3.21 (C)].

These results are quite similar to those reported for single crystals⁵¹, sintered layers³⁴ and thin films of CdS^{35b}.

According to Bube⁵¹, a square-root variation of the photocurrent with the light intensity is the familiar case of bimolecular recombination and it results only when the concentration of free electrons becomes equal to the concentration of traps located between the corresponding quasi-fermi level and the dark conductivity fermi level.

If the distribution of recombination states (having preferential capture cross-section for photo-excited holes) decreases towards the conduction band, one

observes the linear dependence of free electron density (and hence photocurrent) on the light intensity⁴.

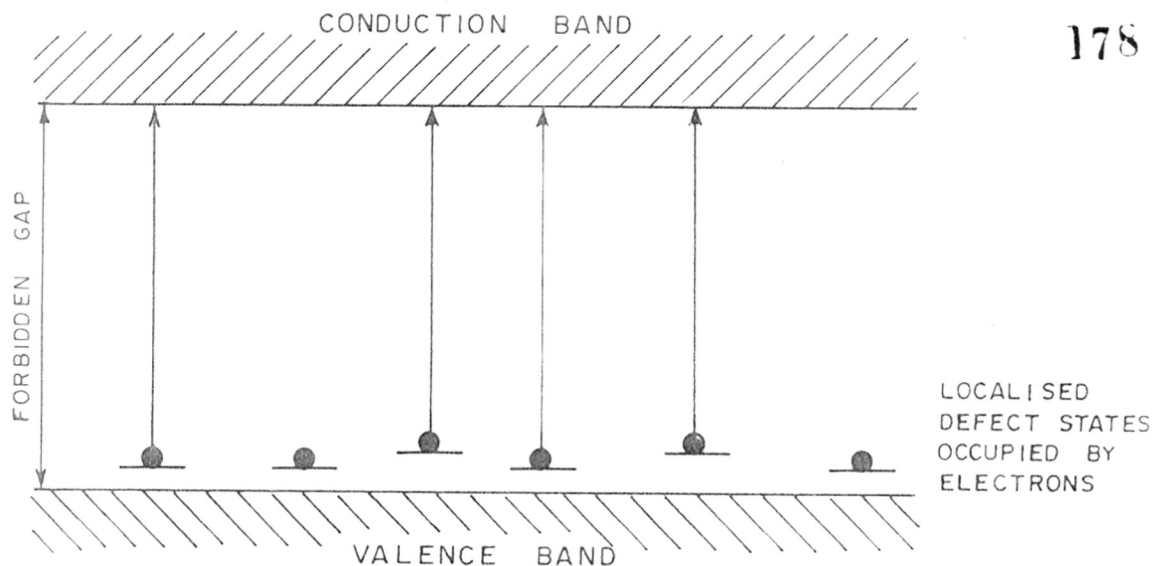
Superlinearity is a well-known phenomenon in the photoconducting CdS doped with high impurity concentrations⁵². As discussed earlier (section 3.1.2), desensitization occurs at the room temperature as a consequence of high impurity concentration, particularly at low excitation intensities. With increase in light intensity, however, the two steady state Fermi levels are moved farther apart which embrace new states in the category of recombination centers having large preferential capture cross-section for photo-excited holes⁴. In other words, lifetime of the photo-excited electrons in the conduction band increases with a power-exponent greater than unity with an increase in the excitation intensity in case of heavily doped films. The photocurrent, therefore, varies superlinearly with the excitation intensity.

Superlinearity is a striking effect since most of the changes that one expects to occur at higher light intensities lead to sublinearity. Moreover, the superlinearity can be experimentally observed even at relatively low light intensities, where saturation of recombination centers is not likely to take place⁴.

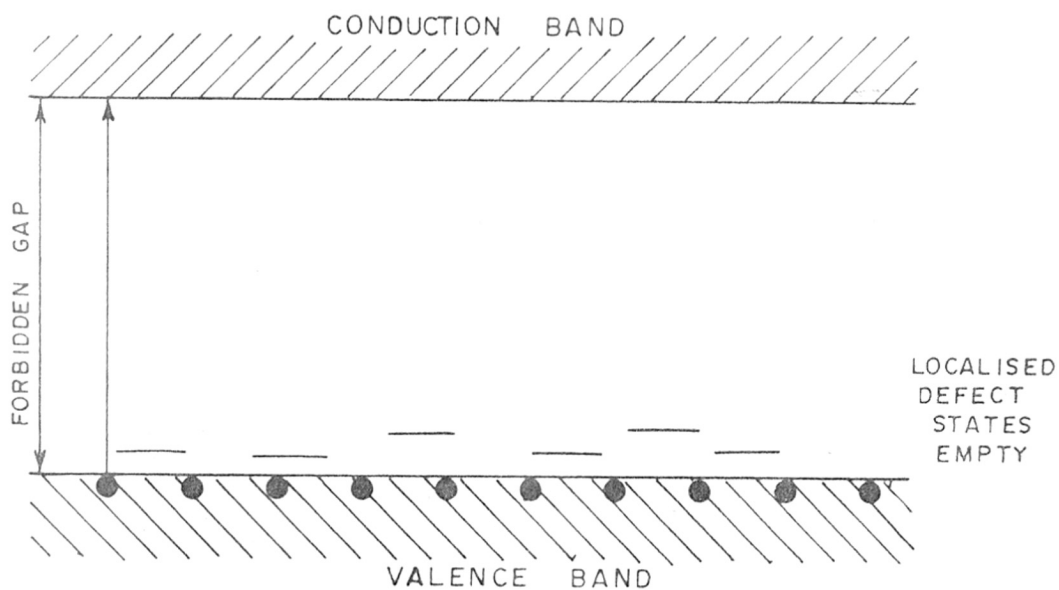
3.8. SPECTRAL RESPONSE

Spectral response curves associated with the undoped thick film of CdS at 300°K and 93°K are depicted in Fig. 3.22. The curve (a) at 300°K shows a response peak in the region of $\lambda = 555$ nm which is followed by a fairly constant response upto $\lambda = 690$ nm. The shape of spectral response curve at 300°K appears to be different from that reported for undoped single crystals³³ and thin films of CdS^{11,12,35}. However, the spectral response curve at 93°K [curve (b)] of the same undoped film indicates a sharp peak at $\lambda = 515$ nm. This curve at 93°K has a close resemblance in shape and peak position with that of undoped single crystals³³ and thin films of CdS^{11,12,35} at 300°K. This is a distinct feature of the present investigation. We suggest two possibilities to account for this anomalous spectral response behaviour:

(1) It can be associated with the localised defect states which lie in the forbidden gap just above the valence band [Fig. 3.23 (A)]. These acceptor-like states are occupied by electrons at room temperature. If transitions of electrons from these localised defect levels to conduction band are to take place under illumination, then such transitions will require relatively low excitation energy than that of band to band transition. The spectral response may, therefore, extend to relatively longer



(A) AT 300°K



(B) AT 93°K

FIG. 3.23 ENERGY-LEVEL DIAGRAM SHOWING THE LOCALISED DEFECT STATES :

(A) POSSIBLE ELECTRONIC TRANSITIONS AT 300°K

(B) ONLY BAND TO BAND TRANSITION AT 93°K

wavelengths characteristic of these defect excitation energies. The shape of the response curve in such a case will, of course, depend upon the actual transition probabilities. At 93°K , these localised defect levels are depopulated and electronic transitions from them are absent. At this temperature, the only possible transition will be band to band transition [Fig. 3.23(B)]. The spectral response at 93°K corresponds to a wavelength which is characteristic of band to band transition. The response peak at $\lambda = 515 \text{ nm}$ [curve (b), Fig. 3.22] corresponds to an excitation energy of 2.4 eV. It is the generally accepted value for the band gap of CdS.

(2) The other possibility may be related to the cubic dominated mixed phase in the undoped film, as the exact band structure of the cubic modification of CdS is not yet determined¹¹. Although photoconductivity in thin films and layers of cubic CdS has been reported earlier⁹⁻¹², this will be the first indication of the photoelectronic behaviour as a function of wavelength for cubic CdS photoconductor which involves high temperature firing in the preparation procedure (see section 3.2.2).

Spectral response curves (at 300°K and 93°K) of the doped film with optimum Cu concentration are presented in Fig. 3.24. The curve (a) at 300°K shows a relatively broad response peak in the region of $\lambda = 660 \text{ nm}$. At 93°K , response peak remains unchanged.

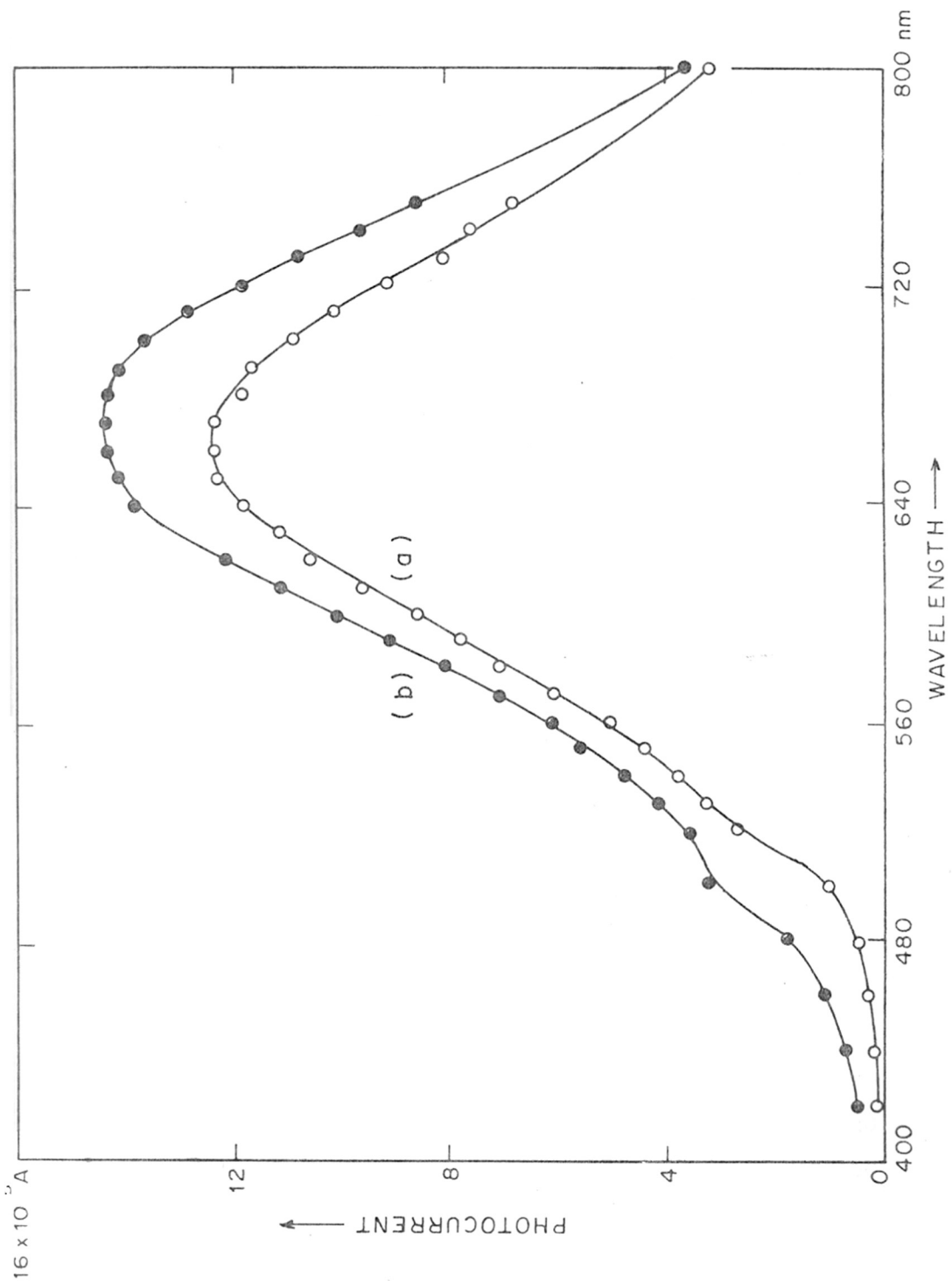


FIG. 3-24 SPECTRAL RESPONSE FOR THE DOPED THICK FILM OF CdS WITH OPTIMUM Cu CONCENTRATION [CURVE (a)-300°K, CURVE (b) -93°K]

For heavily doped films [Cu concentration > 0.25% by wt], a fairly sharp response peak is observed in the region $\lambda = 690$ nm at 300°K and $\lambda = 645$ nm at 93°K (Fig. 3.25).

It is also noticed that for doped films with medium copper concentration (ranging from 0.1 to 0.25% by wt), a fairly sharp response peak occurs in the region of $\lambda = 645$ nm at 300°K and $\lambda = 635$ nm at 93°K .

Table 3.8 presents the dependence of spectral response data on the copper concentration of these films.

TABLE 3.8

EFFECT OF Cu CONCENTRATION ON SPECTRAL
RESPONSE

Concentration of Cu added as CuCl_2 (wt % of CdS)	Spectral response peak nm	
	at 300°K	at 93°K
nil	550-690	510-520
0.05	650-670	660-680
0.10	640-650	630-640
0.15	640-650	630-640
0.20	640-650	630-640
0.25	640-650	630-640
0.30	680-690	640-650
1.00	690-700	640-650

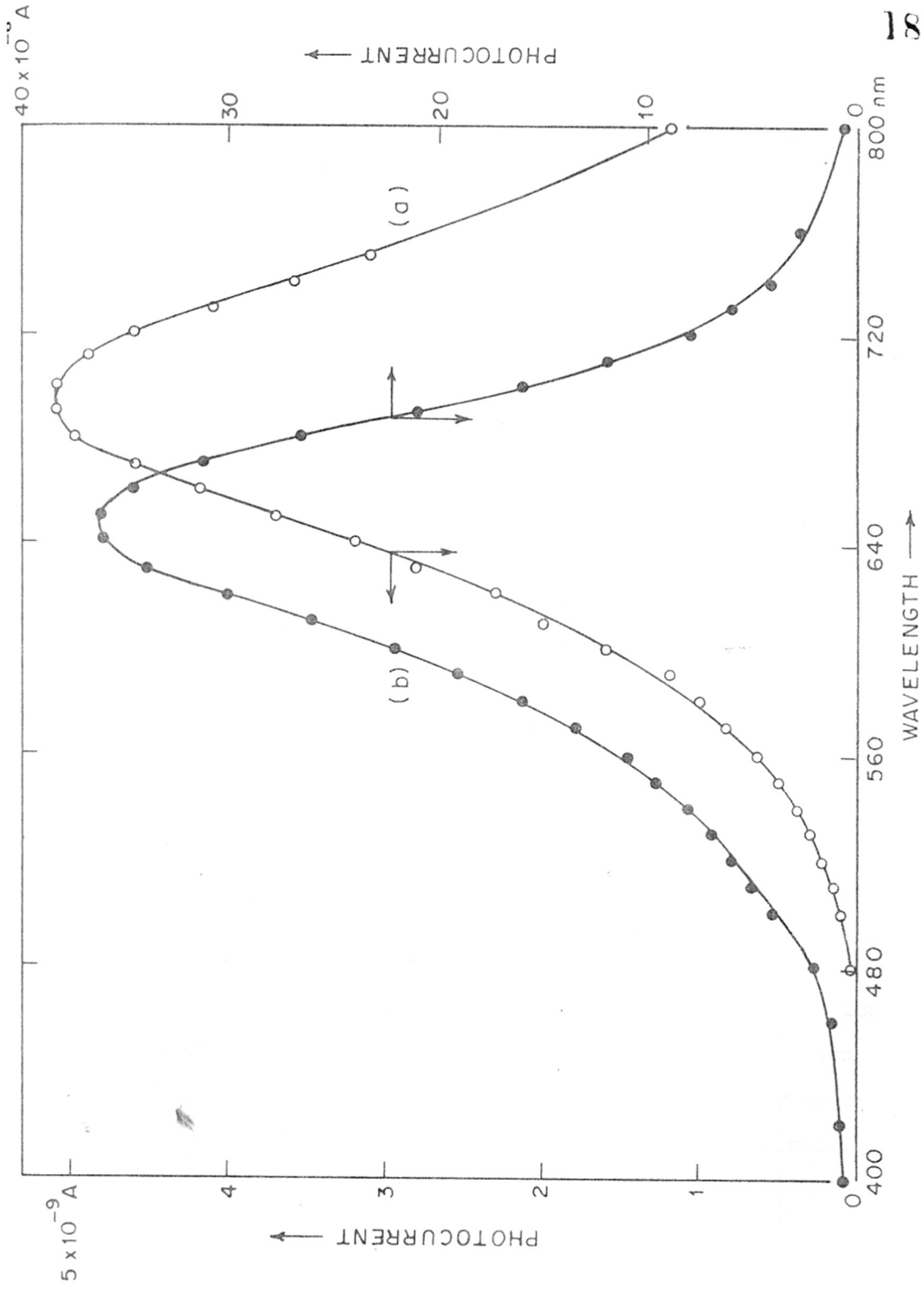


FIG. 3.25 SPECTRAL RESPONSE FOR THE HEAVILY DOPED THICK FILM OF CdS
 [CURVE (a)- 300° K , CURVE (b)- 93° K]

The highlights of the spectral response study on the doped thick films of CdS (Table 3.8) are:

(1) With impurity incorporation (doping), there is a red shift in the spectral response peak. This observation is consistent with the work reported for doped single crystals⁵³, sintered layers^{1,34} and thin films³⁵ of CdS. When there is an appreciable concentration of compensated acceptor type of impurity, the possibility of direct electronic excitation from such impurity level lying in the forbidden gap to the conduction band had been suggested by Rose⁴ and Bube²⁸. Since impurity state excitation requires less energy than that of band gap excitation, spectral response peak shows a shift to longer wavelength side (red shift). Further red shift in the response peak with increasing Cu concentration could be attributed to a higher ratio of Cu to Cl centers¹. This increase in Cu centers over Cl centers produces an observable deepening in the colour of the films. A change in colour of the thick films (from yellow to blackish brown) with increase in Cu concentration also indicates more efficient absorption of longer wavelengths¹. An impurity-band broadening which may occur as a result of an increase in impurity-density can also be expected to have some effect on the observed red shift.

(2) It is observed that on lowering the temperature; (a) there is no shift in response peak for the films doped with optimum Cu concentration, (b) there is a negligible blue shift in response peak for the films doped with medium Cu concentrations and (c) there is an appreciable blue shift in response peak for the films doped with high Cu concentrations.

An appreciable shift in the optical absorption edge of CdS single crystals at low temperature (77°K) is also presented by Lehmann⁵⁴. He has reported the optical absorption edge as a function of impurity concentration for indium doped CdS. He considered a tailing-off of the density of allowed states below the bottom edge of the conduction band because of the crystal disorder. Our observation, (c) in particular, can also be explained on similar lines.

Temperature dependence of the photocurrent as noticed during the spectral response measurements also forms a salient aspect of our study. Under the same conditions of spectral illumination, if the temperature is lowered from 300 to 93°K , then

(i) undoped films show a marked decrease in photocurrent (Fig. 3.22),

(ii) doped films with optimum Cu concentration show a little increase in the photocurrent (Fig. 3.24),

(iii) doped films with medium Cu concentration (viz. 0.1-0.25% by wt) show an incremental increase in the photocurrent,

(iv) highly doped films (Cu concentration $>$ 0.3% by wt) show a remarkable increase in the photocurrent (Fig. 3.25).

It is possible to explain the observation (i), semiquantitatively, on the basis of the model consisting of localised defect states described earlier. These states when filled with electrons at room temperature possess high capture cross-section for photoexcited holes. In other words, these defect states behave as sensitizing centers at room temperature, thereby exhibiting relatively high photoconductivity. But with the electronic depopulation at 93°K , these defect states do not behave as sensitizing centers, thereby exhibiting low photoconductivity. Owing to the complex nature of these defect states, the origin of which is still unknown, this model alone may not provide a satisfactory explanation.

The observations (ii), (iii) and (iv) can be regarded as the consequence of increasingly high impurity concentration effects. It has been already discussed that

beyond a critical impurity concentration, the photosensitivity decreases rapidly at room temperature and this desensitization could be a direct result of the imperfection interactions that reduce thermal hole-ionization energy of the sensitizing centers^{2,3} (see section 3.1.2). At low-temperature (viz. 93°K), however, quite a different type of situation arises in the case of heavily doped films. There might be two possibilities:

(1) Even with the decreased hole ionization energy, thermal excitation of holes from the impurity states to valence band may not be possible at low temperatures.

(2) Under the conditions of constant illumination, two steady state quasi-fermi levels shift towards the respective band-edges on lowering the temperature⁴. As a result of this, more of the impurity states are embraced between the two quasi-fermi levels⁴.

The possibilities (1) and (2) imply that the occupancy of the impurity states is governed more by recombination kinetics than by the thermal behaviour at 93°K. This condition as proposed by A. Rose⁴ favours high photoconductivity.

REFERENCES

1. M. J. B. Thomas and E. J. Zdanuk;
J. Electrochem. Soc., 106, p. 964 (1959).
2. R. H. Bube and A. B. Dreeben;
Phys. Rev., 115, p. 1578 (1959).
3. R. H. Bube, E. L. Lind and A. B. Dreeben;
Phys. Rev., 128, p. 532 (1962).
4. A. Rose;
"Concepts in photoconductivity and allied problems", Interscience Publishers, Wiley, New York (1963), Chapter 3.
5. ASTM Cards for X-ray diffraction data,
No : 6-0314.
6. ASTM Cards for X-ray diffraction data,
No : 2-0454.
7. N. F. Foster;
J. Appl. Phys., 38, p. 149 (1968).
8. C. A. Escoffery;
J. Appl. Phys., 35, p. 2273 (1964).
9. E. L. Lind and R. H. Bube;
J. Chem. Phys., 37, p. 2499 (1962).
10. M. Nagao and S. Watanabe;
Jap. J. Appl. Phys., 7, p. 684 (1968).
11. S. D. Sathaye and A..P. B. Sinha;
Thin Sol. Films, 37, p. 15 (1976).
12. N. R. Pavaskar, C.A. Menezes and A. P. B. Sinha;
J. Electrochem. Soc., 124, p. 743 (1977).
13. Y. Ma and R. H. Bube;
J. Electrochem. Soc., 124, p. 1430 (1977).
14. K. L. Chopra and I. H. Khan;
Surf. Sci., 6, p. 33 (1967).
15. S. Simov; (and the references therein),
Thin Sol. Films, 15, p. 79 (1973).
16. E. S. Rittner and J. H. Schulman;
J. Phys. Chem., 47, p. 537 (1943).

17. J. Kimavicius, A. Alisauskas, A. Sirvaitis;
Liet. Fiz. Rinkinys, 11, p. 493 (1971).
C.A. 76:38400n.
18. W. W. Wendlandt;
"Thermal methods of analysis",
A. Wiley-Interscience Publication, New York
(1974).
19. A. F. Andrushko;
Sov. Phys. - Solid State, 4, p. 424 (1962).
20. Z. I. Kiryashkina, A. G. Rokakh, N. A. Kulikova,
L. M. Beletskaya, O. S. Vdovin, L. D. Zorina and
N. B. Trofimova;
Fiz. Poluprov. Poluprov. Electron. (Russ.),
1, p. 93 (1968).
21. A. Addamiano and M. Aven;
J. Appl. Phys., 31, p. 36 (1960).
22. A. Kremheller;
Sylvania Technologist, 8, p. 11 (1955).
23. A. J. Behringer and L. Corrsin;
J. Electrochem. Soc., 110, p. 1083 (1963).
24. K. V. Shalimova, A. F. Andrushko, V. A. Dmitriev;
and L. P. Pavlov; Sov. Phys. Crystallogr., 8, p.618
(1964).
25. B. D. Galkin, N. V. Troitskaya and R.D. Ivanov;
Sov. Phys. Crystallogr., 12, p. 766 (1968).
26. R. H. Bube;
In M. Aven and J. S. Frener (Eds.);
"Physics and Chemistry of II-VI Compounds",
North-Holland Publishing Co. (1967), p. 661.
27. A. Rose;
"Concepts in Photoconductivity and Allied Problems",
Interscience Publishers (1963), Chapter - 2.
28. R. H. Bube;
"Photoconductivity of Solids", John Wiley and Sons,
New York (1960), Chapter 6.
29. K. H. Nicholas and J. Woods;
Brit. J. Appl. Phys., 15, p. 783 (1964).
30. J. Woods and K. H. Nicholas;
Brit. J. Appl. Phys., 15, p. 1361 (1964).

31. R. H. Bube;
J. Phys. Chem. Solids, 1, p. 234 (1957).
32. R. H. Bube;
In M. Aven and J. S. Prener (Eds.),
"Physics and Chemistry of II-VI Compounds",
North-Holland Publishing Co. (1967),
Section - 13.1.4.
33. R. H. Bube and S. M. Thomsen;
J. Chem. Phys., 23, p. 15 (1955).
34. S. M. Thomsen and R. H. Bube;
Rev. Sci. Instrum., 26, p. 664 (1955).
35. W. Veith;
(a) Compt. Rend., 230, p. 947 (1950).
(b) Z. Angew Physik, 7, p. 1 (1955).
36. D. B. Fraser and H. Melchior;
J. Appl. Phys., 43, p. 3120 (1972).
37. P. K. Gogna, L. K. Malhotra and K. L. Chopra;
Res. and Ind., 22, p. 74 (1977).
38. B. K. Gupta, O. P. Agnihotri and A. Raza;
Thin Sol. Films, 48, p. 153 (1978).
39. N. Croitoru and S. Jakobson;
Thin Sol. Films, 56, L5 (1979).
40. F. B. Micheletti and P. Mark;
J. Appl. Phys., 39, p. 5274 (1968).
41. V. G. Bhide, S. Jatar and A. C. Rastogi;
Pramana, 9, p. 399 (1977).
42. P. Mark;
J. Phys. Chem. Solids, 26, p. 1767 (1965).
43. G. D. Sootha, G. K. Padam and S. K. Gupta;
Phys. Stat. Sol. (a), 58, p. 615 (1980).
44. R. A. Walton;
Coordination Chemistry Reviews, 31, p.183 (1980).
45. J. C. Fuggle;
In D. Briggs (Ed.) "Hand-book of X-ray and
Ultraviolet Photoelectron Spectroscopy",
Heyden and Son Ltd. (1977), p. 295.

46. K. Siegbahn et al.;
"ESCA - Atomic, Molecular and Solid State
Structure Studies by means of Electron
Spectroscopy", Almquist and Wiksells,
Uppasala (1967).
47. M. Lichtensteiger, C. Webb and J. Lagowski;
Surf. Sci., 97, L-375 (1980).
48. D. Lichtman, J. H. Craig, V. Sailer and
M. Drinkwine,
Appl. Surf. Sci., 7, p. 325 (1981).
49. M. Furuyama, K. Kishi and S. Ikeda;
J. Electron Spectrosc. Relat. Phenom.,
13, p. 59 (1978).
50. M. Barber, P. Sharpe and J. C. Vickerman,
Chem. Phys. Lett., 27, p. 436 (1974).
51. R. H. Bube;
J. Chem. Phys., 23, p. 18 (1955).
52. R. H. Bube;
In S. Larach (Ed.); Photoelectronic Materials
and Devices", Van Nostrand Co. Inc., New York
(1965), p. 132 - 137.
53. J. Woods;
J. Electronics and Control, 3, p. 225 (1957).
54. W. Lehmann;
J. Electrochem. Soc., 112, p. 1150 (1965).

CHAPTER - 4

SUMMARY

During the course of this investigation, thick films of CdS with superior photosensitivity and acceptable shelf-life have been successfully prepared. The preparation is based on the standard thick film technology process i. e. screen-printing and firing. It has been demonstrated that photosensitivity of CdS thick films can be greatly modified by preparation conditions, namely, the firing temperature and impurity concentration. These parameters, therefore, have been optimised to get the best and reproducible photosensitivity. The optimum values are:

- (i) Cu concentration = 0.05% by wt of CdS and
- (ii) firing temperature = 600°C.

Structural, electrical and photoconducting properties of these films have been studied by using (i) the instrumental techniques like XRD, SEM, DTA-TG, ESCA, etc. and (ii) methods of measurements of dark conductivity versus temperature, dependence of photo-current on the intensity of illumination and spectral response.

Analysis of the XRD data shows that:

- (i) There exists a cubic dominated mixed phase [cubic (85%) + hexagonal (15%)] in undoped thick films of CdS.
- (ii) There exists a purely hexagonal phase in doped thick films of CdS.

Predominance of cubic phase in undoped films is an interesting observation, since there are scant literature references related to the occurrence of cubic dominated/ cubic phase in photoconducting CdS. A characteristic aspect of the structural investigations is the CdCl_2 assisted cubic to hexagonal phase transformation that occurs during the process of doping. DTA studies support the XRD results and have been used to shed further light on the mechanism underlying such a phase transformation.

An examination of surface morphology of these films with scanning electron microscopy indicates that:

- (i) Undoped film consists of uniform grains of average 1μ grain size and
- (ii) Doped film consists of large but non-uniform grains of size varying from 4μ to 12μ .

Current-voltage (I-V) characteristics for thick films of CdS have been established in the range of 0-60 V in dark as well as under illumination. I-V plots exhibit an ohmic behaviour. All the electrical and photoconducting measurements have been performed by applying a d.c. potential which falls in this ohmic range.

Dark conductivity of these films has been studied as a function of temperature over the temperature

range of 150-370°K. Plots of $\log(I_d)$ versus $10^3/T$ indicate that:

(i) There are two principal ionization energies [0.138 and 0.85 eV] associated with the imperfection centers in undoped film.

(ii) There are three principal ionization energies [0.059, 0.087 and 1.05 eV] associated with the imperfection centers in doped film.

These values are quite comparable with the reported data.

The photosensitivity of the order of 10^9 associated with the thick films of CdS doped with optimum Cu concentration is the highest reported so far for CdS photoconductors.

It was anticipated that oxygen chemisorption could play a key role in the overall photoelectronic behaviour of these films. We have, therefore, carried out dark conductivity measurements as a function of temperature) during the oxygen-adsorption-desorption cycles. These cycles include:(i) heating of the virgin films upto 200°C in dark under vacuum and (ii) heating of these vacuum-treated films upto 200°C in dark and in air. It has been found that room temperature dark conductivity changes by 9 to 10 orders of magnitude as a result of the above thermal treatments. With these results, it is concluded

that a strong oxygen chemisorption is mainly responsible for very low dark conductivity and, in turn, very high photosensitivity of these films.

To investigate the kinetics of oxygen-chemisorption, variation in dark conductivity of a previously vacuum-treated sample has been studied as a function of time when it is exposed to air at a fixed temperature. A plot of $\log(I_d)$ versus $10^3/T$ is further drawn by using the above kinetics data. It yields an activation energy of 0.9 eV for the oxygen chemisorption process which is in good agreement with the reported data.

Recently, the immensely complex issues of surface states originating through gaseous chemisorption on photoconductors have received renewed impetus through advances in surface sensitive techniques like XPS, AES, SIMS etc. We have carried out XPS examination of our films in order to extract information regarding the chemical bonding of an adsorbate with the adsorbent. The significant appearance of a triplet structure of S_{2p} level with the peaks centered at BE values 162.6, 172.8 and 179.7 eV in the XPS spectrum of an as-prepared highly photosensitive [$I_p/I_d = 10^9$] film is particularly interesting. XPS spectrum also offers a direct evidence for the presence of chemisorbed oxygen. By using the finger-print analysis of the available XPS shifts data;

the S2p peak at 162.6 eV is interpreted to originate from S^{--} ions, the one at 172.8 eV from the SO_4^{--} like species and that at 179.7 eV from SO_2 like species, the latter two being formed on the surface due to preferential bonding of chemisorbed oxygen with sulphur. After thermal desorption, the film exhibits no photosensitivity and there is a substantial reduction in the intensities of 172.8 and 179.7 eV peaks. A close link between the existence of SO_4^{--} and SO_2 like species and photoconductivity is clearly manifested.

Depending upon Cu concentration, these films show sublinear, linear and superlinear variation of the photocurrent with the intensity of illumination.

Spectral response measurements on these films have been conducted at $300^\circ K$ and $93^\circ K$. The highlights of the spectral response data are:

(A) Undoped film has a broad spectral response at $300^\circ K$ ranging from $\lambda = 550$ to 690 nm, unlike the thin films, sintered layers and single crystals which gave a sharp peak at $\lambda = 510$ - 520 nm. However, the same film exhibits a sharp peak at $\lambda = 515$ nm at $93^\circ K$. This is a quite distinct feature of the present investigation. It can be attributed to (i) the spectral excitation of the localised defect states which lie just above the valence band in the forbidden gap and/or (ii) to the prevalence of cubic dominated mixed phase.

(B) Doped films show a red shift [$\lambda = 640-650$ nm] in spectral response peak at 300°K which is similar to that obtained for doped thin films, single crystals and sintered layers of CdS.

(C) On lowering the temperature, there is a notable blue shift in response peak only in case of heavily doped films.

Temperature dependence of the photocurrent as noticed during the spectral response measurements also forms a salient part of our study.

Apart from the basic studies, the following features make this technique attractive for the fabrication of photoconductor devices:

- (1) It gives films with superior and reproducible photosensitivity and reasonable shelf-life.
- (2) It is simple and less expensive.
- (3) It possesses most of the advantages of sintered layers i.e. uniformity, high mechanical strength and ease of impurity incorporation for the films.
- (4) It offers a viable method for large area fabrication and mass production which are the prime prerequisites of commercial devices.

ACKNOWLEDGEMENT

I am deeply indebted to Dr. A.P.B. Sinha, FNA, Distinguished Scientist, National Chemical Laboratory, Pune, for suggesting the research problem and also for his valuable guidance, keen interest and constant encouragement during the course of the present investigation.

I am grateful to Dr. S.K. Date for many stimulating discussions and for useful suggestions in the preparation of this dissertation.

I wish to express my sincere thanks to Mr. M.S. Setty, Dr.(Miss) N.R. Pavaskar, Dr. S.T. Kshirsagar and Dr. S.D. Sathaye for their genuine help in the different phases of this work.

The whole-hearted co-operation of Dr. S. Badrinarayanan, Dr. V.G. Gunjekar, Dr.(Mrs) A. Mitra, Mr. J.S. Gujral and Mr. P.D. Godbole is sincerely acknowledged. I am also thankful to Mr. S.M. Kulkarni for his patient typing.

It gives me great pleasure to thank my parents for their unflinching support in the materialization of this work.

Finally, I must thank the Council of Scientific and Industrial Research, New Delhi, for the award of research fellowship and the Director, National Chemical Laboratory, Pune, for allowing me to submit this work in the form of Ph.D. thesis.

D.P. Amalnerkar
27-5-82
[D.P. Amalnerkar]